

# The Effects of Initial Conditions and Liquid Composition on the One-Dimensional Consolidation Behaviour of Clay-Based Sealing Materials

NWMO TR-2008-06

March 2008

**D. G. Priyanto<sup>1</sup>**

**J. A. Blatz<sup>2</sup>**

**G. A. Siemens<sup>3</sup>**

**R. Offman<sup>2</sup>**

**J. S. Boyle<sup>3</sup>**

**D. A. Dixon<sup>1</sup>**

<sup>1</sup>Atomic Energy of Canada Limited

<sup>2</sup>University of Manitoba

<sup>3</sup>Royal Military College of Canada

**nwmo**

NUCLEAR WASTE  
MANAGEMENT  
ORGANIZATION

SOCIÉTÉ DE GESTION  
DES DÉCHETS  
NUCLÉAIRES

**Nuclear Waste Management Organization**  
22 St. Clair Avenue East, 6<sup>th</sup> Floor  
Toronto, Ontario  
M4T 2S3  
Canada

Tel: 416-934-9814  
Web: [www.nwmo.ca](http://www.nwmo.ca)

**The Effects of Initial Conditions and Liquid Composition on the One-Dimensional  
Consolidation Behaviour of Clay-Based Sealing Materials**

**NWMO TR-2008-06**

March 2008

**D. G. Priyanto<sup>1</sup>**  
**J. A. Blatz<sup>2</sup>**  
**G. A. Siemens<sup>3</sup>**  
**R. Offman<sup>2</sup>**  
**J. S. Boyle<sup>3</sup>**  
**D. A. Dixon<sup>1</sup>**

<sup>1</sup>Atomic Energy of Canada Limited;

<sup>2</sup>University of Manitoba;

<sup>3</sup>Royal Military College of Canada

---

Disclaimer:

This report does not necessarily reflect the views or position of the Nuclear Waste Management Organization, its directors, officers, employees and agents (the "NWMO") and unless otherwise specifically stated, is made available to the public by the NWMO for information only. The contents of this report reflect the views of the author(s) who are solely responsible for the text and its conclusions as well as the accuracy of any data used in its creation. The NWMO does not make any warranty, express or implied, or assume any legal liability or responsibility for the accuracy, completeness, or usefulness of any information disclosed, or represent that the use of any information would not infringe privately owned rights. Any reference to a specific commercial product, process or service by trade name, trademark, manufacturer, or otherwise, does not constitute or imply its endorsement, recommendation, or preference by NWMO.

---

## ABSTRACT

**Title:** The Effects of Initial Conditions and Liquid Composition on the One-Dimensional Consolidation Behaviour of Clay-Based Sealing Materials  
**Report No.:** NWMO TR-2008-06  
**Author(s):** D. G. Priyanto<sup>1</sup>, J. A. Blatz<sup>2</sup>, G. A. Siemens<sup>3</sup>, R. Offman<sup>2</sup>, J. S. Boyle<sup>3</sup>, and D. A. Dixon<sup>1</sup>  
**Company:** <sup>1</sup>Atomic Energy of Canada Limited;  
<sup>2</sup>University of Manitoba;  
<sup>3</sup>Royal Military College of Canada  
**Date:** March 2008

### Abstract

Groundwaters at proposed repository depths of 500 to 1000 m can contain significant quantities of soluble salts (Gascoyne et al. 1987; Mazurek 2004). These salts have the potential to affect the hydraulic-mechanical behaviour of clay-based sealing materials installed in a Deep Geologic Repository (DGR) of the type presented by Russell and Simmons (2003) and Maak and Simmons (2005). As a result of the influence of liquid salinity on material behaviour, one of the design decisions for the engineering of a sealing system is whether to prepare the sealing materials with fresh or saline liquid (Baumgartner et al. 2008) and to determine if this will affect the performance of the barrier materials.

The results of one-dimensional (1D) consolidation tests conducted in 2007 on three clay-based sealing materials including: Highly Compacted Bentonite (HCB); Dense Backfill (DBF); and Light Backfill (LBF) are presented and discussed. Testing was conducted at three different laboratories: Atomic Energy of Canada Limited (AECL)'s geotechnical laboratory at the Underground Research Laboratory (URL) (HCB); the University of Manitoba (U of M) (DBF); and the Royal Military College of Canada (RMC) (LBF).

The 1D consolidation tests are used to examine the effects of: boundary conditions and applied load during initial saturation; and high pore liquid salinities (up to 250 g/L CaCl<sub>2</sub>) used in specimen preparation and as a reservoir liquid. Parameters to define the mechanical behaviour (i.e., Compression Index (C<sub>c</sub>) and Swelling Index (C<sub>s</sub>)) of the HCB, DBF, and LBF have been determined from the results of these tests. The values of these parameters were found to decrease with an increase in concentration of calcium chloride (CaCl<sub>2</sub>) solution in pore liquid. The relationship of these parameters to the pore liquid composition is suggested for use in defining the mechanical behaviour of clay-based sealing materials in THM numerical modelling.



**TABLE OF CONTENTS**

	<b><u>Page</u></b>
<b>ABSTRACT .....</b>	<b>v</b>
<b>1. INTRODUCTION .....</b>	<b>1</b>
<b>1.1 BACKGROUND.....</b>	<b>2</b>
<b>1.2 OBJECTIVES .....</b>	<b>3</b>
<b>1.3 SCOPE OF THE WORK.....</b>	<b>3</b>
1.3.1 1D Consolidation of HCB, DBF, and LBF in 2006 .....	3
1.3.2 1D Consolidation of HCB, DBF, and LBF in 2007 .....	4
<b>2. MATERIALS .....</b>	<b>4</b>
<b>3. EQUIPMENT .....</b>	<b>4</b>
<b>4. TESTING PROGRAM (2006 TO 2007).....</b>	<b>5</b>
<b>4.1 ONE-DIMENSIONAL (1D) CONSOLIDATION TESTS IN 2006.....</b>	<b>5</b>
<b>4.2 ONE-DIMENSIONAL (1D) CONSOLIDATION TESTS IN 2007 .....</b>	<b>5</b>
<b>5. SUMMARY OF THE RESULTS .....</b>	<b>14</b>
<b>5.1 MECHANICAL CONSTITUTIVE MODEL PARAMETERS .....</b>	<b>14</b>
<b>5.2 HYDRAULIC CONSTITUTIVE MODELS.....</b>	<b>19</b>
<b>5.3 EFFECTS OF CONCENTRATION OF THE SOLUTION IN THE PORE LIQUID, MIXING LIQUID USED IN SPECIMEN PREPARATION AND BOUNDARY CONDITIONS DURING INITIAL SATURATION .....</b>	<b>20</b>
<b>6. PLANS FOR FUTURE WORKS .....</b>	<b>22</b>
<b>6.1 PLAN FOR 1D CONSOLIDATION TESTS IN 2008.....</b>	<b>22</b>
<b>6.2 PLAN FOR 1D CONSOLIDATION TESTS (2009 and beyond) .....</b>	<b>22</b>
<b>6.3 PROJECTED RESULTS AT THE END OF TESTING PROGRAM .....</b>	<b>23</b>
<b>7. CONCLUDING REMARKS.....</b>	<b>23</b>
<b>REFERENCES .....</b>	<b>25</b>
<b>APPENDIX A: HIGHLY COMPACTED BENTONITE .....</b>	<b>27</b>
<b>APPENDIX B: DENSE BACKFILL .....</b>	<b>95</b>
<b>APPENDIX C: LIGHT BACKFILL.....</b>	<b>103</b>

**LIST OF TABLES**

	<b><u>Page</u></b>
Table 1: Physical Characteristics of Engineering Barriers System Components (after Russell and Simmons 2003).....	2
Table 2: Test Matrix for 1D Consolidation Test of HCB Material (2006 to 2007).....	6
Table 3: Test Matrix Plan for 1D Consolidation Test of HCB Material (2008 and Beyond).....	7
Table 4: Test Matrix for 1D Consolidation Test of DBF Material (2006 to 2007).....	8
Table 5: Test Matrix Plan for 1D Consolidation Test of DBF Material (2008 and Beyond).....	9
Table 6: Test Matrix for 1D Consolidation Test of LBF Material (2006).....	10
Table 7: Test Matrix for 1D Consolidation Test of LBF Material (2007).....	12
Table 8: Test Matrix Plan for 1D Consolidation Test of LBF Material (2008 and Beyond).....	13
Table 9: Compression Indices ( $C_c$ ) and Swelling Indices ( $C_s$ ) of the Highly Compacted Bentonite (HCB) Specimens.....	17
Table 10: Compression Indices ( $C_c$ ) and Swelling Indices ( $C_s$ ) of the Dense Backfill (DBF) Specimens.....	17
Table 11: Compression Indices ( $C_c$ ) and Swelling Indices ( $C_s$ ) of the Light Backfill (LBF) Specimens.....	18

**LIST OF FIGURES**

	<b><u>Page</u></b>
Figure 1: In-room Placement Cross-sectional Geometry (CTECH 2002).....	1
Figure 2: Definition of Parameters $C_c$ and $C_s$ .....	14
Figure 3: Void Ratio ( $e$ ) versus Vertical Stress for HCB Specimens (11 Tests).....	15
Figure 4: Void Ratio ( $e$ ) versus Vertical Stress for LBF Specimens (8 Tests).....	15
Figure 5: Void Ratio ( $e$ ) versus Vertical Stress for LBF Specimens (20 Tests).....	16
Figure 6: Comparison of the Void Ratio ( $e$ ) versus Vertical Stress for the HCB, DBF, and LBF Specimens.....	16
Figure 7: Hydraulic Conductivity ( $K$ ) of the HCB Interpreted from the 1D Consolidation Test Results.....	19
Figure 8: Relationship of the Compression Index ( $C_c$ ) to the Concentration (in TDS) of Calcium Chloride ( $\text{CaCl}_2$ ) in the Pore Liquid.....	20
Figure 9: Relationship of the Compression Index ( $C_c$ ) to the Concentration (in TDS) of Calcium Chloride ( $\text{CaCl}_2$ ) in the Pore Liquid.....	21
Figure 10: The Effect of $\text{CaCl}_2$ Concentration in Pore Liquid on the Swelling Pressure of Highly Compacted Bentonite (HCB).....	21
Figure 11: Possible Relationship of Parameters $C_c$ and $C_s$ and the Concentration of Solution in the Pore Liquid.....	23

## 1. INTRODUCTION

Several sealing-system components are proposed for use in an emplacement-room sealing system (e.g., the CTECH-type in-room placement method shown in Figure 1) in a deep geological repository (DGR) for used nuclear fuel (Russell and Simmons 2003; Gierszewski et al. 2004; Maak and Simmons 2005). For the clay-based portions of the repository sealing system, five sealing-system components are being considered.

1. Highly Compacted Bentonite (HCB) – 100% bentonite clay either installed at high dry density by in-situ compaction or prefabricated as blocks.
2. Bentonite-Sand Buffer (BSB) – a mixture of bentonite clay and silica sand either installed at high dry density by in-situ compaction or prefabricated as blocks (shown in Figure 1 as “Compacted Buffer”).
3. Dense Backfill (DBF) – a mixture of lake clay, crushed host rock and bentonite clay, either installed at high dry density by in-situ compaction or prefabrication as blocks.
4. Light Backfill (LBF) – a mixture of bentonite clay and silica sand, likely installed in the form of dense pellets and installed at low-to-medium dry density.
5. Gapfill (GF) – either bentonite clay, possibly fabricated in the form of dense pellets, silica sand or some combination of the two, which are likely to be installed at low-to-medium average dry density.

Some suggested compositions and fundamental physical characteristics of these candidate sealing-system components are presented in Table 1.

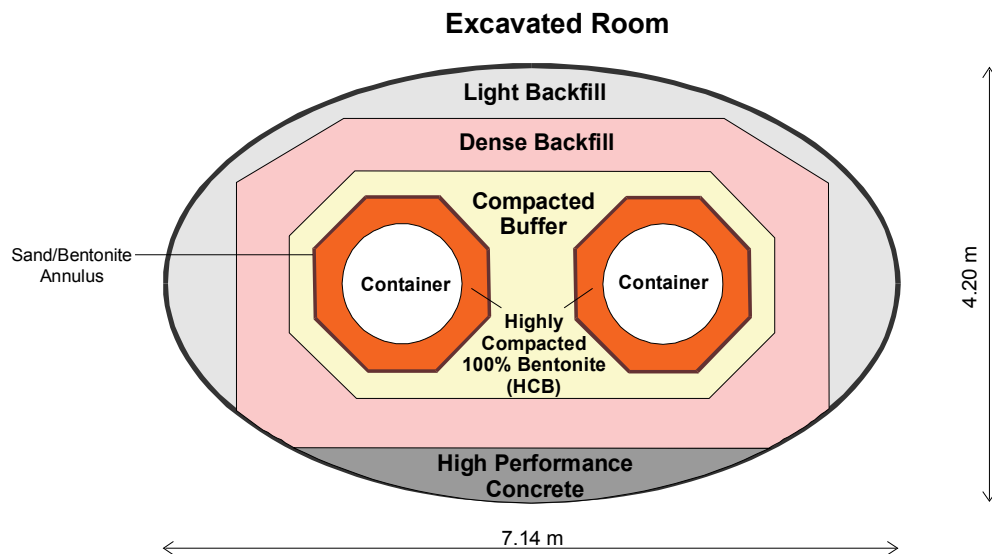


**Figure 1: In-room Placement Cross-sectional Geometry (CTECH 2002)**

**Table 1: Physical Characteristics of Engineering Barriers System Components**  
(after Russell and Simmons 2003)

Property	HCB	BSB	GF	DBF	LBF
Composition (dry mass %)	100% bentonite	50% bentonite 50% sand	100% bentonite	5% bentonite 25% glacial lake clay 70% crushed granite	50% bentonite 50% sand
Initial Gravimetric Water Content (%)	17	18.5	2	8.5	15
As-Placed Saturation (%)	65	80	6	80	33
Dry Density (Mg/m <sup>3</sup> )	1.61	1.69	1.40	2.12	1.24
EMDD (Mg/m <sup>3</sup> )*	1.50	1.15	1.25	0.8	0.66

\* assumes that all bentonites have a minimum 75% montmorillonite content

## 1.1 BACKGROUND

The chemistry of the pore liquid strongly affects the swelling potential and hydraulic conductivity of bentonite clay. Groundwaters at proposed repository depths of 500 to 1000 m can contain significant quantities of soluble salts and an increase in salinity is known to decrease the swelling potential and increase the hydraulic conductivity (Dixon 2000) of barrier materials containing a swelling clay mineral component.

Gascoyne et al. (1987) and Mazurek (2004) have collated data from the crystalline rock of the Canadian Shield and the sedimentary rock in southern Ontario, respectively, and very high concentrations of soluble salts can exist. Salt concentrations also typically vary with depth, tending to be low near the surface and increasing with depth. Salt concentrations also vary considerably throughout the Canadian Shield. Salinities, in terms of Total Dissolved Solids (TDS) at proposed repository depths, can vary from 8 to >100 g/L in the Canadian Shield to greater than 200 g/L in Ordovician-age sediments. Salt speciation is often Na-Ca-Cl at shallow depth trending to Ca-Na-Cl at greater depth.

The observation of the role that the chemistry of the pore liquid plays in the behaviour of bentonite clay has been largely limited to NaCl solutions using constant-volume load cells (Dixon 2000), which does not provide comparative data on Ca-rich groundwaters. The presence of CaCl<sub>2</sub> in groundwater makes testing of clay-based sealing materials with CaCl<sub>2</sub> solutions of importance in confirming their behaviour. One-dimensional (1D) consolidation tests have recently been completed at salinities up to 100 g/L CaCl<sub>2</sub> in order to start the process of increasing the behavioural database for sealing materials (Baumgartner et al. 2008). Baumgartner et al. (2008) observed that specimen preparation affected the behaviour of the clay-based sealing materials. One of the design decisions for the engineering of a sealing system is the choice for preparing the sealing materials with either fresh or saline water.

With identification of high salinity conditions (TDS > 200 g/L) in the Canadian Shield (Gascoyne et al. 1987, Mazurek 2004) the range of liquid concentrations examined by Baumgartner et al.

(2008) needs to be extended. This report investigates the effect of salinities up to 250 g/L  $\text{CaCl}_2$  on the behaviour of HCB, DBF, and LBF using 1D consolidation tests. In response to potential effects of different methods of specimen preparation (mixing with saline solution (i.e., 250 g/L  $\text{CaCl}_2$  solution) and mixing with Distilled Water (DW)), sample preparation with both liquids is examined.

In related studies, the results of the triaxial testing on unsaturated Bentonite-Sand-Buffer material have also shown that boundary conditions affect both the hydraulic (H) and mechanical (M) behaviour (Siemens 2006). In those tests, two types of boundary conditions (i.e., constant volume and constant pressure) were applied during the initial saturation to examine the effect of boundary conditions applied at the early stage of the tests. In the tests described in the current study, both constant pressure and constant volume conditions were also examined.

The primary goal of the stress-strain testing described in this report is to provide physically-measured parameter values. The values are used in Thermal-Hydraulic-Mechanical (THM) models to simulate the behaviour of clay-based sealing materials in a repository. THM numerical modelling requires the parameters of thermal (T), hydraulic (H) and mechanical (M) constitutive models. The results of 1D consolidation tests are used to interpret the parameters of mechanical (M) and hydraulic (H) constitutive models. Comparison of the results of 1D consolidation tests with various pore liquid concentrations provides a measure of to what degree the parameters of these constitutive models are affected by the pore liquid salinity.

## **1.2 OBJECTIVES**

The objectives of the 1D consolidation tests done in 2007 are to:

1. examine the effect of higher pore liquid salinity (up to 250 g/L  $\text{CaCl}_2$ );
2. examine the effects of different mixing liquid used in specimen preparation and boundary conditions during initial saturation; and
3. define mechanical and hydraulics parameters interpreted from the 1D consolidation tests that include the effect of liquid composition in the pore liquid of clay-based sealing materials for use in THM modelling.

## **1.3 SCOPE OF THE WORK**

### **1.3.1 1D Consolidation of HCB, DBF, and LBF in 2006**

The work done during 2006 consisted of a series of laboratory 1D consolidation tests on three clay-based sealing materials (i.e., HCB, DBF, and LBF). Testing was divided between Atomic Energy of Canada Limited (AECL)'s geotechnical laboratory at the Underground Research Laboratory (URL), the Department of Civil Engineering at the University of Manitoba (U of M), and Department of Civil Engineering at Lakehead University (LHU). Each group was assigned a material-type to test. AECL tested the HCB, U of M tested the DBF, and LHU tested the LBF. The 2006 work investigated the effect of pore liquid concentration on the mechanical behaviour of HCB, DBF, and LBF using 1D consolidation tests (i.e., up to 100 g/L  $\text{CaCl}_2$  for DBF and LBF specimens, and 75 g/L  $\text{CaCl}_2$  for HCB specimens).

### 1.3.2 1D Consolidation of HCB, DBF, and LBF in 2007

During 2007 AECL continued testing of HCB specimens, and the U of M continued testing of DBF specimens. Due to resourcing issues at LHU in 2007, testing of LBF specimens was shifted to the Department of Civil Engineering at the Royal Military College of Canada (RMC) under the supervision of Dr. Siemens, who has worked previously in testing of swelling clay materials at the U of M. This report presents the results of 1D consolidation tests on HCB, DBF, and LBF conducted in 2007.

## 2. MATERIALS

The following three sealing-system components are tested in the series of consolidation tests.

- HCB, composed of 100% (by weight) Wyoming MX80 bentonite (montmorillonite content ~75%).
- LBF, composed of 50% (by weight) Avonlea (Saskatchewan) bentonite (montmorillonite content ~80%) and 50% (by weight) silica sand.
- DBF, composed of 75% (by weight) crushed granite, 18.75% crushed illite clay (Sealbond) and 6.25% (by weight) Avonlea bentonite (montmorillonite content ~80%). This DBF composition differs from that provided in Table 1 due to the desire to use a material consistent with that used in previous work on DBF.

## 3. EQUIPMENT

Three different sizes of cells are required since each material has very different swelling and mechanical properties. Conventional 50-mm-diameter consolidation rings that allow 19-thick specimens to be tested are used for the LBF. Larger cells, 101-mm-in-diameter and allowing a 101-mm-thick specimen, are used to test the DBF to accommodate the large size of the aggregate (i.e., up to 35-mm granite chips). Small-diameter oedometer cells (i.e., 28.1 mm diameter) are used to test the HCB, which permit application of high stress (i.e., maximum 16 MPa). All the cells are fabricated from non-corrosive material. No corrosion effects were observed in any of the tests conducted in 2007.

Conventional dead-weight-type oedometers are used to test the DBF and LBF and data are collected by manually monitoring the deformation of these two materials. The very high swelling capacity and associated high swelling pressure in HCB require a different type of testing system to be used for that material. In testing the HCB a small-diameter, thick-walled cell is used in a compression frame that has hydraulic rams installed. Each hydraulic ram is actuated by a high-pressure nitrogen-gas cylinder acting on a gas-over-oil accumulator. An LVDT is used to measure the displacement of the specimen and connected to a data logger. A second frame using a servo-hydraulic testing system manufactured by the MTS® (Materials Testing Services) added in 2007 to test the HCB. This additional equipment enables application of different boundary conditions in the tests (i.e., constant volume or constant pressure).

#### **4. TESTING PROGRAM (2006 TO 2007)**

##### **4.1 ONE-DIMENSIONAL (1D) CONSOLIDATION TESTS IN 2006**

Tables 2, 4, and 6 show the test matrices for the 1D consolidation tests conducted in 2006 on HCB, DBF, and LBF specimens, respectively. Baumgartner et al. (2008) summarized the results of these tests. The objectives of the testing program were: to determine H-M parameters from 1D consolidation test results; and to investigate the effect of pore liquid salinity (up to 75 g/L CaCl<sub>2</sub> for HCB specimens and 100 g/L CaCl<sub>2</sub> for LBF and DBF specimens).

##### **4.2 ONE-DIMENSIONAL (1D) CONSOLIDATION TESTS IN 2007**

Tables 2, 4, and 7 show the test matrices for the 1D consolidation tests conducted in 2007 on the HCB, DBF, and LBF specimens, respectively. The results of these tests are discussed in this report in Appendices A, B, and C for HCB, DBF, and LBF specimens respectively.

Four (4) tests on HCB were planned at AECL, four (4) tests on the DBF were planned at the U of M, and six (6) tests on LBF were planned at the RMC. AECL provided the material (i.e., DBF and LBF) and the specification of initial conditions, including target initial dry density, liquid used in specimen preparation, and liquid added to the tests.

Considering the availability of the equipment and additional work required to prepare additional specimens, HCB11 was added to provide more data defining the relationship of compression index ( $C_c$ ) and swelling index ( $C_s$ ) versus concentration of CaCl<sub>2</sub> in the pore liquid. This relationship can be used to include the effect of concentration of CaCl<sub>2</sub> in the pore liquid to the mechanical behaviour of sealing material.

The testing programs in the year of 2007 were designed to address the objectives presented in Section 1.2 and to compare these results to the results of 1D consolidation tests completed in 2006 (Baumgartner et al. 2008).

**Table 2: Test Matrix for 1D Consolidation Test of HCB Material (2006 to 2007)**

Test No.	Sample No.	Mixing Liquid	Reservoir Liquid	Dry Density (Mg/m <sup>3</sup> )	Degree of Saturation (%)	Gravimetric Water Content (%)	Boundary Condition during Initial Water Uptake	Target Swelling on Initial Water Uptake (%)	Loading Sequence	Status	Testing Location	Reference
<b>2006</b>												
<b>Effect of pore fluid concentration on mechanical behaviour of HCB (up to 75 g/L CaCl<sub>2</sub>)</b>												
1	HCB1	DW	DW	1.65	90	21.5	CP	100% at 1 MPa Attempt rigid confinement with no LVDT displacement beginning at 1 MPa	Load to 1, 2, 4, 8, & 16 MPa; Unload to 8, 4, & 2 MPa	Completed	AECL	Baumgartner et al. (2008)
2	HCB2	DW	DW	1.65	90	21.5	CP		Load to 1 & 16 MPa; Unload to 8, 4, 2, & 1 MPa	Completed	AECL	Baumgartner et al. (2008)
3	HCB3	75 g/L CaCl <sub>2</sub>	75 g/L CaCl <sub>2</sub>	1.65	90	21.5	CP	100% at 1 MPa	Load to 1, 2, 4, & 8 MPa; Unload to 4, 2, & 1 MPa; Load to 4, 8, & 16 MPa	Completed	AECL	Baumgartner et al. (2008)
4	HCB4	75 g/L CaCl <sub>2</sub>	75 g/L CaCl <sub>2</sub>	1.65	90	21.5	CP	100% at 8 MPa	Load to 8 MPa; Unload to 4, 2, & 1 MPa; Load to 1, 2, 4, 8, & 16 MPa	Completed	AECL	Baumgartner et al. (2008)
5	HCB5	DW	DW	1.40	91	31	CP	100% at 1 MPa	Load to 1, 2, 4, 8, & 16 MPa; Unload to 8, 4, 2, & 1 MPa; Load to 2, 4, 8, & 16 MPa	Completed	AECL	Baumgartner et al. (2008)
6	HCB6	75 g/L CaCl <sub>2</sub>	75 g/L CaCl <sub>2</sub>	1.40	91	31	CP	100% at 1 MPa	Load to 1, 2, 4, 8, & 16 MPa; Unload to 8, 4, 2, & 1 MPa; Load to 2, 4, 8, & 16 MPa	Completed	AECL	Baumgartner et al. (2008)
<b>2007</b>												
<b>Effect of pore fluid concentration, mixing liquid, initial boundary condition on mechanical behaviour of HCB (higher concentration: 250 g/L CaCl<sub>2</sub>)</b>												
7	HCB7	DW	250 g/L CaCl <sub>2</sub>	1.65	95	23	CP	100% at 1 MPa	Load to 1, 2, 4, 8, & 16 MPa; Unload to 8, 4, 2, & 1 MPa.	Completed	AECL	Priyanto et al. (2008)
8	HCB8	250 g/L CaCl <sub>2</sub>	250 g/L CaCl <sub>2</sub>	1.65	95	20	CP	100% at 1 MPa	Load to 1, 2, 4, 8, & 16 MPa; Unload to 8, 4, 2, & 1 MPa.	Completed	AECL	Priyanto et al. (2008)
9	HCB9	DW	DW	1.65	95	23	CV	0	Load to 1, 2, 4, 8, & 16 MPa; Unload to 8, 4, 2, & 1 MPa.	Completed	AECL	Priyanto et al. (2008)
10	HCB10	250 g/L CaCl <sub>2</sub>	250 g/L CaCl <sub>2</sub>	1.65	95	20	CV	0	Load to 1, 2, 4, 8, & 16 MPa; Unload to 8, 4, 2, & 1 MPa.	Completed	AECL	Priyanto et al. (2008)
11	HCB11*	DW	150 g/L CaCl <sub>2</sub>	1.65	95	23	CP	100% at 1 MPa	Load to 1, 2, 4, 8, & 16 MPa; Unload to 8, 4, 2, & 1 MPa.	Completed	AECL	Priyanto et al. (2008)

Note: \*HCB11 was added to the original test matrix in 2007  
 CP = Constant Pressure; CV = Constant Volume; DW = Distilled Water

**Table 3: Test Matrix Plan for 1D Consolidation Test of HCB Material (2008 and Beyond)**

Test No.	Sample No.	Mixing Liquid	Reservoir Liquid	Dry Density (Mg/m <sup>3</sup> )	Degree of Saturation (%)	Gravimetric Water Content (%)	Boundary Condition during Initial Water Uptake	Target Swelling on Initial Water Uptake (%)	Loading Sequence	Status	Testing Location	Reference
<b>2008</b>												
<b>Effect of different fluid type (250 g/L NaCl)</b>												
12	???	DW	250 g/L NaCl	1.65	95	23	CP	100% at 1 MPa	Load to 1, 2, 4, 8, & 16 MPa; Unload to 8, 4, 2, & 1 MPa.	Planned	AECL	NA
13	???	DW	250 g/L NaCl	1.65	95	23	CV	0	Load to 1, 2, 4, 8, & 16 MPa; Unload to 8, 4, 2, & 1 MPa.	Planned	AECL	NA
14	???	250 g/L NaCl	250 g/L NaCl	1.65	95	NA	CP	100% at 1 MPa	Load to 1, 2, 4, 8, & 16 MPa; Unload to 8, 4, 2, & 1 MPa.	Planned	AECL	NA
15	???	250 g/L NaCl	250 g/L NaCl	1.65	95	NA	CV	0	Load to 1, 2, 4, 8, & 16 MPa; Unload to 8, 4, 2, & 1 MPa.	Planned	AECL	NA
<b>2009 - ....</b>												
<b>Alternative 1: More data to define the effect of NaCl concentration (Cc &amp; Cs versus NaCl concentration)</b>												
16	???	DW	150 g/L NaCl	1.65	95	23	CP	100% at 1 MPa	Load to 1, 2, 4, 8, & 16 MPa; Unload to 8, 4, 2, & 1 MPa.	Planned	AECL	NA
17	???	DW	150 g/L NaCl	1.65	95	23	CV	0	Load to 1, 2, 4, 8, & 16 MPa; Unload to 8, 4, 2, & 1 MPa.	Planned	AECL	NA
18	???	150 g/L NaCl	150 g/L NaCl	1.65	95	NA	CP	100% at 1 MPa	Load to 1, 2, 4, 8, & 16 MPa; Unload to 8, 4, 2, & 1 MPa.	Planned	AECL	NA
19	???	150 g/L NaCl	150 g/L NaCl	1.65	95	NA	CV	0	Load to 1, 2, 4, 8, & 16 MPa; Unload to 8, 4, 2, & 1 MPa.	Planned	AECL	NA
<b>Alternative 2: Examining the effect of artificial ground water (NaCl+CaCl<sub>2</sub>)</b>												
20	???	DW	Artificial GW	1.65	95	23	CP	100% at 1 MPa	Load to 1, 2, 4, 8, & 16 MPa; Unload to 8, 4, 2, & 1 MPa.	Planned	AECL	NA
21	???	DW	Artificial GW	1.65	95	23	CV	0	Load to 1, 2, 4, 8, & 16 MPa; Unload to 8, 4, 2, & 1 MPa.	Planned	AECL	NA
22	???	Artificial GW	Artificial GW	1.65	95	NA	CP	100% at 1 MPa	Load to 1, 2, 4, 8, & 16 MPa; Unload to 8, 4, 2, & 1 MPa.	Planned	AECL	NA
23	???	Artificial GW	Artificial GW	1.65	95	NA	CV	0	Load to 1, 2, 4, 8, & 16 MPa; Unload to 8, 4, 2, & 1 MPa.	Planned	AECL	NA

Note: \*HCB11 was added to the original test matrix in 2007  
 CP = Constant Pressure; CV = Constant Volume; DW = Distilled Water  
 Artificial GW = mixture of NaCl and CaCl<sub>2</sub> solution.

**Table 4: Test Matrix for 1D Consolidation Test of DBF Material (2006 to 2007)**

Test No.	Sample No.	Mixing Liquid	Reservoir Liquid	Bulk Density (Mg/m <sup>3</sup> )	Degree of Saturation (%)	Gravimetric Water Content (%)	Boundary Condition during Initial Water Uptake	Target Swelling on Initial Water Uptake (%)	Loading Sequence	Status	Testing Location	Reference
<b>2006</b>												
<b>Effect of pore fluid concentration on mechanical behaviour of DBF (up to 100 g/L CaCl<sub>2</sub>)</b>												
1	DBF1	DW	DW	2.3	NA	10.6	CP	20% at low load*	Load to 245, 490, 975, 1950, 3900 kPa; Unload to 975, 245 kPa	Completed	U of M	Baumgartner et al. (2008)
2	DBF2	DW	DW	2.3	NA	10.6	CV	Rigidly confined**	Load to 245, 490, 975, 1950, 3900 kPa; Unload to 975, 245 kPa	Completed	U of M	Baumgartner et al. (2008)
3	DBF3	100 g/L CaCl <sub>2</sub>	100 g/L CaCl <sub>2</sub>	2.3	NA	10.6	CP	20% at low load*	Load to 245, 490, 975, 1950, 3900 kPa; Unload to 975, 245 kPa	Completed	U of M	Baumgartner et al. (2008)
4	DBF4	100 g/L CaCl <sub>2</sub>	100 g/L CaCl <sub>2</sub>	2.3	NA	10.6	CV	Rigidly confined**	Load to 245, 490, 975, 1950, 3900 kPa; Unload to 975, 245 kPa	Completed	U of M	Baumgartner et al. (2008)
5	DBF5	DW	DW	2.3	NA	10.6	NA	Immediately loaded to 1 MPa	Load to 1, 2, and 4 MPa; Unload to 2, 1, and 0.5 MPa; Load to 1, 2, and 4 MPa	Completed	U of M	Baumgartner et al. (2008)
6	DBF6	100 g/L CaCl <sub>2</sub>	100 g/L CaCl <sub>2</sub>	2.3	NA	10.6	CP	Immediately loaded to 1 MPa	Load to 1, 2, and 4 MPa; Unload to 2, 1, and 0.5 MPa; Load to 1, 2, and 4 MPa	Completed	U of M	Baumgartner et al. (2008)
<b>2007</b>												
<b>Effect of pore fluid concentration, mixing liquid, initial boundary condition on mechanical behaviour of DBF (higher concentration: 250 g/L CaCl<sub>2</sub>)</b>												
7	DBF1 (2007)	DW	250 g/L CaCl <sub>2</sub>	2.3	NA	10.6	CP	100% at 1 MPa	Load to 1, 2, 4 MPa; Unload to 2, 1, and 0.5 MPa	In progress	U of M	Priyanto et al. (2008)
8	DBF2 (2007)	250 g/L CaCl <sub>2</sub>	250 g/L CaCl <sub>2</sub>	2.3	NA	10.6	CP	100% at 1 MPa	Load to 1, 2, 4 MPa; Unload to 2, 1, and 0.5 MPa	In progress	U of M	Priyanto et al. (2008)
9	DBF3 (2007)	DW	DW	2.3	NA	10.6	CV	0	Load to 1, 2, 4 MPa; Unload to 2, 1, and 0.5 MPa	In progress	U of M	Priyanto et al. (2008)
10	DBF4 (2007)	250 g/L CaCl <sub>2</sub>	250 g/L CaCl <sub>2</sub>	2.3	NA	10.6	CV	0	Load to 1, 2, 4 MPa; Unload to 2, 1, and 0.5 MPa	In progress	U of M	Priyanto et al. (2008)

**Note: CP = Constant Pressure; CV = Constant Volume; DW = Distilled Water**

**Table 5: Test Matrix Plan for 1D Consolidation Test of DBF Material (2008 and Beyond)**

Test No.	Sample No.	Mixing Liquid	Reservoir Liquid	Bulk Density (Mg/m <sup>3</sup> )	Degree of Saturation (%)	Gravimetric Water Content (%)	Boundary Condition during Initial Water Uptake	Target Swelling on Initial Water Uptake (%)	Loading Sequence	Status	Testing Location	Reference
<b>2008</b>												
<b>Effect of different fluid type (250 g/L NaCl)</b>												
11	???	DW	250 g/L NaCl	2.3	NA	10.6	CP	100% at 1 MPa	Load to 1, 2, 4 MPa; Unload to 2, 1, and 0.5 MPa?	Planned	U of M	NA
12	???	DW	250 g/L NaCl	2.3	NA	10.6	CV	0	Load to 1, 2, 4 MPa; Unload to 2, 1, and 0.5 MPa?	Planned	U of M	NA
13	???	NaCl	250 g/L NaCl	2.3	NA	10.6	CP	100% at 1 MPa	Load to 1, 2, 4 MPa; Unload to 2, 1, and 0.5 MPa?	Planned	U of M	NA
14	???	NaCl	250 g/L NaCl	2.3	NA	10.6	CV	0	Load to 1, 2, 4 MPa; Unload to 2, 1, and 0.5 MPa?	Planned	U of M	NA
<b>Alternative 1: More data to define the effect of NaCl concentration (Cc &amp; Cs versus NaCl concentration)</b>												
15	???	DW	150 g/L NaCl	1.65	95	23	CP	100% at 1 MPa	Load to 1, 2, 4 MPa; Unload to 2, 1, and 0.5 MPa?	Planned	U of M	NA
16	???	DW	150 g/L NaCl	1.65	95	23	CV	0	Load to 1, 2, 4 MPa; Unload to 2, 1, and 0.5 MPa?	Planned	U of M	NA
17	???	NaCl	150 g/L NaCl	1.65	95	NA	CP	100% at 1 MPa	Load to 1, 2, 4 MPa; Unload to 2, 1, and 0.5 MPa?	Planned	U of M	NA
18	???	NaCl	150 g/L NaCl	1.65	95	NA	CV	0	Load to 1, 2, 4 MPa; Unload to 2, 1, and 0.5 MPa?	Planned	U of M	NA
<b>Alternative 2: Examining the effect of artificial ground water (NaCl+CaCl<sub>2</sub>)</b>												
19	???	DW	Artificial GW	1.65	95	23	CP	100% at 1 MPa	Load to 1, 2, 4 MPa; Unload to 2, 1, and 0.5 MPa?	Planned	U of M	NA
20	???	DW	Artificial GW	1.65	95	23	CV	0	Load to 1, 2, 4 MPa; Unload to 2, 1, and 0.5 MPa?	Planned	U of M	NA
21	???	Artificial GW	Artificial GW	1.65	95	NA	CP	100% at 1 MPa	Load to 1, 2, 4 MPa; Unload to 2, 1, and 0.5 MPa?	Planned	U of M	NA
22	???	Artificial GW	Artificial GW	1.65	95	NA	CV	0	Load to 1, 2, 4 MPa; Unload to 2, 1, and 0.5 MPa?	Planned	U of M	NA

Note: CP = Constant Pressure; CV = Constant Volume; DW = Distilled Water  
Artificial GW = mixture of NaCl and CaCl<sub>2</sub> solution.

**Table 6: Test Matrix for 1D Consolidation Test of LBF Material (2006)**

Test No.	Sample No.	Mixing Liquid	Reservoir Liquid	Dry Density (Mg/m <sup>3</sup> )	Degree of Saturation (%)	Gravimetric Water Content (%)	Boundary Condition during Initial Water Uptake	Swelling on Initial Water Uptake (%)	Loading Sequence	Status	Testing Location	Reference
<b>2006</b>												
<b>Effect of pore fluid concentration on mechanical behaviour of LBF (up to 100 g/L CaCl<sub>2</sub>)</b>												
1	HB3	As supplied by AECL*	DW	1.24	NA	NA	NA	19.50%	After initial swelling; Load to , 111, 221, 332, 667, 1326 kPa; Unload to 668, 336, 166, 55 kPa	Completed	LHU	Baumgartner et al. (2008)
	HB6	As supplied by AECL*	DW	1.24	NA	NA	NA	20.80%	After initial swelling; Load to 166, 332, 664, 1326, 2652, 3986 kPa; Unload to 1326, 668, 336, 167, 57 kPa	Completed	LHU	Baumgartner et al. (2008)
	HB8	As supplied by AECL*	DW	1.24	NA	NA	NA	22.40%	After initial swelling; Load to 166, 332, 664, 1326, 2652 kPa; Unload to 1326, 668 kPa	Completed	LHU	Baumgartner et al. (2008)
2a	HB2	As supplied by AECL*	DW	1.24	NA	NA	NA	Rigidly confined	Load to 55, 81, 161, 332, 663, 1326, 2651 kPa	Completed	LHU	Baumgartner et al. (2008)
	HB4	As supplied by AECL*	DW	1.24	NA	NA	NA	Rigidly confined	Load to 55, 80, 166, 332, 665, 1328, 2654 kPa; Unload to 1328, 666 kPa	Completed	LHU	Baumgartner et al. (2008)
2b	HB7	As supplied by AECL*	DW	1.3	NA	NA	NA	Rigidly confined	Unload (let swell to 21.2%); Load to 167, 332, 664, 1326, 2652, 3986 kPa; Unload to 2652, 1326, and 664 kPa	Completed	LHU	Baumgartner et al. (2008)
	HB9	As supplied by AECL*	DW	1.3	NA	NA	NA	Rigidly confined	Unload (let swell to 21.2%); Load to 165, 331, 663, 1336, 2659 kPa; Unload to 1336, 663, 331, 165, and 55 kPa	Completed	LHU	Baumgartner et al. (2008)

Note: CP = Constant Pressure; CV = Constant Volume; DW = Distilled Water

**Table 6: Test Matrix for 1D Consolidation Test of LBF Material (2006) (concluded)**

Test No.	Sample No.	Mixing Liquid	Reservoir Liquid	Dry Density (Mg/m <sup>3</sup> )	Degree of Saturation (%)	Gravimetric Water Content (%)	Boundary Condition during Initial Water Uptake	Swelling on Initial Water Uptake (%)	Loading Sequence	Status	Testing Location	Reference
<b>2006</b>												
<b>Effect of pore fluid concentration on mechanical behaviour of LBF (up to 100 g/L CaCl<sub>2</sub>)</b>												
3	HB11	As supplied by AECL*	100 g/L CaCl <sub>2</sub>	1.3	NA	NA	NA	10.40%	After initial swelling; Load to 25, 55, 166, 332, 664, 1326, 2661, 3990 kPa; Unload to 2661, 1326, 664, 166, 55 kPa	Completed	LHU	Baumgartner et al. (2008)
	HB12	As supplied by AECL*	100 g/L CaCl <sub>2</sub>	1.3	NA	NA	NA	7.50%	After initial swelling; Load to 25, 55, 166, 336, 676, 1340, 2675 kPa; Unload to 1340, 676, 167, 57 kPa	Completed	LHU	Baumgartner et al. (2008)
	HB19	As supplied by AECL*	100 g/L CaCl <sub>2</sub>	1.3	NA	NA	NA	6.30%	After initial swelling; Load to 1, 25, 55, 166, 332, 663, 1326, 2660 kPa; Unload to 1326, 668, 166, 55 kPa	Completed	LHU	Baumgartner et al. (2008)
4	HB14	As supplied by AECL*	100 g/L CaCl <sub>2</sub>	1.3	NA	NA	NA	Rigidly confined	Unload, let swell to 3.6%, Load to 57, 167, 336, 668, 1343, 2673, 4000 kPa; Unload to 2673, 1343, 668, 336, 167, 57 kPa	Completed	LHU	Baumgartner et al. (2008)
5	HB13	100 g/L CaCl <sub>2</sub>	100 g/L CaCl <sub>2</sub>	1.3	NA	NA	NA	6.40%	After initial swelling, Load to 25, 55, 166, 332, 663, 1327, 2650 kPa; Unload to 1327, 663, 332, 166, and 55 kPa	Completed	LHU	Baumgartner et al. (2008)
	HB15	100 g/L CaCl <sub>2</sub>	100 g/L CaCl <sub>2</sub>	1.3	NA	NA	NA	7.10%	After initial swelling, Load to 25, 55, 166, 332, 664, 1327, 2656, 3985 kPa; Unload to 1327, 336, 166, 55 kPa	Completed	LHU	Baumgartner et al. (2008)
6	HB16	As supplied by AECL*	200 g/L CaCl <sub>2</sub>	1.3	NA	NA	NA	6.10%	After initial swelling, Load to 25, 55, 166, 332, 663, 1327, 2650 kPa; Unload to 1327, 663, 332, 166, 55 kPa	Completed	LHU	Baumgartner et al. (2008)

Note: CP = Constant Pressure; CV = Constant Volume; DW = Distilled Water

**Table 7: Test Matrix for 1D Consolidation Test of LBF Material (2007)**

Test No.	Sample No.	Mixing Liquid	Reservoir Liquid	Dry Density (Mg/m <sup>3</sup> )	Degree of Saturation (%)	Gravimetric Water Content (%)	Boundary Condition during Initial Water Uptake	Swelling on Initial Water Uptake (%)	Loading Sequence	Status	Testing Location	Reference
<b>2007</b>												
<b>Effect of pore fluid concentration, mixing liquid, initial boundary condition on mechanical behaviour of LBF (higher concentration: 250 g/L CaCl<sub>2</sub>)</b>												
7	LBF_1	250 g/L CaCl <sub>2</sub>	250 g/L CaCl <sub>2</sub>	1.3	NA	19.1	CP	8.3% at 1 MPa	After initial swelling, Load to 55, 110, 220, 439, 878, 1702 kPa; Unload to 878, 439, 220, 110, 55 kPa.	Completed	RMC	Priyanto et al. (2008)
8	LBF_2	DW	250 g/L CaCl <sub>2</sub>	1.3	NA	19.1	CP	4.2% at 1 MPa	After initial swelling, Load to 55, 110, 220, 441, 882, 1709 kPa; Unload to 882, 220, 110, and 55 kPa.	Completed	RMC	Priyanto et al. (2008)
9	LBF_3	250 g/L CaCl <sub>2</sub>	250 g/L CaCl <sub>2</sub>	1.3	NA	19.1	CV	Rigidly confined	After initial swelling, Load to 55, 110, 220, 441, 879, 1703 kPa; Unload to 879, 440, 220, 110 and 55 kPa.	Completed	RMC	Priyanto et al. (2008)
10	LBF_4	DW	250 g/L CaCl <sub>2</sub>	1.3	NA	19.1	CV	Rigidly confined	After initial swelling, Load to 55, 110, 220, 441, 882, 1709 kPa; Unload to 882, 441, 220, 110 and 55 kPa.	Completed	RMC	Priyanto et al. (2008)
11	LBF_5B	100 g/L CaCl <sub>2</sub>	100 g/L CaCl <sub>2</sub>	1.3	NA	19.1	CP	7.7% at 1 MPa	After initial swelling, Load to 55, 110, 220, 439, 878, 1701 kPa; Unload to 878, 439, 220, 110 and 55 kPa.	Completed	RMC	Priyanto et al. (2008)
12	LBF_6	DW	100 g/L CaCl <sub>2</sub>	1.3	NA	19.1	CV	Rigidly confined	After initial swelling, Load to 55, 110, 220, 441, 883, 1711 kPa; Unload to 883, 441, 220, 110 and 55 kPa.	Completed	RMC	Priyanto et al. (2008)

**Note: CP = Constant Pressure; CV = Constant Volume; DW = Distilled Water**

**Table 8: Test Matrix Plan for 1D Consolidation Test of LBF Material (2008 and Beyond)**

Test No.	Sample No.	Mixing Liquid	Reservoir Liquid	Dry Density (Mg/m <sup>3</sup> )	Degree of Saturation (%)	Gravimetric Water Content (%)	Boundary Condition during Initial Water Uptake	Swelling on Initial Water Uptake (%)	Loading Sequence	Status	Testing Location	Reference
<b>2008</b>												
<b>Effect of different fluid type (250 g/L NaCl)</b>												
13	???	DW	250 g/L NaCl	1.3	NA	19.1	CP	NA?	Load to 1700 kPa; Unload to 55 kPa?	Planned	RMC	NA
14	???	DW	250 g/L NaCl	1.3	NA	19.1	CV	NA?	Load to 1700 kPa; Unload to 55 kPa?	Planned	RMC	NA
15	???	250 g/L NaCl	250 g/L NaCl	1.3	NA	19.1	CP	NA?	Load to 1700 kPa; Unload to 55 kPa?	Planned	RMC	NA
16	???	250 g/L NaCl	250 g/L NaCl	1.3	NA	19.1	CV	NA?	Load to 1700 kPa; Unload to 55 kPa?	Planned	RMC	NA
<b>2009 - ....</b>												
<b>Alternative 1: More data to define the effect of NaCl concentration (Cc &amp; Cs versus NaCl concentration)</b>												
17	???	DW	150 g/L NaCl	1.3	NA	19.1	CP	100% at 1 MPa	Load to 1, 2, 4, 8, & 16 MPa; Unload to 8, 4, 2, & 1 MPa?	Planned	AECL	NA
18	???	DW	150 g/L NaCl	1.3	NA	19.1	CV	0	Load to 1, 2, 4, 8, & 16 MPa; Unload to 8, 4, 2, & 1 MPa?	Planned	AECL	NA
19	???	150 g/L NaCl	150 g/L NaCl	1.3	NA	19.1	CP	100% at 1 MPa	Load to 1, 2, 4, 8, & 16 MPa; Unload to 8, 4, 2, & 1 MPa?	Planned	AECL	NA
20	???	150 g/L NaCl	150 g/L NaCl	1.3	NA	19.1	CV	0	Load to 1, 2, 4, 8, & 16 MPa; Unload to 8, 4, 2, & 1 MPa?	Planned	AECL	NA
<b>Alternative 2: Examining the effect of artificial ground water (NaCl+CaCl<sub>2</sub>)</b>												
21	???	DW	Artificial GW	1.3	NA	19.1	CP	100% at 1 MPa	Load to 1, 2, 4, 8, & 16 MPa; Unload to 8, 4, 2, & 1 MPa?	Planned	AECL	NA
22	???	DW	Artificial GW	1.3	NA	19.1	CV	0	Load to 1, 2, 4, 8, & 16 MPa; Unload to 8, 4, 2, & 1 MPa?	Planned	AECL	NA
23	???	Artificial GW	Artificial GW	1.3	NA	19.1	CP	100% at 1 MPa	Load to 1, 2, 4, 8, & 16 MPa; Unload to 8, 4, 2, & 1 MPa?	Planned	AECL	NA
24	???	Artificial GW	Artificial GW	1.3	NA	19.1	CV	0	Load to 1, 2, 4, 8, & 16 MPa; Unload to 8, 4, 2, & 1 MPa?	Planned	AECL	NA

Note: CP = Constant Pressure; CV = Constant Volume; DW = Distilled Water  
 Artificial GW = mixture of NaCl and CaCl<sub>2</sub> solution.

## 5. SUMMARY OF THE RESULTS

### 5.1 MECHANICAL CONSTITUTIVE MODEL PARAMETERS

Mechanical constitutive model parameters for the HCB, DBF, and LBF are interpreted from the results of 1D consolidation tests. Log-linear relationships are used to interpret the mechanical behaviour of the soils. The parameters  $C_c$  and  $C_s$  are the slope in loading and reloading, respectively, obtained from the void ratio ( $e$ ) versus vertical stress ( $\sigma_v$ ) plot as illustrated in Figure 2. Figures 3, 4, and 5 show the void ratio ( $e$ ) versus vertical stress ( $\sigma_v$ ) of the HCB, DBF, and LBF, respectively. Currently, a total of thirty-nine (39) 1D consolidation tests have been completed: 11 tests on the HCB; 8 tests on the DBF; and 20 tests on the LBF. Figure 6 shows the comparison of the HCB, DBF, and LBF. The compression index ( $C_c$ ) and swelling index ( $C_s$ ) are interpreted from the results of 1D consolidation tests. The parameters  $C_c$  and  $C_s$  for the HCB, DBF, and LBF are presented in Tables 9, 10, and 11, respectively. A discussion of the testing program for each type of material is presented in Appendices A, B, and C.

Combined with the results of triaxial tests that define the behaviour of soil during shearing and the failure criteria, these parameters can be used to evaluate soil behaviour using a critical state model (e.g., modified cam-clay (MCC) (Roscoe and Burland 1968)).

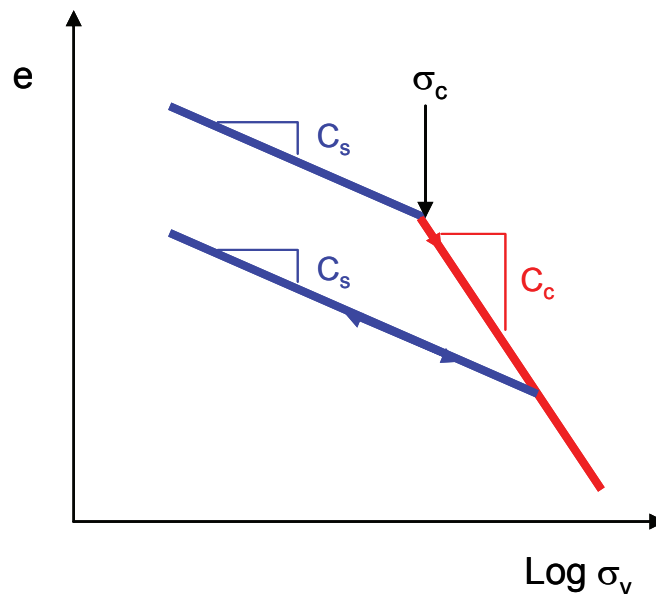
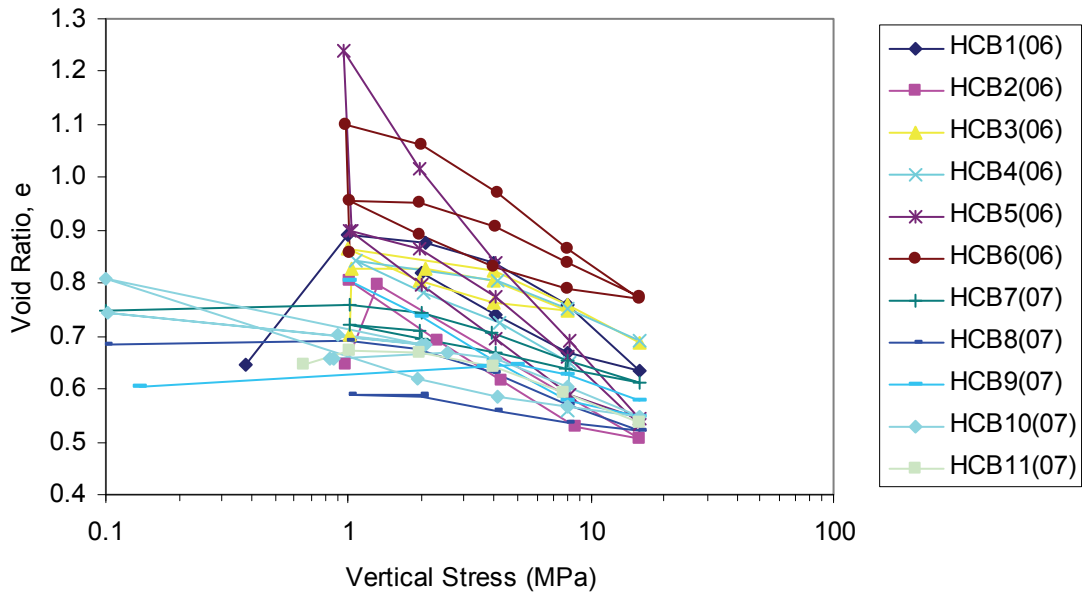
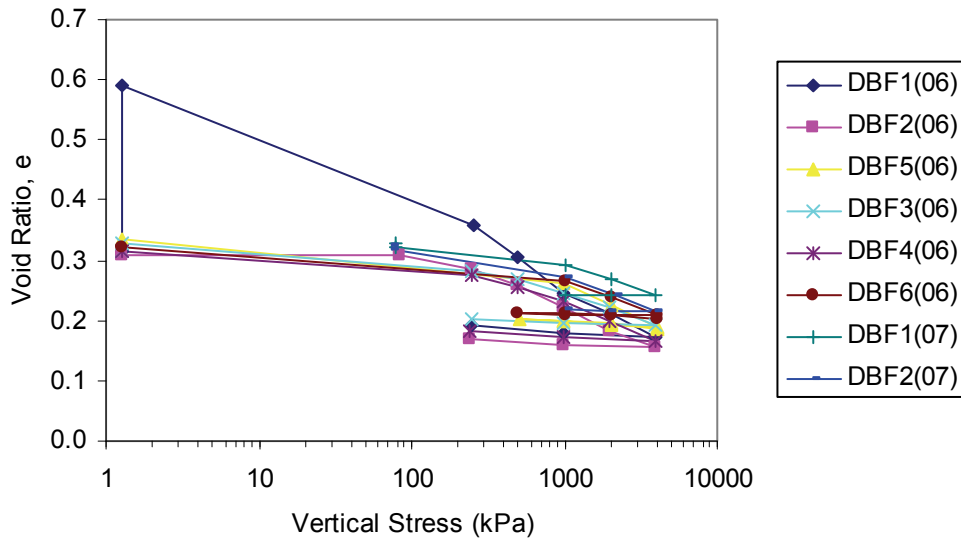


Figure 2: Definition of Parameters  $C_c$  and  $C_s$



**Figure 3: Void Ratio (e) versus Vertical Stress for HCB Specimens (11 Tests)**



**Figure 4: Void Ratio (e) versus Vertical Stress for LBF Specimens (8 Tests)**

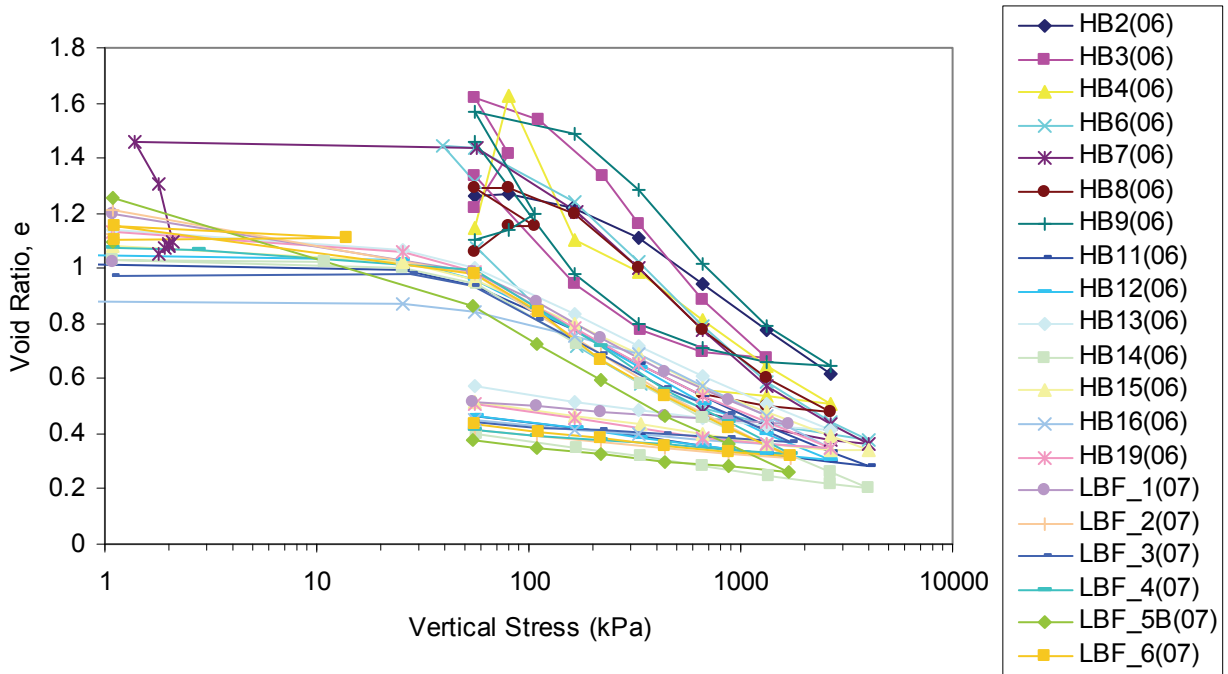


Figure 5: Void Ratio ( $e$ ) versus Vertical Stress for LBF Specimens (20 Tests)

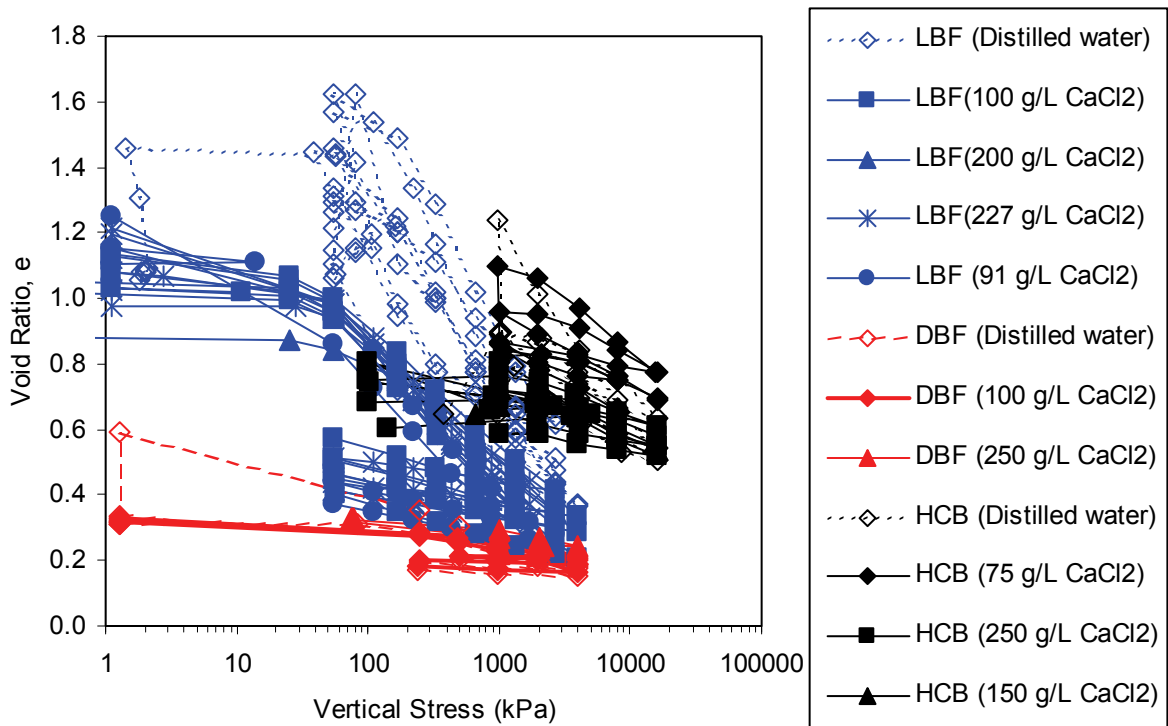


Figure 6: Comparison of the Void Ratio ( $e$ ) versus Vertical Stress for the HCB, DBF, and LBF Specimens

**Table 9: Compression Indices ( $C_c$ ) and Swelling Indices ( $C_s$ ) of the Highly Compacted Bentonite (HCB) Specimens**

No.	Sample No.	Mixing Liquid	Reservoir Liquid	$C_c$	$C_s$	References
1	HCB1(06)	DW	DW	0.42	0.11	Baumgartner et al. 2008
2	HCB2(06)	DW	DW	0.27	0.09	Baumgartner et al. 2008
3	HCB3(06)	75 g/L CaCl <sub>2</sub>	75 g/L CaCl <sub>2</sub>	0.15	0.09	Baumgartner et al. 2008
4	HCB4(06)	75 g/L CaCl <sub>2</sub>	75 g/L CaCl <sub>2</sub>	0.19	0.07	Baumgartner et al. 2008
5	HCB5(06)	DW	DW	0.57	0.30	Baumgartner et al. 2008
6	HCB6(06)	75 g/L CaCl <sub>2</sub>	75 g/L CaCl <sub>2</sub>	0.32	0.15	Baumgartner et al. 2008
7	HCB7(07)	DW	250 g/L CaCl <sub>2</sub>	0.16	0.09	Priyanto et al. 2008
8	HCB8(07)	250 g/L CaCl <sub>2</sub>	250 g/L CaCl <sub>2</sub>	0.18	0.06	Priyanto et al. 2008
9	HCB9(07)	DW	DW	0.16	0.09	Priyanto et al. 2008
10	HCB10(07)	250 g/L CaCl <sub>2</sub>	250 g/L CaCl <sub>2</sub>	0.19	0.06	Priyanto et al. 2008
11	HCB11(07)	DW	150 g/L CaCl <sub>2</sub>	0.18	0.02	Priyanto et al. 2008

**Table 10: Compression Indices ( $C_c$ ) and Swelling Indices ( $C_s$ ) of the Dense Backfill (DBF) Specimens**

No.	Sample No.	Mixing Liquid	Reservoir Liquid	$C_c$	$C_s$	Reference
1	DBF1(06)	DW	DW	0.153	0.013	Baumgartner et al. 2008
2	DBF2(06)	DW	DW	0.116	0.013	Baumgartner et al. 2008
3	DBF5(06)	DW	DW	0.116	0.014	Baumgartner et al. 2008
4	DBF3(06)	100 g/L CaCl <sub>2</sub>	100 g/L CaCl <sub>2</sub>	0.091	0.008	Baumgartner et al. 2008
5	DBF4(06)	100 g/L CaCl <sub>2</sub>	100 g/L CaCl <sub>2</sub>	0.106	0.013	Baumgartner et al. 2008
6	DBF6(06)	100 g/L CaCl <sub>2</sub>	100 g/L CaCl <sub>2</sub>	0.095	0.001	Baumgartner et al. 2008
7	DBF1(07)	250 g/L CaCl <sub>2</sub>	250 g/L CaCl <sub>2</sub>	0.085	0.002	Priyanto et al. 2008
8	DBF2(07)	DW	250 g/L CaCl <sub>2</sub>	0.094	0.004	Priyanto et al. 2008

**Table 11: Compression Indices ( $C_c$ ) and Swelling Indices ( $C_s$ ) of the Light Backfill (LBF) Specimens**

Test No.	Sample No.	Mixing Liquid	Reservoir Liquid	$C_c$	$C_s$	References
1	HB2(06)	Distilled Water	Distilled Water	0.537	NA	Baumgartner et al. 2008
2	HB3(06)	Distilled Water	Distilled Water	0.851	0.169	Baumgartner et al. 2008
3	HB4(06)	Distilled Water	Distilled Water	0.531	0.077	Baumgartner et al. 2008
4	HB6(06)	Distilled Water	Distilled Water	0.629	0.158	Baumgartner et al. 2008
5	HB7(06)	Distilled Water	Distilled Water	0.608	0.149	Baumgartner et al. 2008
6	HB8(06)	Distilled Water	Distilled Water	0.600	0.113	Baumgartner et al. 2008
7	HB9(06)	Distilled Water	Distilled Water	0.713	0.114	Baumgartner et al. 2008
8	HB11(06)	Distilled water	100 g/L $\text{CaCl}_2$	0.353	0.097	Baumgartner et al. 2008
9	HB12(06)	Distilled water	100 g/L $\text{CaCl}_2$	0.387	0.095	Baumgartner et al. 2008
10	HB13(06)	100 g/L $\text{CaCl}_2$	100 g/L $\text{CaCl}_2$	0.351	0.097	Baumgartner et al. 2008
11	HB14(06)	Distilled water	100 g/L $\text{CaCl}_2$	0.398	0.105	Baumgartner et al. 2008
12	HB15(06)	100 g/L $\text{CaCl}_2$	100 g/L $\text{CaCl}_2$	0.334	0.095	Baumgartner et al. 2008
13	HB16(06)	Distilled water	200 g/L $\text{CaCl}_2$	0.380	0.062	Baumgartner et al. 2008
14	HB19(06)	Distilled water	100 g/L $\text{CaCl}_2$	0.379	0.094	Baumgartner et al. 2008
15	LBF_1(07)	227 g/L $\text{CaCl}_2$	227 g/L $\text{CaCl}_2$	0.366	0.050	Priyanto et al. 2008
16	LBF_2(07)	Distilled water	227 g/L $\text{CaCl}_2$	0.446	0.065	Priyanto et al. 2008
17	LBF_3(07)	227 g/L $\text{CaCl}_2$	227 g/L $\text{CaCl}_2$	0.378	0.046	Priyanto et al. 2008
18	LBF_4(07)	Distilled water	227 g/L $\text{CaCl}_2$	0.445	0.056	Priyanto et al. 2008
19	LBF_5B(07)	91 g/L $\text{CaCl}_2$	91 g/L $\text{CaCl}_2$	0.400	0.074	Priyanto et al. 2008
20	LBF_6(07)	Distilled water	91 g/L $\text{CaCl}_2$	0.446	0.081	Priyanto et al. 2008

## 5.2 HYDRAULIC CONSTITUTIVE MODELS

Coefficient of consolidation ( $c_v$ ) for each load increment can be interpreted from the results of 1D consolidation. The coefficient of consolidation ( $c_v$ ) is a parameter that couples hydraulic and mechanical behaviour of the soil. Assuming soil has linear-elastic behaviour for each load increment, the hydraulic conductivity ( $K$ ) can be calculated from the coefficient of consolidation ( $c_v$ ) using the relationships developed by Terzhagi (1943). The assumption of linear-elastic behaviour for each load increment is reasonable, because constant load for each load increment was used during the 1D consolidation test. The coefficient of consolidation ( $c_v$ ) and hydraulic conductivity ( $K$ ) of HCB material have been interpreted from the results and shown in Figure 7. Detailed discussion on the result is presented in Appendix A. The 1D consolidation tests of DBF and LBF specimens are still in progress, complete test results are required to calculate the coefficient of consolidation ( $c_v$ ) and hydraulic conductivity ( $K$ ). These values for DBF and LBF will be presented in the report for the final report.

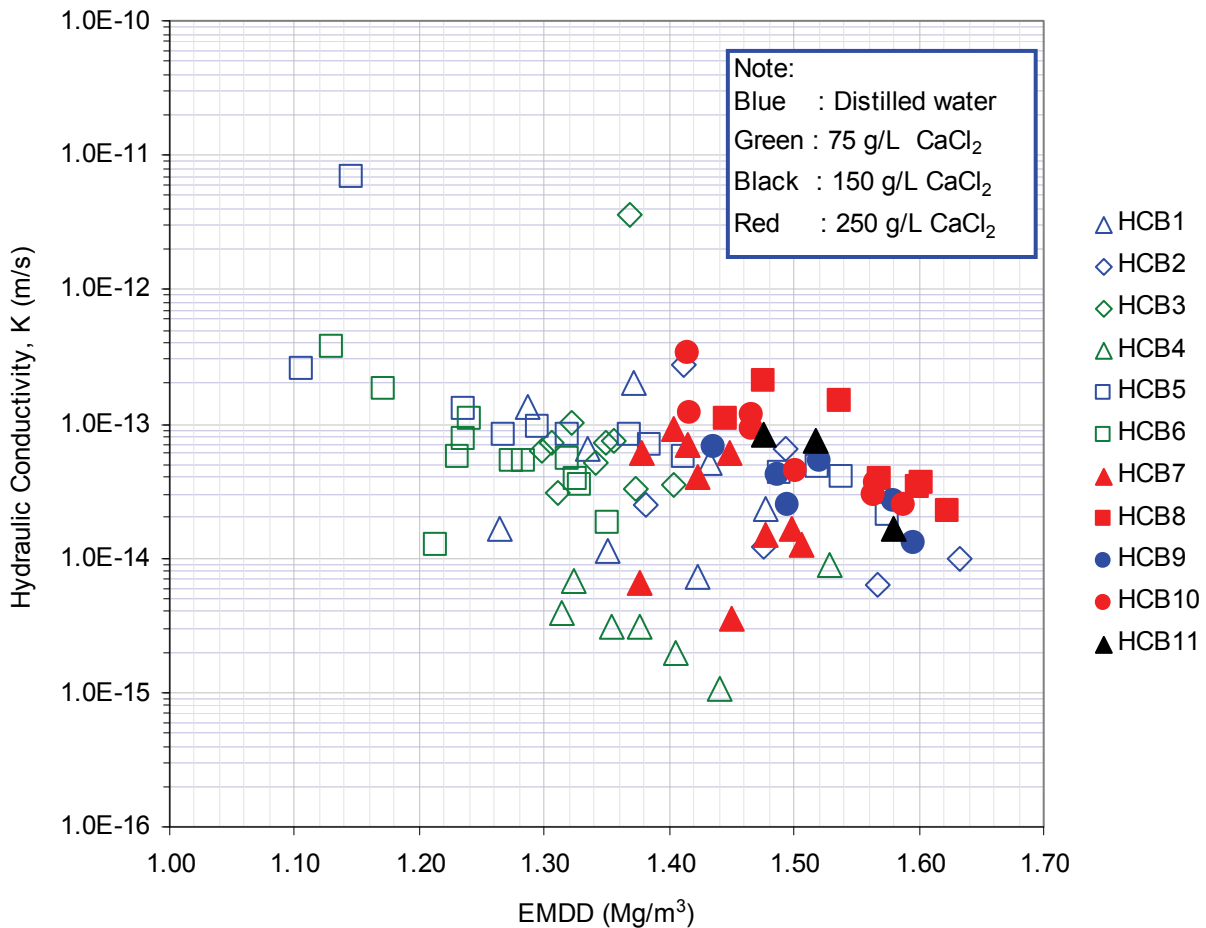


**Figure 7: Hydraulic Conductivity ( $K$ ) of the HCB Interpreted from the 1D Consolidation Test Results**

### 5.3 EFFECTS OF CONCENTRATION OF THE SOLUTION IN THE PORE LIQUID, MIXING LIQUID USED IN SPECIMEN PREPARATION AND BOUNDARY CONDITIONS DURING INITIAL SATURATION

The effects of pore liquid concentration, mixing liquid used in specimen preparation and boundary condition during initial saturation for each type of material are discussed in Appendices A, B, and C. The results show that parameters  $C_c$  and  $C_s$  decrease (i.e., the soil becomes stiffer) with increasing of pore-liquid concentration for all materials. This relationship can be used to include the effect of pore liquid salinity on the mechanical behaviour of the clay-based sealing materials using THM numerical models. The relationship of the concentration of Calcium Chloride ( $\text{CaCl}_2$ ) in the pore liquid and the compression indices ( $C_c$ ) and swelling indices ( $C_s$ ) for the three clay-based sealing materials are illustrated in Figures 8 and 9 respectively, which indicates that the compression indices ( $C_c$ ) and swelling indices ( $C_s$ ) decrease with an increase in the concentration of  $\text{CaCl}_2$  in the pore liquid for the three clay-based sealing material. A decrease in the compression index ( $C_c$ ) indicates that the materials become stiffer and less compressible; while a decrease of the swelling index ( $C_s$ ) indicates a reduction in the ability of the material to swell. The effects of the concentration of the solution in the pore liquid and mixing liquid used in specimen preparation, and the boundary condition during initial saturation are discussed in Appendices A, B, and C for each material.

Under constant volume boundary conditions during initial saturation, the vertical stress increases up to a certain pressure required to maintain constant volume. Figure 10 shows the swelling pressure for specimen HCB9 prepared with distilled water is higher than specimen HCB10 with 250 g/L  $\text{CaCl}_2$  (5 MPa versus 2.5 MPa). This result shows a reduction of 2.5 MPa of swelling pressure of the Highly Compacted Bentonite (HCB) specimen with an increase of concentration of Calcium Chloride ( $\text{CaCl}_2$ ) from 0 g/L to 250 g/L in pore liquid.

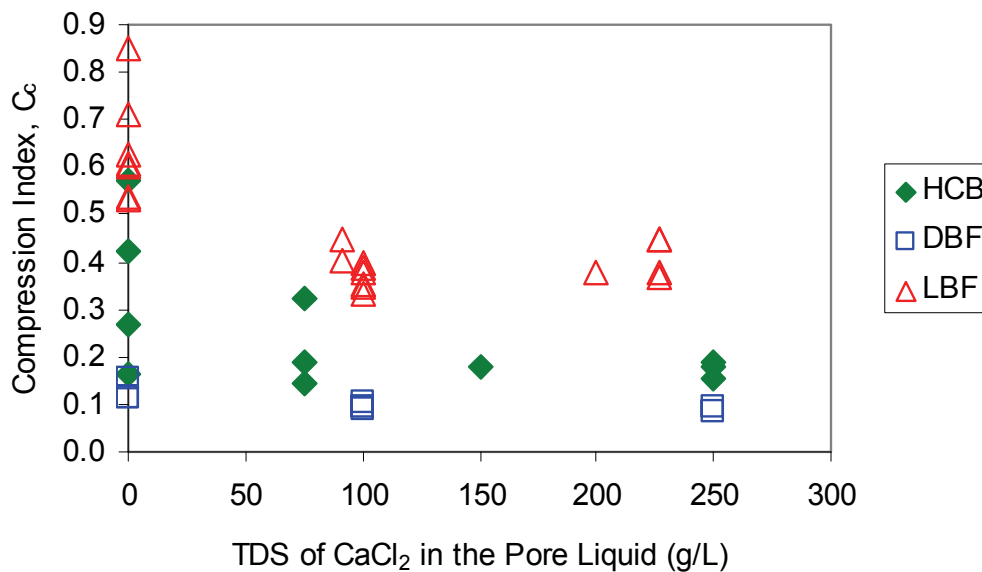


Figure 8: Relationship of the Compression Index ( $C_c$ ) to the Concentration (in TDS) of Calcium Chloride ( $\text{CaCl}_2$ ) in the Pore Liquid



## **6. PLANS FOR FUTURE WORKS**

### **6.1 PLAN FOR 1D CONSOLIDATION TESTS IN 2008**

The placement of a repository will likely be a ground water environment that consists of a mixture of  $\text{CaCl}_2$  and  $\text{NaCl}$  as the dominant dissolved species that will vary with location and depth (Gascoyne et al. 1987; Mazurek 2004). As most of the initial 1D-consolidation testing was done using fresh water or calcium chloride solutions, there is a need to establish what the effects of sodium dominated solutions will have on system behaviour and ultimately a limited number of tests should be done using mixed cation solutions. The focus of the 1D-consolidation testing in 2008 is investigation of the sodium chloride solutions as shown in Tables 3, 5, and 8. Variation of liquid used in the specimen mixing and initial boundary condition applied during initial saturation will be included to allow a comparison with the previous work (2006 and 2007).

The 1D consolidation tests of the DBF materials with various sand contents (i.e., 70% to 85%) (N. Chandler, personal communication, 2007) show that the swelling index ( $C_s$ ) increases significantly during unloading under low pressure resulting in hysteretic behaviour. The same behaviours have also been observed for HCB material (Appendix A) and suggest the need to modify the currently used constitutive models for these clay-based sealing materials. Unloading to lower pressure than is currently done is included in 2008 test plan to allow for evaluation of this phenomenon.

### **6.2 PLAN FOR 1D CONSOLIDATION TESTS (2009 and beyond)**

Two potential test plans have been identified for work in 2009 and beyond. The option selected will depend on the results obtained in the work from 2006 through 2008 and identification of what parameters are most important to evaluate. The two alternatives are described below.

Alternative 1: Establish the relationship of  $C_c$  and  $C_s$  to concentration of  $\text{NaCl}$  and  $\text{CaCl}_2$  in the pore liquid. Currently, the THM numerical modelling assumes that the pore liquid salinity is constant during the analysis. Mass transport formulation is used to define the flow of fluid (i.e., liquid and gas). Addition of mass transport formulation describing the flow of solvent in the pore liquid in the THM numerical modelling may be used to incorporate the change of pore liquid concentration. The relationship of  $C_c$  and  $C_s$  to pore liquid concentration can be used to incorporate the effect of pore liquid concentration to the mechanical behaviour of clay-based sealing material in the THM numerical modelling. This relationship of  $C_c$  and  $C_s$  to pore liquid concentration may also be used to consider the change of salt type (i.e.,  $\text{NaCl}$  and  $\text{CaCl}_2$ ) and their concentration. Additional data are still required to define this relationship. Tables 3, 5, and 8 show alternative 1 for 2009 to include 150 g/L  $\text{NaCl}$  in 1D consolidation tests.

Alternative 2: Examine the effect of artificial groundwater (e.g., mixture of  $\text{NaCl}$  and  $\text{CaCl}_2$ ). Natural groundwater consists of mixtures of various types of salts at different concentrations. Examining the effect of artificial groundwater on the mechanical behaviour of sealing materials is important if the mechanical behaviour of sealing materials is dependent on the types of salts or their ratios (i.e.,  $\text{NaCl}$  and  $\text{CaCl}_2$ ). Table 3, 5, and 8 shows alternative 2 for 2009 to include artificial water in 1D consolidation test.

### 6.3 PROJECTED RESULTS AT THE END OF TESTING PROGRAM

In the end of the outlined testing program it is hoped that the following relationships can be generated from the results of 1D consolidation tests of HCB, DBF, and LBF.

- The effects of salt types and their concentrations used as mixing and reservoir liquids, and boundary conditions during initial saturation on the mechanical behaviour of HCB, DBF, and LBF.
- Parameters  $C_c$ ,  $C_s$ , and  $c_v$  for each test.
- Parameters  $C_c$  and  $C_s$  as a function of pore liquid concentration and salt type to incorporate the effect of pore liquid salinity in numerical modelling for each material (i.e., HCB, DBF, and LBF). Examples of the type of relationship that may be developed from the tests are shown in Figure 11. These relationships for the specimens with Calcium Chloride ( $\text{CaCl}_2$ ) in the pore liquid are shown in Figures 8 and 9.

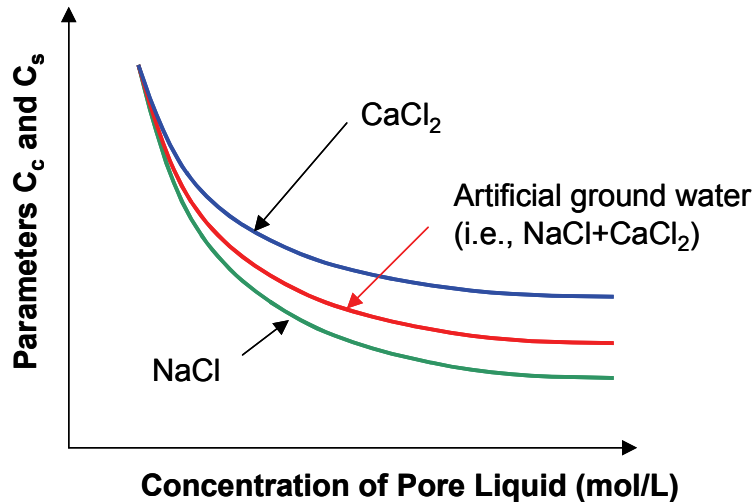


Figure 11: Possible Relationship of Parameters  $C_c$  and  $C_s$  and the Concentration of Solution in the Pore Liquid

### 7. CONCLUDING REMARKS

- Based on the results of the 1D-consolidation tests of the three clay-based sealing materials, the following conclusions can be made.
- The compression indices ( $C_c$ ) and swelling indices ( $C_s$ ) decrease with increasing concentration of  $\text{CaCl}_2$  in the pore liquid for the three clay-based sealing materials (i.e., HCB, DBF, and LBF). A decrease in the compression index ( $C_c$ ) indicates that the materials become stiffer and less compressible; while a decrease of the swelling index ( $C_s$ ) indicates a reduction of the ability of the material to swell.

- The results of the 1D consolidation tests of the Highly Compacted Bentonite (HCB) show a loss of 2.5 MPa in its swelling pressure with an increase of concentration of Calcium Chloride ( $\text{CaCl}_2$ ) solution from 0 g/L to 250 g/L in pore liquid.

## REFERENCES

- Baumgartner, P., D. G. Priyanto, J. R. Baldwin, J. A. Blatz, B. H. Kjartanson, and H. Batenipour. 2008. Preliminary Results of One-Dimensional Consolidation Testing on Bentonite Clay-Based Sealing Components Subjected to Two Pore-Fluid Chemistry Conditions. Nuclear Waste Management Organization (NWMO) Technical Report No. TR-2008-04. Toronto, Canada.
- CTECH (CTECH Radioactive Materials Management). 2002. Conceptual design for a deep geologic repository for used nuclear fuel. CTECH Report 1106/MD18085/REP/01, Nuclear Waste Management Organization, Toronto, Canada ([www.nwmo.ca](http://www.nwmo.ca)).
- Dixon, D.A. 2000. Porewater salinity and the development of swelling pressure in bentonite-based buffer and backfill materials. Helsinki, Posiva Report, POSIVA 2000-04 (ISBN 951-652-090-1).
- Gascoyne, M., C.C. Davison, J.D. Ross and R. Pearson. 1987. Saline groundwaters and brines in plutons in the Canadian Shield. *In* Saline Water and Gases in Crystalline Rocks. Editors: Fritz, P. and Frape, S.K.; Geological Association of Canada Special Paper 33, Ottawa.
- Gierszewski, P., J. Avis, N. Calder, A. D'Andrea, F. Garisto, C. Kitson, T. Melnyk, K. Wei and L. Wojciechowski. 2004. Third case study – Postclosure safety assessment. Ontario Power Generation, Nuclear Waste Management Division Report 06819-REP-01200-10109-R00. Toronto, Ontario.
- Maak P and Simmons G R. 2005. Deep geologic repository concepts for isolation of used fuel in Canada, Canadian Nuclear Society, Waste Management, Decommissioning and Environmental Restoration for Canada's Nuclear Activities: Current Practices and Future Needs, Ottawa May 8-11 2005.
- Mazurek, M. 2004. Long-term used nuclear fuel waste management – Geoscientific review of the sedimentary sequence in southern Ontario. Institute of Geological Sciences, Univ. of Bern, Technical Report TR 04-01, Bern, Switzerland, available from Nuclear Waste Management Organization, Toronto, Canada ([www.nwmo.ca](http://www.nwmo.ca)).
- Russell, S.B. and G.R. Simmons. 2003. Engineered barrier system for a deep geologic repository. Presented at the 2003 International High-Level Radioactive Waste Management Conference. 2003 March 30-April 2, Las Vegas, NV.
- Siemens, G. A. 2006. Influence of Boundary Conditions on the Hydraulic-Mechanical Behaviour of an Unsaturated Swelling Soil. Ph.D Thesis, University of Manitoba, Canada.
- Terzaghi, K. 1943. Theoretical Soil Mechanics. Wiley, New York.



**APPENDIX A:  
HIGHLY COMPACTED BENTONITE**

D. G. Priyanto and D. A. Dixon  
Atomic Energy of Canada Limited

**CONTENTS**

	<b><u>Page</u></b>
<b>A1. HIGHLY COMPACTED BENTONITE (HCB) .....</b>	<b>33</b>
<b>A2. EQUIPMENT .....</b>	<b>33</b>
<b>A2.1 OEDOMETER CELL AND FILTER STONE.....</b>	<b>33</b>
<b>A2.2 COMPRESSION FRAME AND LOADING SYSTEM .....</b>	<b>33</b>
<b>A2.3 STRAIN AND PRESSURE MEASUREMENT .....</b>	<b>33</b>
<b>A3. TEST PROCEDURE .....</b>	<b>34</b>
<b>A3.1 TEST MATRIX FOR HCB SPECIMENS .....</b>	<b>34</b>
<b>A3.2 SPECIMEN PREPARATION.....</b>	<b>35</b>
<b>A3.3 SPECIMEN LOADING, RESERVOIR LIQUID MAINTENANCE, AND DISMANTLING .....</b>	<b>36</b>
<b>A4. RESULTS .....</b>	<b>42</b>
<b>A4.1 THICKNESS AND VERTICAL STRESS VERSUS TIME .....</b>	<b>42</b>
<b>A4.2 VOID RATIO (E), DRY DENSITY (<math>\rho_{DRY}</math>), AND EMDD VERSUS VERTICAL STRESS (<math>\sigma_v</math>) .....</b>	<b>45</b>
A4.2.1 HCB7 .....	45
A4.2.2 HCB8 .....	47
A4.2.3 HCB9 .....	48
A4.2.4 HCB10 .....	50
A4.2.5 HCB11 .....	52
<b>A4.3 COEFFICIENT OF CONSOLIDATION (<math>C_v</math>) .....</b>	<b>53</b>
<b>A4.4 HYDRAULIC CONDUCTIVITY (K) .....</b>	<b>67</b>
<b>A4.5 1D-MODULUS.....</b>	<b>69</b>
<b>A5. DISCUSSION .....</b>	<b>76</b>
<b>A5.1 BOUNDARY CONDITIONS DURING INITIAL SATURATION .....</b>	<b>76</b>
<b>A5.2 MECHANICAL CONSTITUTIVE MODEL .....</b>	<b>76</b>
A5.2.1 Model 1: Log-Linear Relationship.....	77
A5.2.2 Model 2: Modification Of Model 1 .....	82
<b>A5.3 APPLICATIONS OF PARAMETERS IN NUMERICAL MODELLING .....</b>	<b>83</b>

<b>A5.4</b>	<b>EFFECTS OF PORE LIQUID CHEMISTRY, LIQUID USED IN SPECIMEN PREPARATION, AND BOUNDARY CONDITIONS APPLIED DURING INITIAL SATURATION.....</b>	<b>83</b>
A5.4.1	Effect Of Pore Liquid Chemistry.....	83
A5.4.1.1	Specimens Prepared with Distilled Water .....	83
A5.4.1.2	Specimens Prepared with Salt Solution .....	85
A5.4.2	Effect Of Pore Liquid Used In Specimen Preparation .....	87
A5.4.3	Effect Of Boundary Conditions During Initial Saturation.....	88
<b>A6.</b>	<b>CONCLUDING REMARKS.....</b>	<b>91</b>
	<b>ACKNOWLEDGEMENTS.....</b>	<b>92</b>
	<b>REFERENCES .....</b>	<b>93</b>

**LIST OF TABLES**

	<b><u>Page</u></b>
Table A1: 1-D Consolidation Test Matrix for HCB Specimens in 2007 .....	35
Table A2: Dimension, Mass Composition, Liquid Properties, Water Contents, Densities, Void Ratio, and Porosity of Specimens HCB7, HCB8, HCB9, HCB10, and HCB11 at Installation.....	38
Table A3: Summary of Equations for Calculation of Mass-Volume Relationships of Soil with Saline Pore Liquid .....	39
Table A4: Properties of Highly Compacted Bentonite (HCB).....	42
Table A5: Properties of the Liquid.....	42
Table A6: Coefficient of Consolidation ( $c_v$ ) for Specimen HCB7.....	60
Table A7: Coefficient of Consolidation ( $c_v$ ) for Specimen HCB8.....	61
Table A8: Coefficient of Consolidation ( $c_v$ ) for Specimen HCB9.....	62
Table A9: Coefficient of Consolidation ( $c_v$ ) for Specimen HCB10.....	63
Table A10: Coefficient of Consolidation ( $c_v$ ) for Specimen HCB11.....	64
Table A11: 1D-Constrained Modulus for Specimens HCB1 .....	70
Table A12: 1D-Constrained Modulus for Specimens HCB2 .....	70
Table A13: 1D-Constrained Modulus for Specimens HCB3 .....	71
Table A14: 1D-Constrained Modulus for Specimens HCB4 .....	71
Table A15: 1D-Constrained Modulus for Specimens HCB5 .....	72
Table A16: 1D-Constrained Modulus for Specimens HCB6 .....	73
Table A17: 1D-Constrained Modulus for Specimens HCB7 .....	73
Table A18: 1D-Constrained Modulus for Specimens HCB8 .....	74
Table A19: 1D-Constrained Modulus for Specimens HCB9 .....	74
Table A20: 1D-Constrained Modulus for Specimens HCB10 .....	75
Table A21: 1D-Constrained Modulus for Specimens HCB11 .....	75
Table A22: Compression Index ( $C_c$ ), Swelling Index ( $C_s$ ), and Initial Consolidation Pressure of HCB Specimens.....	78

**LIST OF FIGURES**

	<b><u>Page</u></b>
Figure A1: Loading and Displacement History of Specimen HCB7 (Mixing Liquid = Distilled Water; Reservoir Liquid = 250 g/L $\text{CaCl}_2$ ).....	43
Figure A2: Loading and Displacement History of Specimen HCB8 (Mixing Liquid = Reservoir Liquid = 250 g/L $\text{CaCl}_2$ ).....	43
Figure A3: Loading and Displacement History of Specimen HCB9 (Mixing Liquid = Reservoir Liquid = Distilled Water).....	44
Figure A4: Loading and Displacement History of Specimen HCB10 (Mixing Liquid = Reservoir Liquid = 250 g/L $\text{CaCl}_2$ ).....	44
Figure A5: Loading and Displacement History of Specimen HCB11 (Mixing Liquid = Distilled Water; Reservoir Liquid = 150 g/L $\text{CaCl}_2$ ).....	45
Figure A6: Void Ratio versus Vertical Stress of Specimen HCB7 (Reduced data = data point at the end of each load increment) .....	46
Figure A7: Dry Density versus Vertical Stress of Specimen HCB7.....	46

Figure A8: Void Ratio versus Vertical Stress of Specimen HCB8 (Reduced data = data point at the end of each load increment) .....	47
Figure A9: Dry Density versus Vertical Stress of Specimen HCB8.....	47
Figure A10: Void Ratio versus Vertical Stress of Specimen HCB9 (Note: numbers show load sequence).....	48
Figure A11: Dry Density versus Vertical Stress of Specimen HCB9 (Note: numbers show load sequence).....	49
Figure A12: The Displacement and Vertical Stress during Initial Saturation of Specimen HCB9.....	49
Figure A13: Void Ratio versus Vertical Stress of Specimen HCB10 (Note: numbers show load sequence; reduced data = data point at the end of each load increment).....	50
Figure A14: Dry Density versus Vertical Stress of Specimen HCB10 (Note: numbers show load sequence).....	51
Figure A15: The Displacement and Vertical Stress during Initial Saturation of Specimen HCB10.....	51
Figure A16: Void Ratio versus Vertical Stress of Specimen HCB11 (Reduced data = data point at the end of each load increment) .....	52
Figure A17: Dry Density versus Vertical Stress of Specimen HCB11.....	52
Figure A18: Displacement versus Time in Logarithmic Scale for Specimen HCB7 .....	54
Figure A19: Displacement versus Square Root of Time for Specimen HCB7 .....	54
Figure A20: Displacement versus Time in Logarithmic Scale for Specimen HCB8 .....	55
Figure A21: Displacement versus Square Root of Time for Specimen HCB8 .....	55
Figure A22: Displacement versus Time in Logarithmic Scale for Specimen HCB9 .....	56
Figure A23: Displacement versus Square Root of Time for Specimen HCB9 .....	56
Figure A24: Displacement versus Time in Logarithmic Scale for Specimen HCB10 .....	57
Figure A25: Displacement versus Square Root of Time for Specimen HCB10 .....	57
Figure A26: Displacement versus Time in Logarithmic Scale for Specimen HCB11 .....	58
Figure A27: Displacement versus Square Root of Time for Specimen HCB11 .....	58
Figure A28: Displacement Calculated Using the Parameters Generated from SQRT and Log-T Methods Compared with the Laboratory Test Data for Specimen HCB 8, Load 5 (16 MPa, Compression) .....	59
Figure A29: Void Ratio versus Coefficient of Consolidation ( $c_v$ ) of Specimen HCB7 .....	65
Figure A30: Void Ratio versus Coefficient of Consolidation ( $c_v$ ) of Specimen HCB8 .....	65
Figure A31: Void Ratio versus Coefficient of Consolidation ( $c_v$ ) of Specimen HCB9.....	66
Figure A32: Void Ratio versus Coefficient of Consolidation ( $c_v$ ) of Specimen HCB10 .....	66
Figure A33: Void Ratio versus Coefficient of Consolidation ( $c_v$ ) of Specimen HCB11 .....	67
Figure A34: Hydraulic Conductivity Estimated from 1D-Consolidation Test for Highly Compacted Bentonite (HCB) .....	68
Figure A35: Hydraulic Conductivity (K) of Bentonite Measured using Hydraulic Conductivity Cell (Dixon et al. 1999) .....	68
Figure A36: 1D-Constrained Modulus versus EMDD .....	69
Figure A37: Displacement During Initial Saturation Under Constant Vertical Stress of 1 MPa for Specimen HCB7 .....	76
Figure A38: Model 1: Critical State Soil Mechanics Model for 1D-Consolidation .....	77
Figure A39: Calculated Response using Critical State Constitutive Model Compared with the Laboratory Results for Specimen HCB7 .....	79
Figure A40: Calculated Response using Critical State Constitutive Model Compared with the Laboratory Results for Specimen HCB8 .....	79

Figure A41: Calculated Response using Critical State Constitutive Model (Model 1) and Modified Model (Model 2) Compared with the Laboratory Results for Specimen HCB9.....	80
Figure A42: Calculated Response using Critical State Constitutive Model (Model 1) and Modified Model (Model 2) Compared with the Laboratory Results for Specimen HCB10.....	80
Figure A43: Calculated Response using Critical State Constitutive Model (Model 1) Compared with the Laboratory Results for Specimen HCB11.....	81
Figure A44: Compression Index ( $C_c$ ) for HCB Specimens.....	81
Figure A45: Swelling Index ( $C_s$ ) for HCB Specimens .....	82
Figure A46: Model 2: Modification of Log-Linear Relationship (Model 1) for HCB Specimen ...	83
Figure A47: Void Ratio ( $e$ ) versus Vertical Stress ( $\sigma_v$ ) for Specimens Prepared with Distilled Water with Different Reservoir Liquid .....	84
Figure A48: Compression Index ( $C_c$ ) versus Concentration of $\text{CaCl}_2$ in Pore Liquid for Specimens Prepared using Distilled Water with Different Reservoir Liquid.....	85
Figure A49: Swelling Index ( $C_s$ ) versus Concentration of $\text{CaCl}_2$ in Pore Liquid for Specimens Prepared using Distilled Water with Different Reservoir Liquid .....	85
Figure A50: Void Ratio ( $e$ ) versus Vertical Stress ( $\sigma_v$ ) for Specimens Prepared with Different Mixing and Reservoir Liquid.....	86
Figure A51: Compression Index ( $C_c$ ) versus Concentration of $\text{CaCl}_2$ in Pore Liquid for Specimens Prepared with Different Mixing and Reservoir Liquid .....	86
Figure A52: Swelling Index ( $C_s$ ) versus Concentration of $\text{CaCl}_2$ in Pore Liquid for Specimens Prepared with Similar Mixing and Reservoir Liquid .....	87
Figure A53: Compression Index ( $C_c$ ) versus Concentration of $\text{CaCl}_2$ in Pore Liquid.....	88
Figure A54: Swelling Index ( $C_s$ ) versus Concentration of $\text{CaCl}_2$ in Pore Liquid .....	88
Figure A55: Void Ratio ( $e$ ) versus Vertical Stress ( $\sigma_v$ ) for Specimens having Distilled Water as Mixing and Reservoir Liquid with Different Boundary Condition during Initial Saturation (HCB1-Constant Pressure; HCB9 - Constant Volume) .....	89
Figure A56: Void Ratio ( $e$ ) versus Vertical Stress ( $\sigma_v$ ) for Specimens having 250 g/L $\text{CaCl}_2$ as Mixing and Reservoir Liquid with Different Boundary Condition during Initial Saturation (HCB8-Constant Pressure; HCB10-Constant Volume) .....	90
Figure A57: Compression Index ( $C_c$ ) versus Pore Liquid Concentration for Specimens with Different Boundary Condition during Initial Saturation.....	90
Figure A58: Swelling Index ( $C_s$ ) versus Pore Liquid Concentration for Specimens with Different Boundary Condition during Initial Saturation .....	91



## **A1. HIGHLY COMPACTED BENTONITE (HCB)**

Highly Compacted Bentonite (HCB) is a clay-based sealing-system component proposed for use in either full contact or very close proximity to the used-fuel container (Maak and Simmons 2005). HCB is composed of 100% bentonite (Russell and Simmons 2003), compacted to high dry densities. The test specimens are fabricated from 80-mesh granules of Wyoming bentonite (MX80) with an assumed minimum Na-montmorillonite content of 75%. The 1D consolidation tests of HCB specimens are conducted at the Atomic Energy of Canada Limited (AECL)'s geotechnical engineering laboratory.

## **A2. EQUIPMENT**

### **A2.1 OEDOMETER CELL AND FILTER STONE**

Small-diameter oedometer cells (28.1-mm diameter) are used in this test series to permit high stresses to be applied (i.e., maximum 16 MPa). Similar diameter filter stones (28.1 mm) are used in the tests to allow liquid to enter or leave the faces of the specimens. All components of the oedometer cells were fabricated from stainless steel to avoid corrosion, which can be a problem, particularly in those done using the saline solution. No corrosion was observed during the test series and so interaction of iron with the HCB is assumed to be a non-issue in these tests.

### **A2.2 COMPRESSION FRAME AND LOADING SYSTEM**

Standard dead weight oedometers are unable to apply the high loads needed to generate stresses exceeding the expected swelling pressures for HCB. In order to complete these tests, two custom-built loading systems were constructed; each uses a different method to achieve the testing goals.

1. A compression frame similar to that used by Baumgartner et al. (2008) is used. This system has a double-action hydraulic ram (e.g., a 222 kN spring-return ram and a 445 kN double acting ram) to produce the required loads. Each hydraulic ram is actuated by a high-pressure nitrogen-gas cylinder acting on a gas-over-oil accumulator rather than the conventional mechanical hydraulic pumps. This allows the most stable possible loading condition to be achieved.
2. A new frame using a servo-hydraulic testing system manufactured by the MTS<sup>®</sup> (Materials Testing Services) was added in 2007 to test HCB. This equipment enables an application of different boundary conditions during initial saturation in tests (i.e., constant volume or constant pressure).

### **A2.3 STRAIN AND PRESSURE MEASUREMENT**

Displacements are measured with calibrated linear variable differential transformers (LVDT). Loads are measured with calibrated strain-gauge load cells (i.e., 17.8-kN capacity). All instruments are connected to a data logger and logger scan rates are set at 5 minutes for the

first 24 hours of a load/unload increment and every hour thereafter until the load/unload increment is deemed complete. The laboratory seasonal temperature ranges between 19°C and 24°C, producing maximum dimensional variance of 0.011 mm or about a 0.1% variation for 10-mm-thick specimen (Baumgartner et al. 2008). This small variation is considered insignificant and no thermal compensation is included in any calculation.

### **A3. TEST PROCEDURE**

#### **A3.1 TEST MATRIX FOR HCB SPECIMENS**

The test matrix for HCB specimens is shown in Table A1. Four specimens are initially planned for 1D consolidation of the HCB (i.e., Specimens HCB7, 8, 9, and 10). One additional specimen with 150 g/L  $\text{CaCl}_2$  is added to the specimen matrix (i.e., Specimen HCB11) to define the relationship of the pore liquid concentration and the mechanical behaviour of the HCB. The availability of a load frame and only minor additional work in preparing specimen HCB11 are also the reasons of this additional specimen. Combined with the previous tests (Baumgartner et al. 2008), this test matrix examines the effect of the  $\text{CaCl}_2$  concentration, different mixing liquid (Distilled Water (DW) or  $\text{CaCl}_2$ ), and different boundary conditions during initial saturation on the mechanical behaviour of HCB.

**Table A1: 1-D Consolidation Test Matrix for HCB Specimens in 2007**

<b>Specimen No.</b>	<b>Mixing Liquid</b>	<b>Reservoir Liquid</b>	<b>Target Initial Dry Density (kg/m<sup>3</sup>)</b>	<b>Target Initial Degree of Saturation (%)</b>	<b>Initial Boundary Condition During Saturation</b>	<b>Load Sequence</b>
HCB7	Distilled water	250 g/L CaCl <sub>2</sub>	1650	95	Constant pressure at 1 MPa	Load to 1, 2, 4, 8, & 16 MPa Unload to 8, 4, 2, & 1 MPa
HCB8	250 g/L CaCl <sub>2</sub>	250 g/L CaCl <sub>2</sub>	1650	95	Constant pressure at 1 MPa	Load to 1, 2, 4, 8, & 16 MPa Unload to 8, 4, 2, & 1 MPa
HCB9	Distilled water	Distilled water	1650	95	Constant volume	Load to 1, 2, 4, 8, & 16 MPa Unload to 8, 4, 2, & 1 MPa
HCB10	250 g/L CaCl <sub>2</sub>	250 g/L CaCl <sub>2</sub>	1650	95	Constant volume	Load to 1, 2, 4, 8, & 16 MPa Unload to 8, 4, 2, & 1 MPa
HCB11*	Distilled water	150 g/L CaCl <sub>2</sub>	1650	95	Constant pressure at 1 MPa	Load to 1, 2, 4, 8, & 16 MPa Unload to 8, 4, 2, & 1 MPa

\* This specimen was added to the test plan at the end of 2007.

### **A3.2 SPECIMEN PREPARATION**

Two different mixing liquids are used in the tests to examine the type of liquid that should be considered in the preparation of sealing-system components for a placement-room in a Deep Geological Repository (DGR). All the specimens are compacted with the target dry density of ~1650 kg/m<sup>3</sup> with a target degree of saturation of ~95%. This result in a target gravimetric water content (w) of 23% for specimens mixed with distilled water and 27% for specimens mixed with 250 g/L CaCl<sub>2</sub>. The salt remaining in the specimen during the oven-dry process changes the value of gravimetric water content. Baumgartner et al. (2008) discussed the pore-liquid concentration affecting the volume-mass relationships.

The HCB specimens are fabricated from 80-mesh granules of Wyoming bentonite (MX80). Dry Wyoming bentonite (MX80) is mixed with the liquid in a small beaker. Liquid is added slowly with a syringe to achieve uniform gravimetric water content and avoid lumps during the mixing process. The mixing of the HCB with 250 g/L CaCl<sub>2</sub> is easier as compared to mixing with

distilled water with less formation of lumps. Heat is generated in the mixing of the HCB with 250 g/L CaCl<sub>2</sub>, which is not observed when mixing with distilled water. This may be due to a reaction between the salt solution and the bentonite.

The target mass to be compacted in the cell is calculated based on the target dry density and degree of saturation. This calculated mass is added to the cell and the gravimetric water content analysis is made from the remaining specimen mixture. Filter papers and filter stones are installed on top and bottom of the specimen, and the specimen assembly is installed in the oedometer. The specimen is compacted in one lift in the oedometer ring with a hydraulic press (target thickness ~10-mm). The compaction piston has a scribed mark on its outer surface, which permits the technologist to observe when the specimen has reached its required initial density. The actual initial thickness is measured using calipers by measuring the piston stick-up of the cell.

For specimens HCB7, HCB8, and HCB11 a constant pressure load of 1 MPa was applied to settle the specimen assembly. The specified liquid was added to the reservoir after that. For specimens HCB9 and HCB10 with the initial constant volume boundary condition during initial saturation, the servo-hydraulic testing system was set to zero strain and a small vertical stress of approximately 0.1 MPa was initially applied. After liquid is added to the reservoir, the pressure increases due to the constrained swelling of the specimen.

### A3.3 SPECIMEN LOADING, RESERVOIR LIQUID MAINTENANCE, AND DISMANTLING

The specimen load is adjusted with the regulator on the nitrogen (N<sub>2</sub>) cylinder. The duration of the load increment is dependent on the response of the tests and specimens. Plastic shrouding encloses the assembly and reservoir to minimize evaporation. Three different liquids are used as the reservoir liquid in the tests: distilled water, 250 g/L CaCl<sub>2</sub>, and 150 g/L CaCl<sub>2</sub>. Due to evaporation of the reservoir liquid over the period of the test, liquid levels need to be replenished periodically. During the evaporation, only water is removed from the cell, the amount of the salt within the cell is constant. Therefore, distilled water is periodically added in the cell during the test to maintain a relatively constant salt concentration in the liquid reservoir.

At the end of the test the thickness and the gravimetric water content of the specimen are measured. The values of gravimetric water content, dry density, and Effective Montmorillonite Dry Density (EMDD) upon the installation are summarized in Table A2. Considering the high concentration of the pore liquid (i.e., 250 g/L CaCl<sub>2</sub>), the four-component soil system volume-mass relationships (Baumgartner et al. 2008) are used to calculate these values. The definition of the 'apparent' gravimetric water ( $w_{(app)}$ ), the 'true' gravimetric water content ( $w_w$ ), and the gravimetric liquid content ( $w_l$ ) in the four-component soil system are summarized as follows.

The 'apparent' gravimetric water content ( $w_{(app)}$ ) is:

$$w_{(app)} = \frac{M_{wet} - M_{dry}}{M_{dry}} = \frac{M_w}{M_s + M_{salt}} \quad (A1)$$

where:  $M_{\text{wet}}$  - mass of wet specimen;  
 $M_{\text{dry}}$  - the mass of oven-dry specimen;  
 $M_{\text{w}}$  - the mass of water;  
 $M_{\text{salt}}$  - mass of salt;  
 $M_{\text{s}}$  - mass of solid.

The 'true' gravimetric water content ( $w_w$ ) is:

$$w_w = \frac{M_w}{M_s} \quad (\text{A2})$$

The gravimetric liquid content ( $w_l$ ) is:

$$w_l = \frac{M_l}{M_s} = \frac{M_w + M_{\text{salt}}}{M_s} \quad (\text{A3})$$

The relationships of all three gravimetric water contents are presented in Baumgartner et al. (2008). These relationships and the required formulas to calculate volume-mass relationships of soil with saline pore liquid are summarized in Table A3.

The smectite minerals dominate the behaviour of the clay fraction in the bentonites and the smectite content varies in bentonite from different global sources. The term effective montmorillonite dry density (EMDD) was derived (Baumgartner and Snider 2002, JNC 2000) to single out the role of montmorillonite in soil behaviour and is expressed as follows:

$$\text{EMDD} = \frac{M_m}{(V_m + V_v)} = \frac{f_m \cdot f_c \cdot \rho_d}{\left[ 1 - \left( \frac{(1-f_c) \cdot \rho_d}{G_a \cdot \rho_w} \right) - \left( \frac{(1-f_m) \cdot f_c \cdot \rho_d}{G_n \cdot \rho_w} \right) \right]} \quad (\text{A4})$$

where  $M_m$  = mass of montmorillonite component (kg);  
 $V_m$  = volume occupied by montmorillonite component ( $\text{m}^3$ );  
 $V_v$  = volume of void ( $\text{m}^3$ );  
 $f_m$  = mass fraction of montmorillonite in clay fraction  $f_c$  (e.g., > 75% in MX80);  
 $f_c$  = mass fraction of clay in dry solids (e.g., ~100% in bentonite clay);  
 $G_a$  = relative density of aggregate solid (e.g., quartz sand = 2.65);  
 $G_n$  = relative density of non-montmorillonite component in clay (e.g., 2.645);  
 $\rho_w$  = density of water ( $\text{kg}/\text{m}^3$ ); and  
 $\rho_d$  = dry density of soil ( $\text{kg}/\text{m}^3$ ).

Tables A4 and A5 shows the properties of the HCB and the liquid to calculate the EMDD of HCB, respectively.

**Table A2: Dimension, Mass Composition, Liquid Properties, Water Contents, Densities, Void Ratio, and Porosity of Specimens HCB7, HCB8, HCB9, HCB10, and HCB11 at Installation**

<b>Specimen No.</b>	<b>HCB7</b>	<b>HCB8</b>	<b>HCB9</b>	<b>HCB10</b>	<b>HCB11</b>
<b>DIMENSION</b>					
Thickness (mm)	10.45	10.27	9.60	10.38	9.74
Diameter (mm)	28.20	28.19	28.12	28.1	28.17
Volume (cm <sup>3</sup> )	6.53	6.41	5.96	6.44	6.07
<b>LIQUID PROPERTIES</b>					
Liquid	Distilled Water	CaCl <sub>2</sub> Solution	Distilled Water	CaCl <sub>2</sub> Solution	Distilled Water
TDS (g/L)	0	250	0	250	0
Concentration (mol/L)	0	2.253	0	2.253	0
Density of liquid (Mg/m <sup>3</sup> )	1	1.1879	1	1.1879	1
<b>VOLUME-MASS PROPERTIES</b>					
"Apparent" gravimetric water content, $w_{(app)}$ (%)	22.5	18.60	23.10	19.1	23.10
Gravimetric liquid content, $w_l$ (%)	22.5	24.79	23.10	25.49	23.10
Gravimetric water content, $w_w$ (%)	22.5	19.57	23.10	20.13	23.10
Bulk density (Mg/m <sup>3</sup> )	1.92	2.03	2.10	2.02	2.07
Dry density (Mg/m <sup>3</sup> )	1.57	1.63	1.71	1.61	1.68
Effective Montmorillonite Dry Density (EMDD) (Mg/m <sup>3</sup> )	1.38	1.44	1.529	1.425	1.499
Void ratio, $e$	0.75	0.69	0.606	0.704	0.633
Porosity, $n$	0.43	0.41	0.377	0.413	0.388
<b>MASS COMPOSITION</b>					
Bulk Mass (g)	12.55	13.03	12.55	13.01	12.56
Mass of Soil Solids (g)	10.25	10.44	10.20	10.37	10.20
Mass of Liquid (g)	2.30	2.59	2.35	2.64	2.36
Mass of Water (g)	2.30	2.04	2.35	2.09	2.36
Mass of CaCl <sub>2</sub> (g)	0.00	0.54	0.00	0.56	0.00

**Table A3: Summary of Equations for Calculation of Mass-Volume Relationships of Soil with Saline Pore Liquid**

Input Data
<p>Data measured in the laboratory test:  <math>M_{\text{wet}}</math> = Mass of wet soil specimen;  <math>M_{\text{dry}}</math> = Mass of dry soil specimen; and  <math>V_{\text{total}}</math> = total volume.</p> <p>Data required to calculate mass-volume relationship:  <math>G_s</math> = specific gravity of the soil solid phase;  TDS = total dissolved solid of the solution (g/L); and  <math>\rho_l</math> = density of the solution (liquid phase) (<math>\text{Mg}/\text{m}^3</math>)</p>
Ratio of mass of solute to the mass of solution ( $C_m$ )
$C_m = \frac{\text{TDS (g/L)}}{\rho_l (\text{Mg}/\text{m}^3) \times 1000}$
“Apparent” gravimetric water content ( $w_{(\text{app})}$ ), gravimetric water content ( $w_w$ ), and gravimetric liquid content ( $w_l$ )
<p>“Apparent” gravimetric water content (<math>w_{(\text{app})}</math>)</p> $w_{(\text{app})} = \frac{M_{\text{wet}} - M_{\text{dry}}}{M_{\text{dry}}} \times 100\% = \frac{M_w}{M_s + M_{\text{salt}}} \times 100\%$ <p>Gravimetric water content (<math>w</math>)</p> $w = \frac{M_w}{M_s} \times 100\% = \frac{w_{(\text{app})} \cdot (1 - C_m)}{1 - C_m(1 + w_{(\text{app})})}$ <p>Gravimetric liquid content (<math>w_l</math>)</p> $w_l = \frac{M_l}{M_s} \times 100\% = \frac{w_{(\text{app})}}{1 - C_m(1 + w_{(\text{app})})}$

**Summary of Equations for Calculation of Mass-Volume Relationships of Soil with Saline Pore Liquid (Table A3 Continued)**

**Bulk Density ( $\rho_{\text{bulk}}$ )**

$$\rho_{\text{bulk}} = \frac{M_{\text{wet}}}{V_{\text{total}}} = \frac{M_s + M_w + M_{\text{salt}}}{V_{\text{total}}}$$

**Dry Density ( $\rho_{\text{dry}}$ )**

$$\rho_{\text{dry}} = \frac{\rho_{\text{bulk}}}{1 + w_l}$$

**Void ratio (e) and porosity (n)**

$$e = \frac{G_s \cdot \rho_w}{\rho_{\text{dry}}} - 1$$

$$n = \frac{e}{1 + e}$$

**Degrees of saturation (S)**

Degree of saturation ( $S_l$ )

$$S = \frac{V_l}{V_v} \times 100\% = \frac{V_w + V_{\text{salt}}}{V_v} \times 100\% = \frac{w_l \cdot G_s \cdot \rho_w}{e \cdot \rho_l} \times 100\%$$

**Saturated density ( $\rho_{\text{sat}}$ )**

$$\rho_{\text{sat}} = \frac{G_s \cdot \rho_w + e \cdot \rho_l}{1 + e}$$

**Summary of Equations for Calculation of Mass-Volume Relationships of  
Soil with Saline Pore Liquid (Table A3 Concluded)**

**List of symbols**

$\rho_{\text{bulk}}$	= bulk density	[Mg/m <sup>3</sup> ]
$\rho_{\text{dry}}$	= dry density	[Mg/m <sup>3</sup> ]
$\rho_l$	= density of the solution (liquid phase)	[Mg/m <sup>3</sup> ]
$\rho_{\text{sat}}$	= density of specimen at 100% saturation	[Mg/m <sup>3</sup> ]
$\rho_w$	= density of water	[Mg/m <sup>3</sup> ]
$C_m$	= ratio of the mass of solute to the mass of solution	[no unit]
$e$	= void ratio (i.e., ratio of the volume of void ( $V_v$ ) to the volume of solid ( $V_s$ ))	[no unit]
$G_s$	= specific gravity of the soil solid phase	[no unit]
$M_{\text{wet}}$	= mass of wet soil specimen, before oven-drying process	[Mg]
$M_{\text{dry}}$	= mass of dry soil specimen, after oven-drying process	[Mg]
$M_w$	= mass of water	[Mg]
$M_{\text{salt}}$	= mass of salt	[Mg]
$M_s$	= mass of solid phase	[Mg]
$n$	= porosity	[no unit]
$S$	= degree of saturation (i.e., ratio of the volume of liquid phase to the volume of void)	[%]
TDS	= total dissolved solid of the solution (liquid phase)	[g/L]
$V_l$	= volume of liquid phase	[m <sup>3</sup> ]
$V_{\text{salt}}$	= volume of salt	[m <sup>3</sup> ]
$V_s$	= volume of solid	[m <sup>3</sup> ]
$V_{\text{total}}$	= total volume of soil specimen	[m <sup>3</sup> ]
$V_v$	= Volume of void	[m <sup>3</sup> ]
$V_w$	= volume of water	[m <sup>3</sup> ]
$w_{\text{app}}$	= "Apparent" gravimetric water content (i.e., the gravimetric water content measured directly from the oven-drying process)	[%]
$w$	= gravimetric water content (i.e., ratio of the mass of water to the mass of solid)	[%]
$w_l$	= gravimetric liquid content (i.e., ratio of the mass of liquid phase to the mass of solid)	[%]

**Table A4: Properties of Highly Compacted Bentonite (HCB)**

Material	HCB (Highly Compacted Bentonite)
Material Composition	100% Wyoming Bentonite
Relative density of solid, $G_s$	2.745
Relative density of aggregate, $G_a$	1
Relative density of non-montmorillonite component in clay, $G_n$	2.645
Mass fraction of clay in dry solids, $f_c$	100%
Mass fraction of montmorillonite in clay fraction, $f_m$	75%
Density of water, $r_w$ ( $\text{g/cm}^3$ ) =	1

**Table A5: Properties of the Liquid**

Liquid	Distilled water ( $\text{H}_2\text{O}$ )	Calcium Chloride ( $\text{CaCl}_2$ )	
TDS (g/L)	0	150	250
Salt concentration, $c$ (mol/L)	0	1.352	2.253
Density of liquid, $\rho_l$ ( $\text{Mg/m}^3$ )	1	1.1147*	1.1879*

\* Lide (2007)

## A4. RESULTS

### A4.1 THICKNESS AND VERTICAL STRESS VERSUS TIME

Figures A1 to A5 show the applied vertical stress and thickness of the specimens HCB7, 8, 9, 10, and 11. Some issues experienced during the tests that cannot be avoided include the unintended pressure loss due to the depletion of nitrogen-gas cylinder (i.e., Specimens HCB7, 8, 9, 10, and 11). A two-cylinder set up will be employed in the future tests to eliminate this problem. During the testing of HCB11, the LVDT was found to stick periodically during the unload portion of the test, resulting in a less-smooth plot of displacement than would otherwise have been anticipated. This stick-release of the sensor did not affect the ability of the data to be analysed.

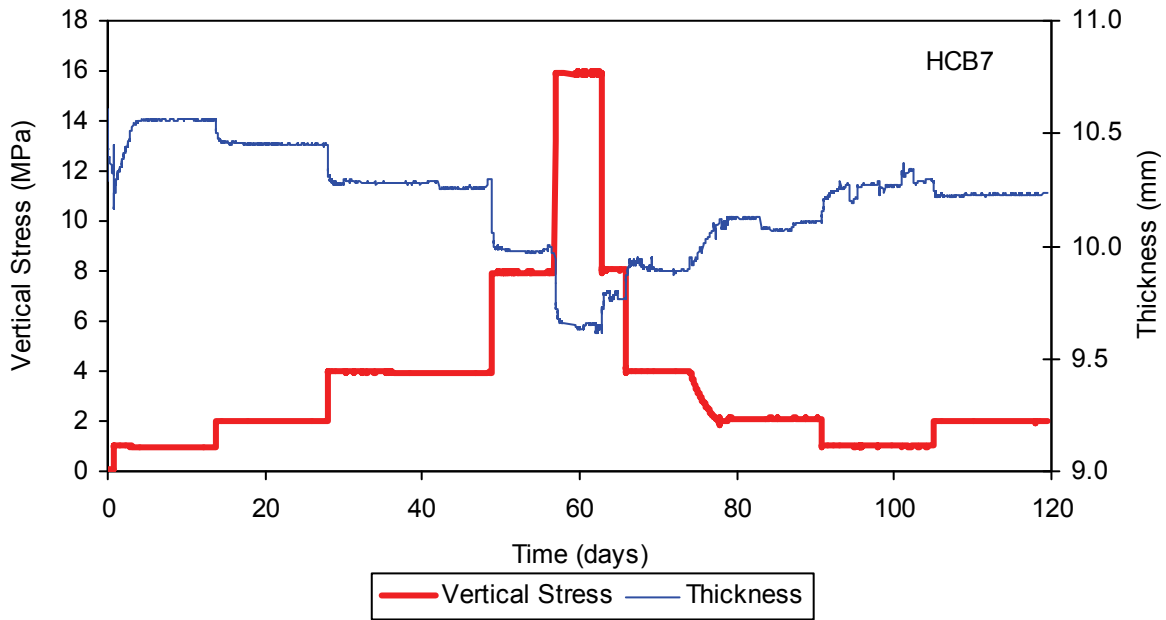


**Figure A1: Loading and Displacement History of Specimen HCB7**  
(Mixing Liquid = Distilled Water; Reservoir Liquid = 250 g/L CaCl<sub>2</sub>)

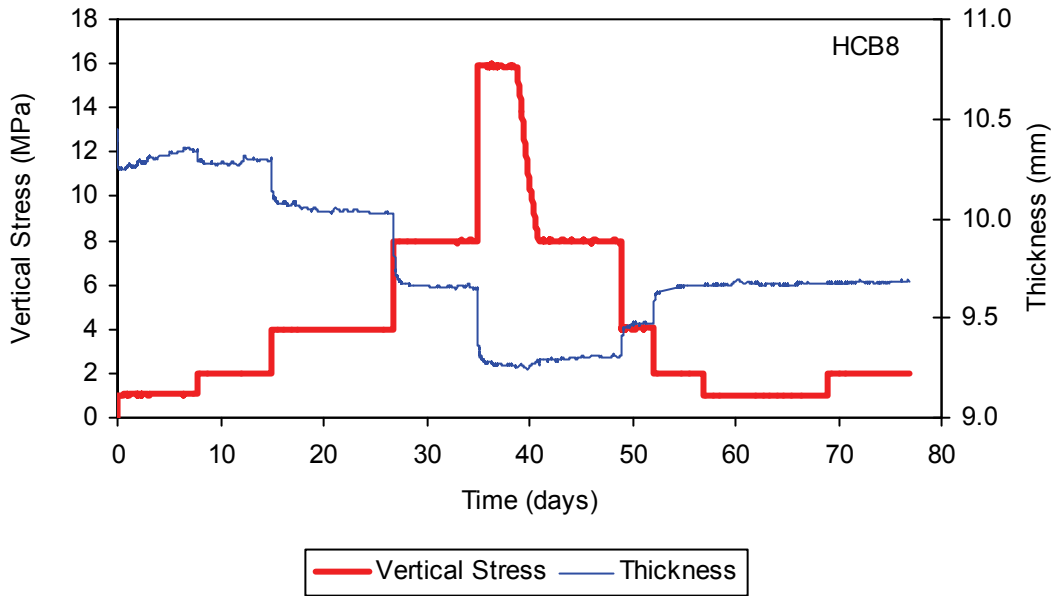


**Figure A2: Loading and Displacement History of Specimen HCB8**  
(Mixing Liquid = Reservoir Liquid = 250 g/L CaCl<sub>2</sub>)

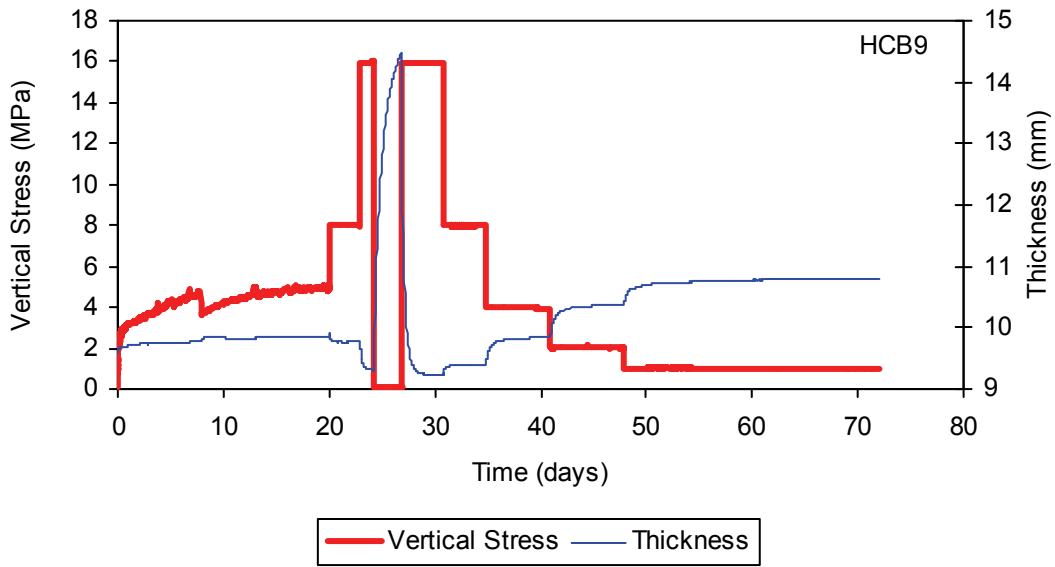


**Figure A3: Loading and Displacement History of Specimen HCB9 (Mixing Liquid = Reservoir Liquid = Distilled Water)**

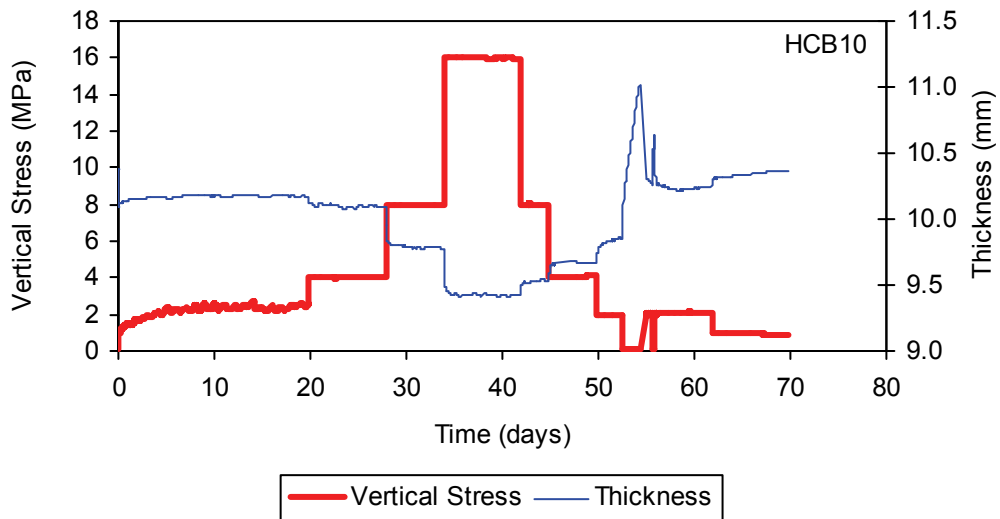


**Figure A4: Loading and Displacement History of Specimen HCB10 (Mixing Liquid = Reservoir Liquid = 250 g/L CaCl<sub>2</sub>)**

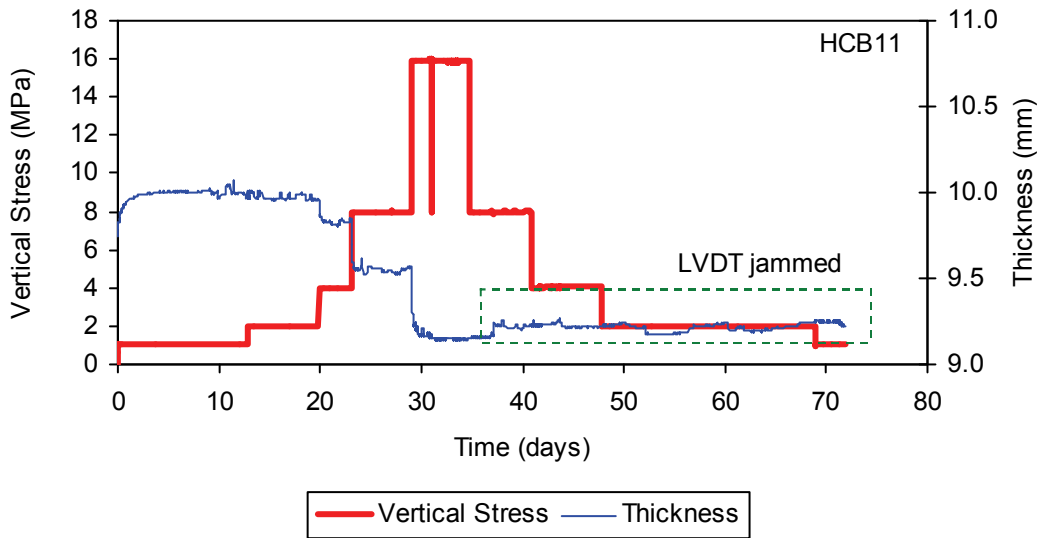


**Figure A5: Loading and Displacement History of Specimen HCB11 (Mixing Liquid = Distilled Water; Reservoir Liquid = 150 g/L CaCl<sub>2</sub>)**

#### **A4.2 VOID RATIO ( $e$ ), DRY DENSITY ( $\rho_{\text{DRY}}$ ), AND EMDD VERSUS VERTICAL STRESS ( $\sigma_v$ )**

##### **A4.2.1 HCB7**

Specimen HCB7 was prepared with distilled water as a mixing liquid and 250 g/L CaCl<sub>2</sub> as a reservoir liquid. Figure A6 shows the void ratio ( $e$ ) versus vertical stress ( $\sigma_v$ ) of Specimen HCB7. Constant pressure of 1 MPa was applied to Specimen HCB7 at the initial saturation. The vertical stress was increased up to maximum 16 MPa and decreased back to 1 MPa. This vertical stress was increased to 2 MPa before the test was ended. The corresponding dry density ( $\rho_{\text{dry}}$ ) versus vertical stress ( $\sigma_v$ ) is illustrated in Figures A7.

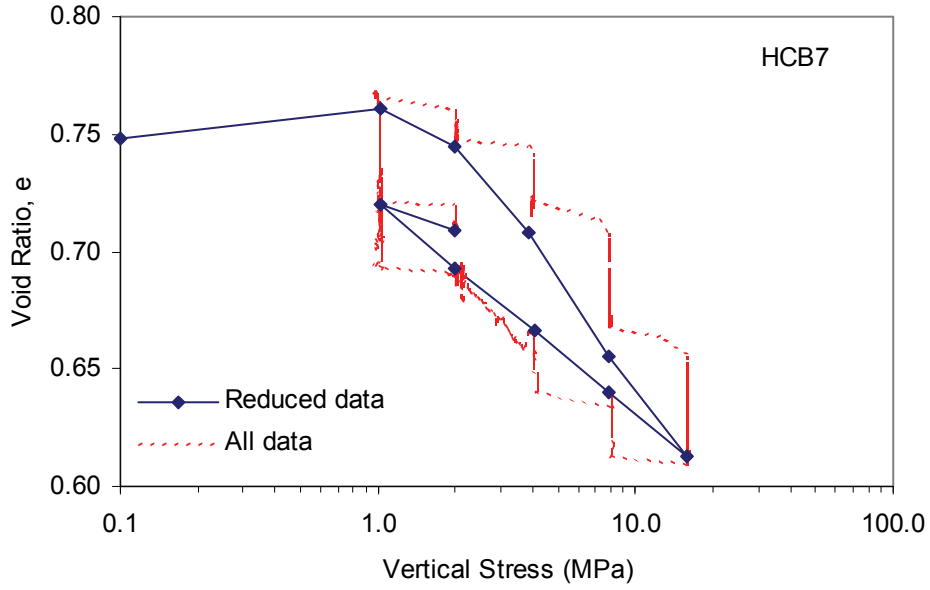


**Figure A6: Void Ratio versus Vertical Stress of Specimen HCB7**  
(Reduced data = data point at the end of each load increment)

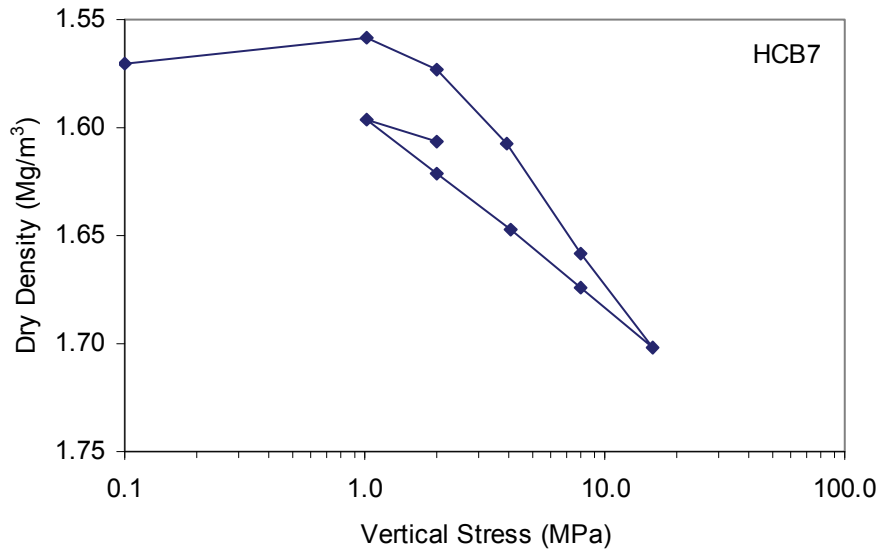


**Figure A7: Dry Density versus Vertical Stress of Specimen HCB7**

### A4.2.2 HCB8

Specimen HCB8 was prepared with distilled water containing 250 g/L CaCl<sub>2</sub> as mixing liquid and reservoir liquid. Figure A8 shows the void ratio ( $e$ ) versus vertical stress ( $\sigma_v$ ) of Specimen HCB8. Constant pressure of 1 MPa is applied on Specimen HCB8 at the initial saturation. The specimen HCB8 has a similar loading sequence as Specimen HCB7. The corresponding dry density ( $\rho_{dry}$ ) versus vertical stress ( $\sigma_v$ ) is illustrated in Figure A9.

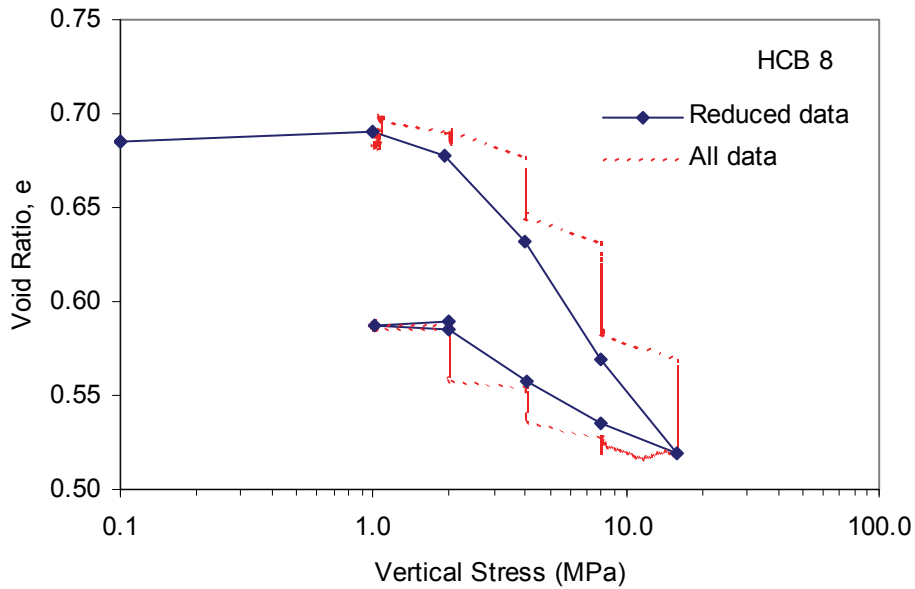


**Figure A8: Void Ratio versus Vertical Stress of Specimen HCB8**  
(Reduced data = data point at the end of each load increment)

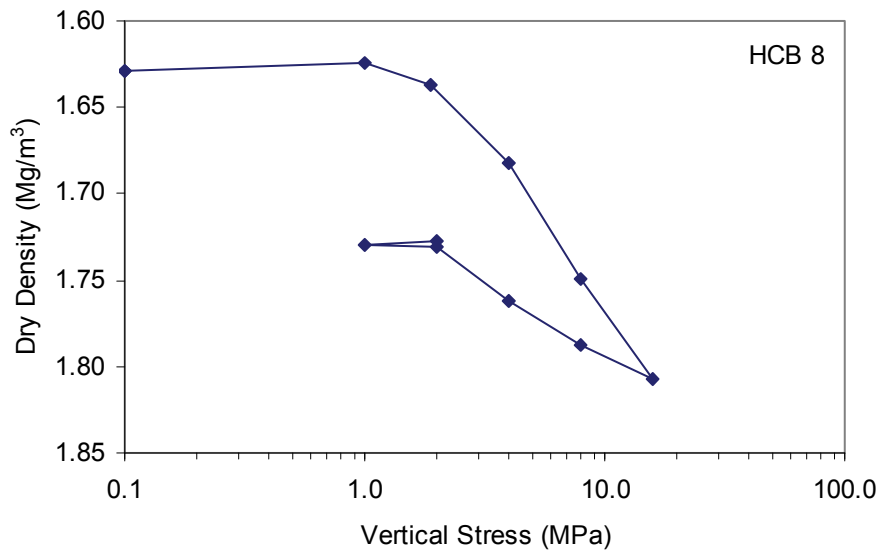


**Figure A9: Dry Density versus Vertical Stress of Specimen HCB8**

### A4.2.3 HCB9

Specimen HCB9 was prepared with distilled water as mixing and reservoir liquids. Figure A10 shows the void ratio ( $e$ ) versus vertical stress ( $\sigma_v$ ) for Specimen HCB9. The corresponding dry density versus vertical stress for Specimen HCB9 is shown in Figures A11. The numbers in Figures A10 and A11 indicate the load sequence of the test. A constant volume boundary condition was applied during the initial saturation (i.e., load sequence no 1 to 2 in Figures A10 and A11). The change of the vertical stress during initial saturation is shown in Figure A12 with a maximum vertical stress of approximately 5 MPa applied. The vertical stress was increased up to 16 MPa (i.e., load sequence no 2 to 3 in Figure A10 and A11). An unintended pressure loss occurred due to the depletion of nitrogen-gas cylinder after the vertical stress of 16 MPa was reached (i.e., load sequence no 3 to 4 in Figure A10 and A11). It was decided to continue the test, despite of the pressure loss, considering the length of the test. The vertical stress was decreased up to 1 MPa before removal of the specimen from the apparatus (i.e., load sequence no 4 to 5 in Figure A10 and A11). The data during the pressure loss section are not included in Figures A10 and A11.

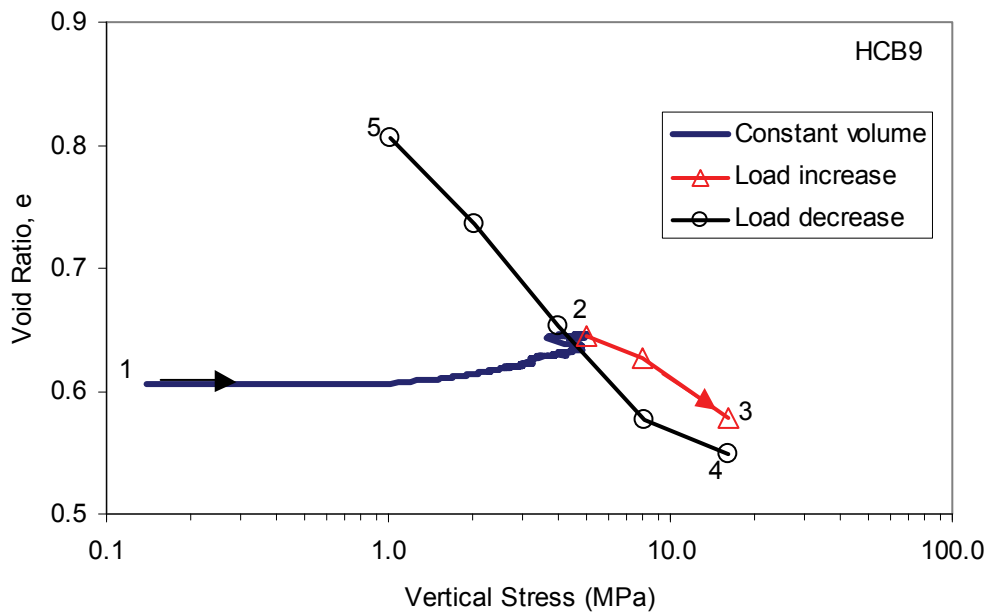


**Figure A10: Void Ratio versus Vertical Stress of Specimen HCB9**  
(Note: numbers show load sequence)

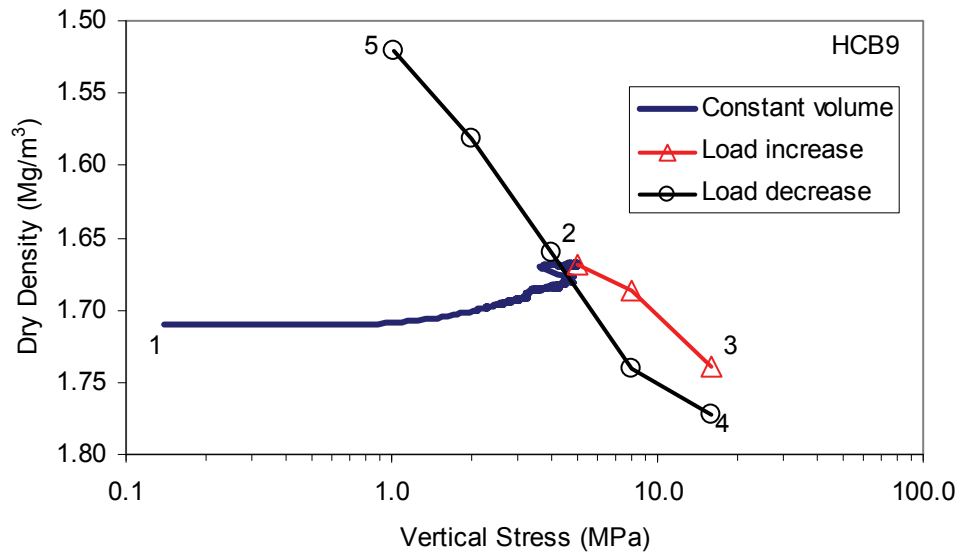


**Figure A11: Dry Density versus Vertical Stress of Specimen HCB9**  
(Note: numbers show load sequence)

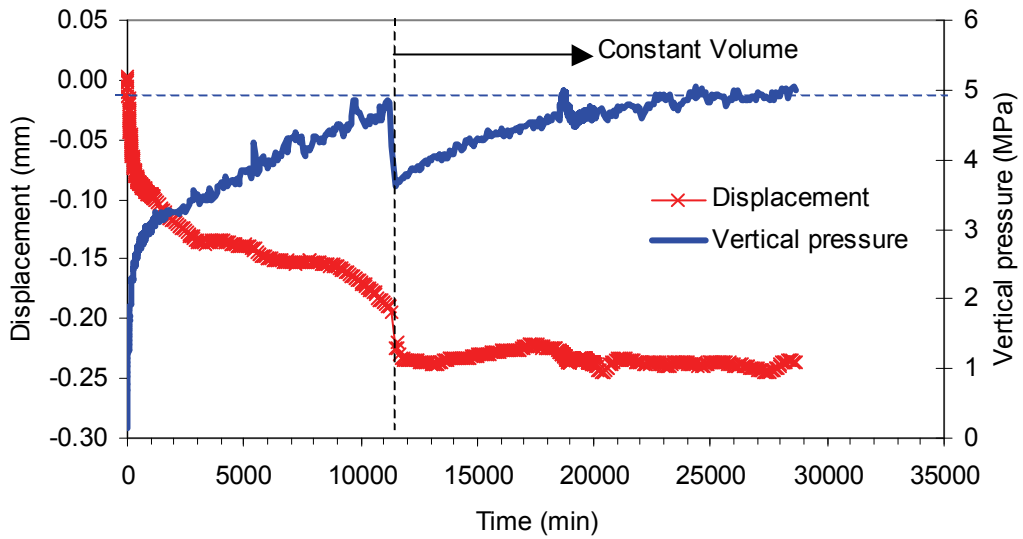


**Figure A12: The Displacement and Vertical Stress during Initial Saturation of Specimen HCB9**

#### A4.2.4 HCB10

Specimen HCB10 was prepared with distilled water containing 250 g/L CaCl<sub>2</sub> as mixing and reservoir liquids. Figure A13 shows the void ratio ( $e$ ) versus vertical stress ( $\sigma_v$ ) for Specimen HCB10. The corresponding dry density versus vertical stress of Specimen HCB10 is shown in Figure A14. A constant volume boundary condition was applied during the initial saturation. The maximum vertical stress at the initial saturation was approximately 2.3 MPa as shown in Figure A15. The vertical stress is increased up to 16 MPa and then decreased up to 2 MPa. Unintended pressure loss occurred in this test after the 2 MPa increment and so the data associated with this event are not included in Figures A13 and A14.

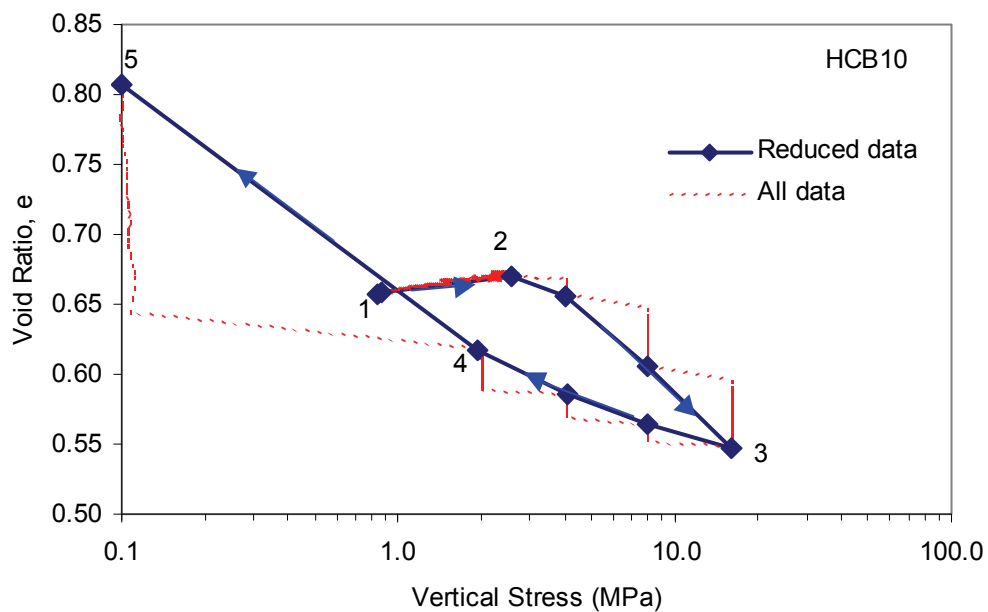


**Figure A13: Void Ratio versus Vertical Stress of Specimen HCB10**

(Note: numbers show load sequence;  
reduced data = data point at the end of each load increment)

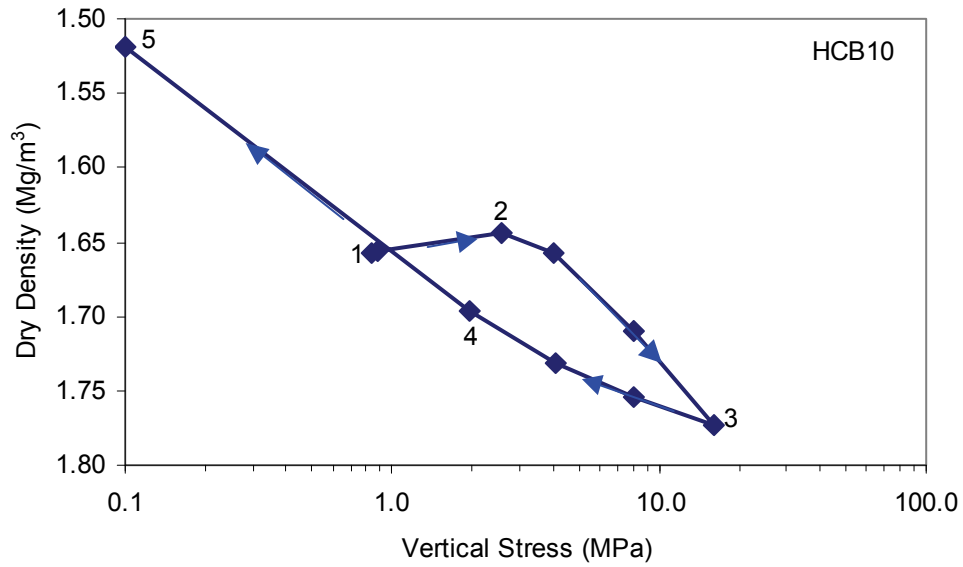


**Figure A14: Dry Density versus Vertical Stress of Specimen HCB10**  
(Note: numbers show load sequence)

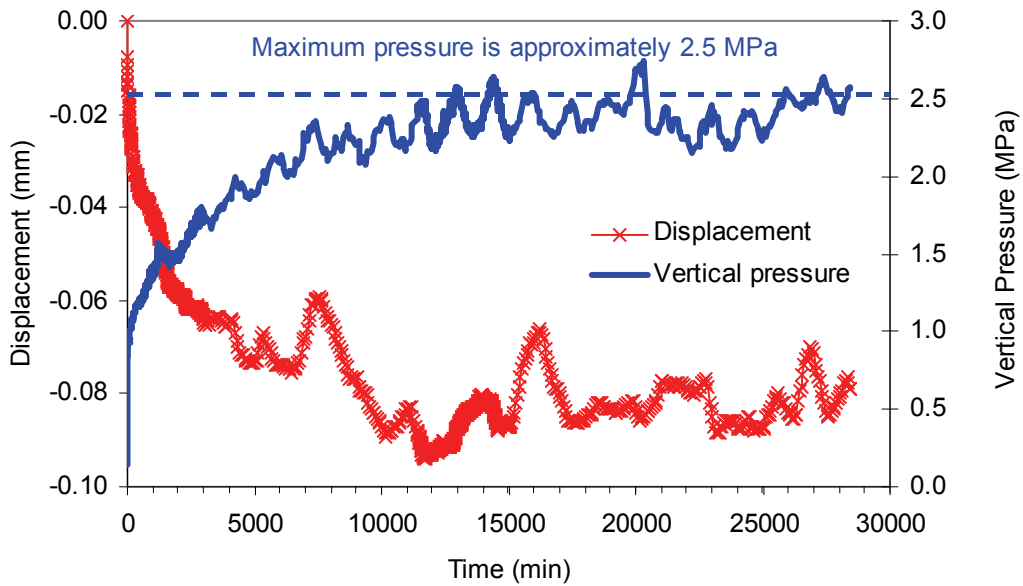


**Figure A15: The Displacement and Vertical Stress during Initial Saturation of Specimen HCB10**

### A4.2.5 HCB11

Specimen HCB11 was prepared with distilled water as the mixing liquid and 150 g/L  $\text{CaCl}_2$  as the reservoir liquid. Figures A17 and A18 show the void ratio ( $e$ ) and dry density versus vertical stress ( $\sigma_v$ ) of Specimen HCB11, respectively. A constant pressure of 1 MPa was applied during the initial saturation. The vertical stress was increased up to 16 MPa and then stepwise decreased to 1 MPa. The LVDT did not move during the decrease of vertical stress stage of testing. It was discovered at the end of this test that the LVDT was jammed. Data from this unloading portion of the experiment therefore cannot be used for consolidation calculations.

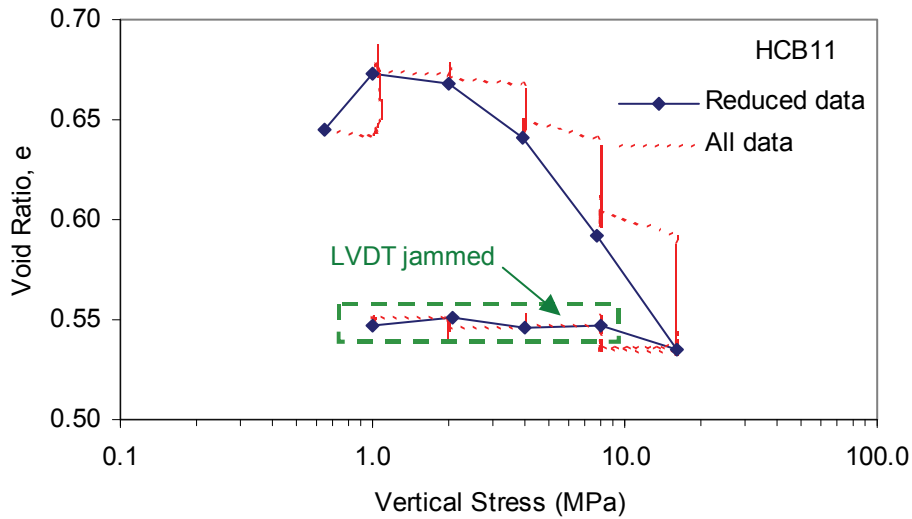


**Figure A16: Void Ratio versus Vertical Stress of Specimen HCB11**  
(Reduced data = data point at the end of each load increment)

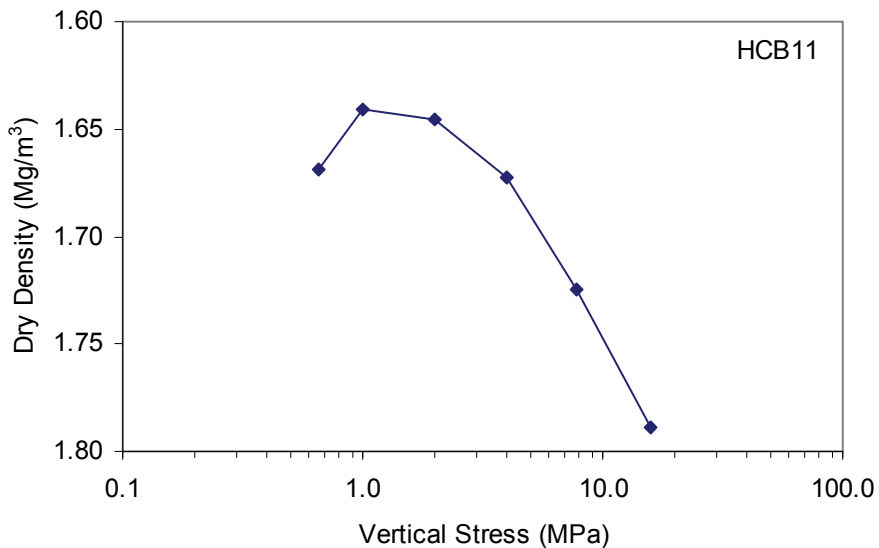


**Figure A17: Dry Density versus Vertical Stress of Specimen HCB11**

### A4.3 COEFFICIENT OF CONSOLIDATION ( $C_v$ )

The coefficient of consolidation ( $c_v$ ) can be generated from the results of 1D consolidation test from each load increment based on consolidation theory (Terzhagi 1943). The coefficient of consolidation ( $c_v$ ) is a hydraulic-mechanical (H-M) parameter that couples the coefficient of hydraulic conductivity in vertical direction ( $K_v$ ) and modulus of volume change ( $m_v$ ). The formulation of the coefficient of consolidation ( $c_v$ ) is limited to situations where the following assumptions apply (Budhu 2000).

1. The soil is saturated, isotropic, and homogeneous.
2. Darcy's law is valid.
3. Flow is only vertical.
4. The strains are small.

There are two common methods that can be used to calculate  $c_v$ .

1. The square root of time method (SQRT) (Taylor 1942).
2. The log time method (LogT) (Casagrande and Fadum 1940).

The procedures for determining the coefficient of consolidation can be found in most geotechnical engineering books (e.g., Budhu 2000, Craig 1992, Das 1998, etc.). The plots of displacement versus square root of time and displacement versus log of time for Specimens HCB7, 8, 9, 10, and 11 are shown in Figures A18 to A27, respectively.

Both methods were used to determine the coefficient of consolidation for each load increment. A comparison of the laboratory data and the calculated displacements based on the parameters determined by the two methods is shown in Figure A28 for Specimen HCB8 during compression under vertical stress of 16 MPa. There is only a slight difference in the coefficient of consolidation ( $c_v$ ) determined using the two different methods as shown by Figure A28. The coefficient of consolidation ( $c_v$ ) determined from the SQRT method is based on the matching of the data at the beginning of the primary consolidation, while  $c_v$  from the LogT method is based on the matching of the data at the end of the primary consolidation. The results of these analyses for Specimens HCB7 to HCB11 are shown in Tables A8 to A12, respectively.

The coefficient of consolidation ( $c_v$ ) versus the void ratio ( $e$ ) is shown in Figures A29 to A33 for Specimens HCB7 to HCB11 respectively. All specimens show that the coefficient of consolidation ( $c_v$ ) during compression is greater than that during swelling.

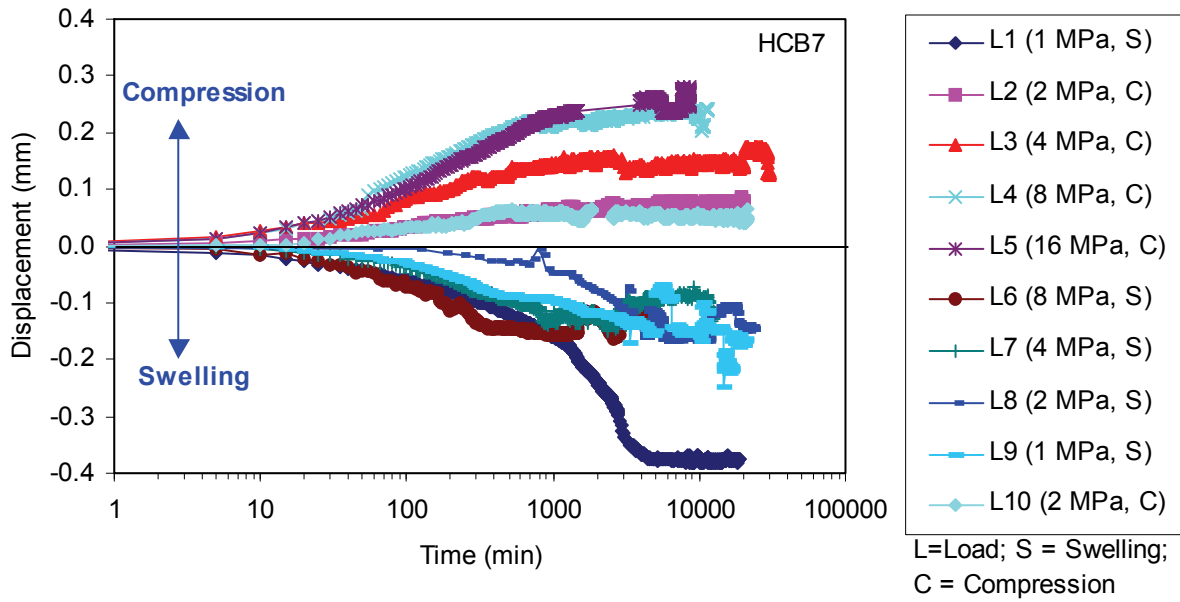


Figure A18: Displacement versus Time in Logarithmic Scale for Specimen HCB7

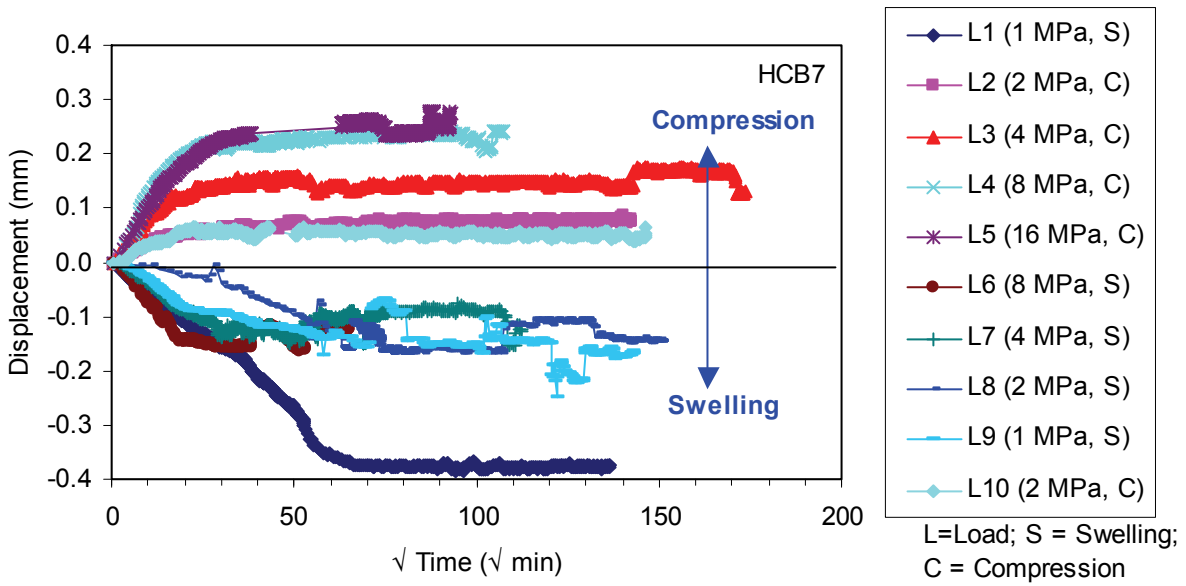


Figure A19: Displacement versus Square Root of Time for Specimen HCB7

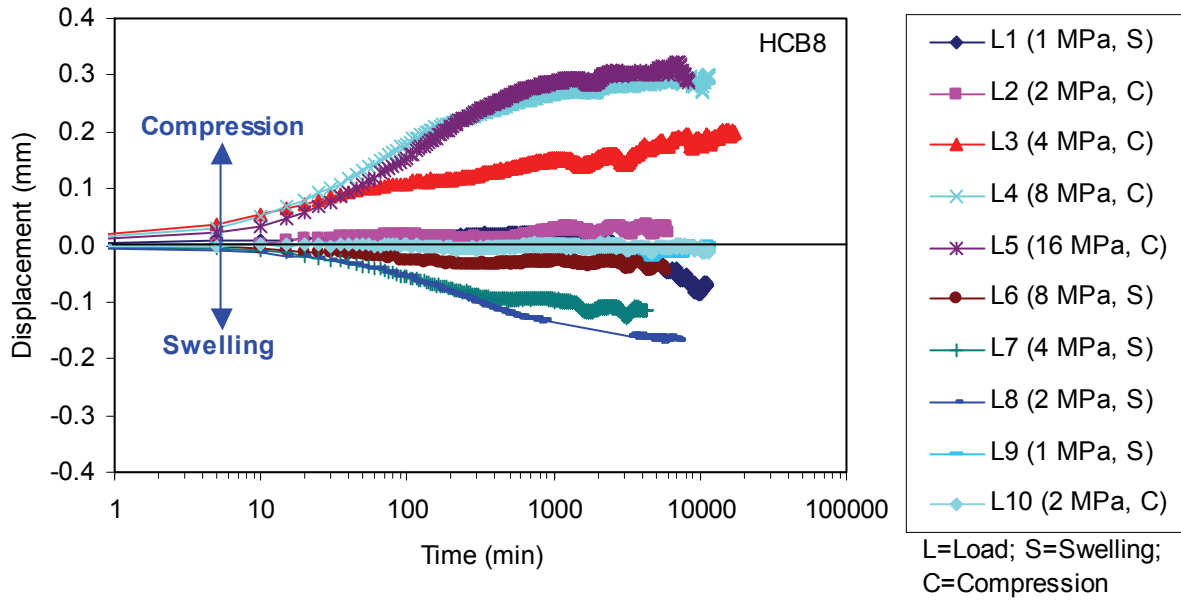


Figure A20: Displacement versus Time in Logarithmic Scale for Specimen HCB8

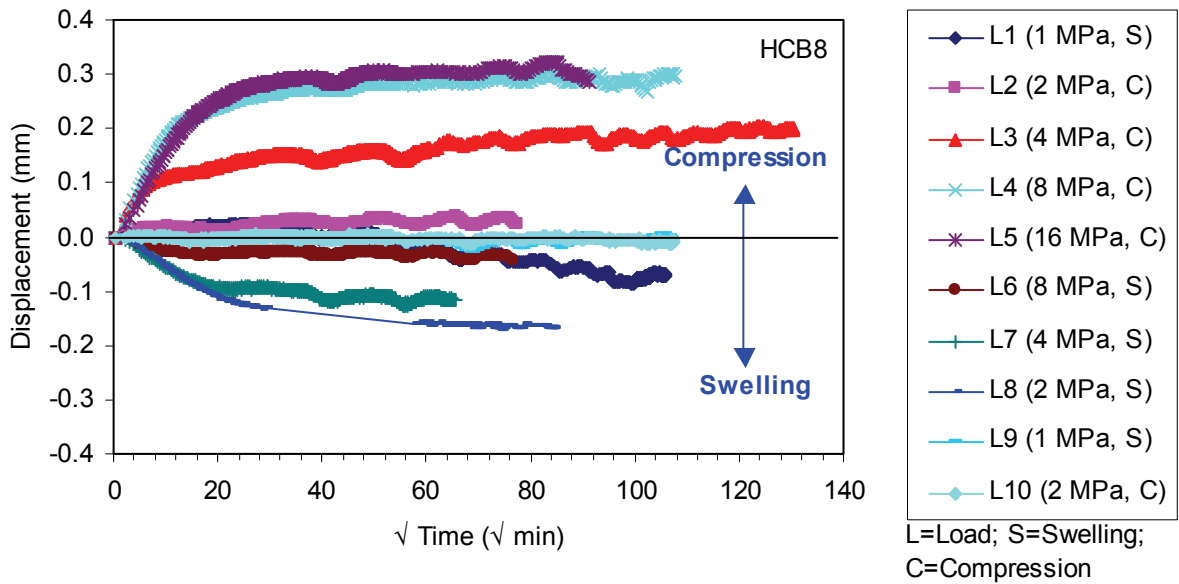


Figure A21: Displacement versus Square Root of Time for Specimen HCB8

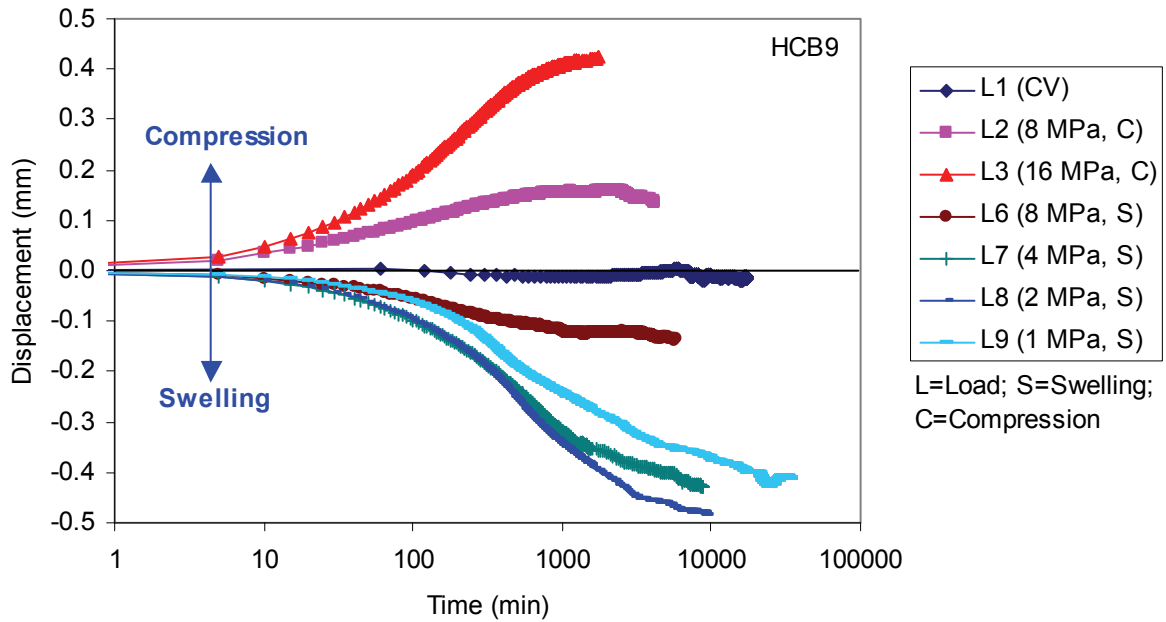


Figure A22: Displacement versus Time in Logarithmic Scale for Specimen HCB9

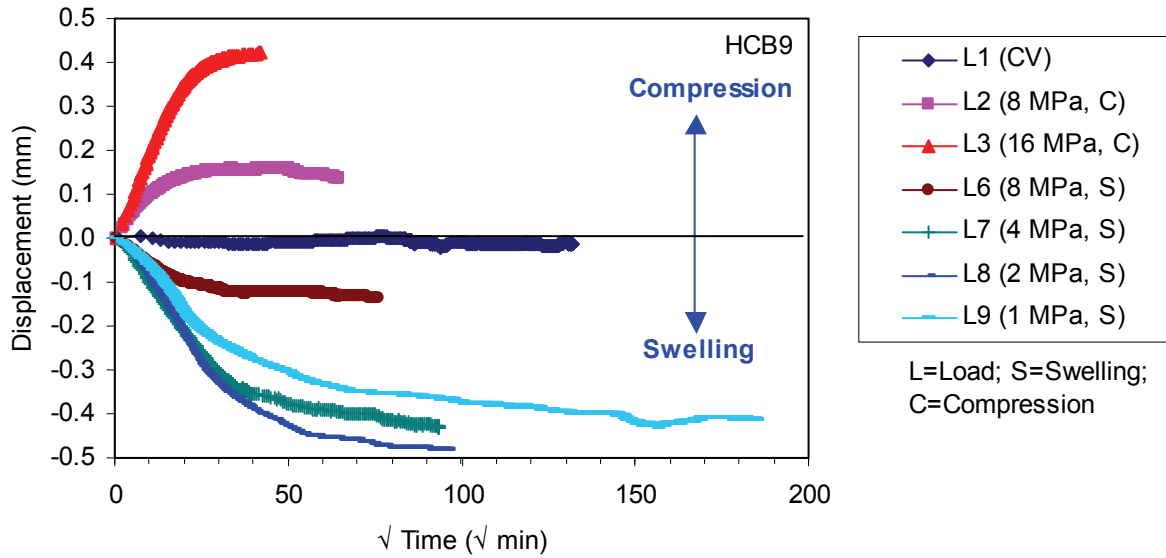


Figure A23: Displacement versus Square Root of Time for Specimen HCB9

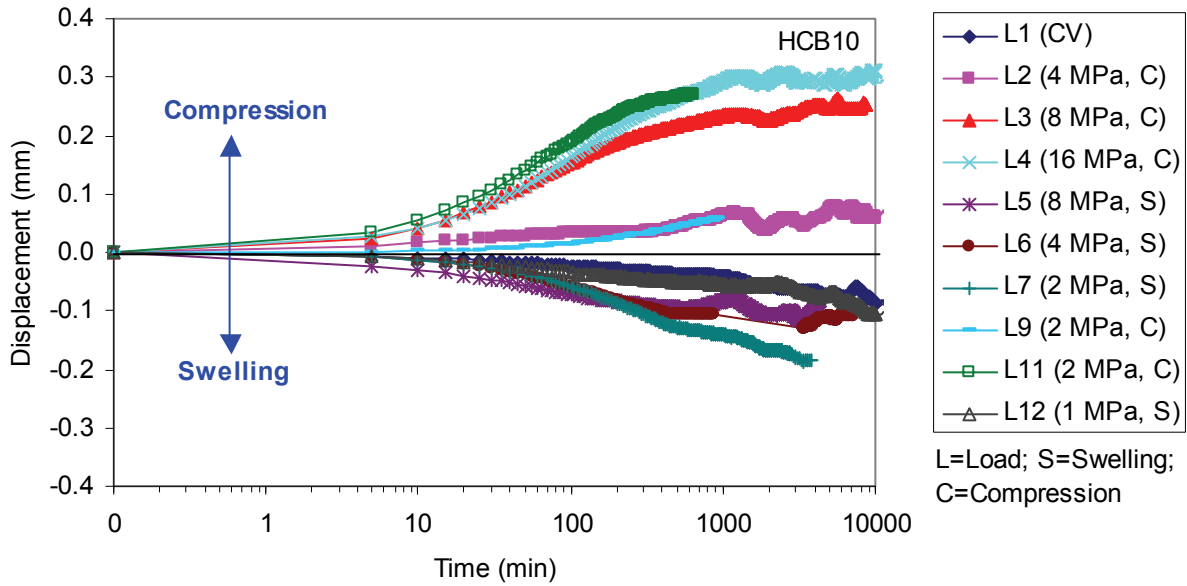


Figure A24: Displacement versus Time in Logarithmic Scale for Specimen HCB10

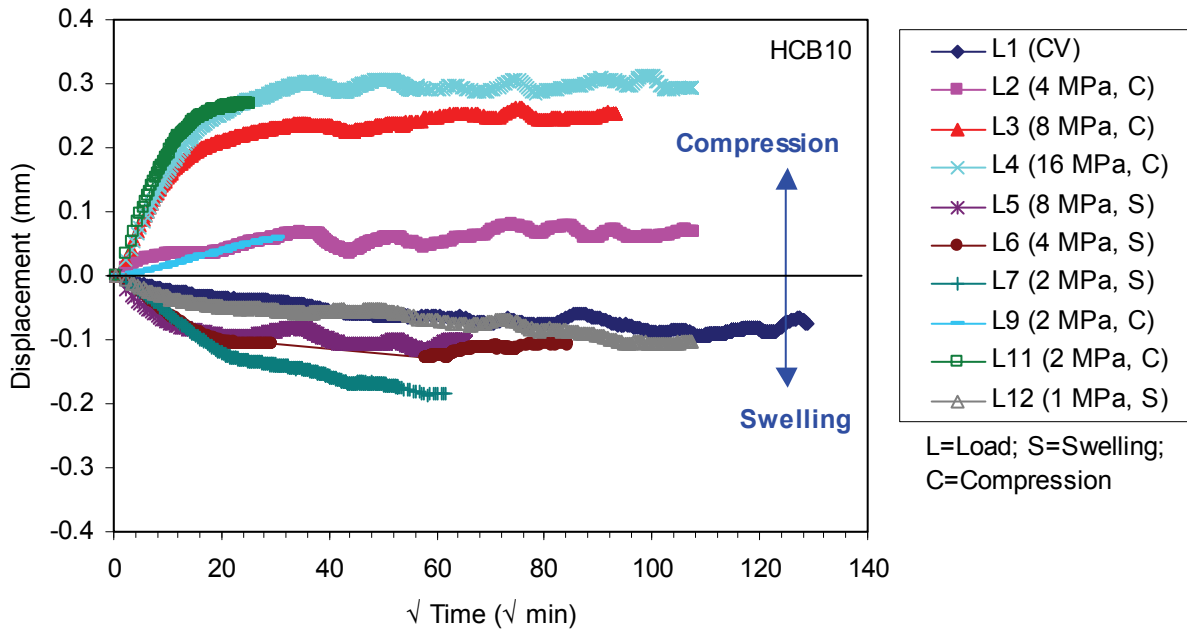


Figure A25: Displacement versus Square Root of Time for Specimen HCB10

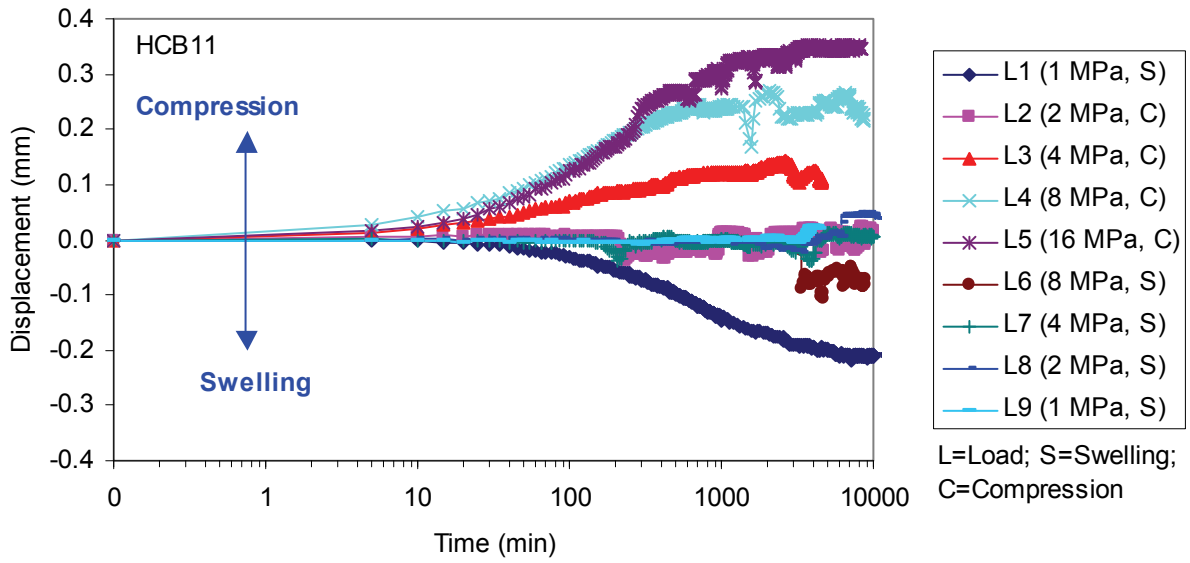


Figure A26: Displacement versus Time in Logarithmic Scale for Specimen HCB11

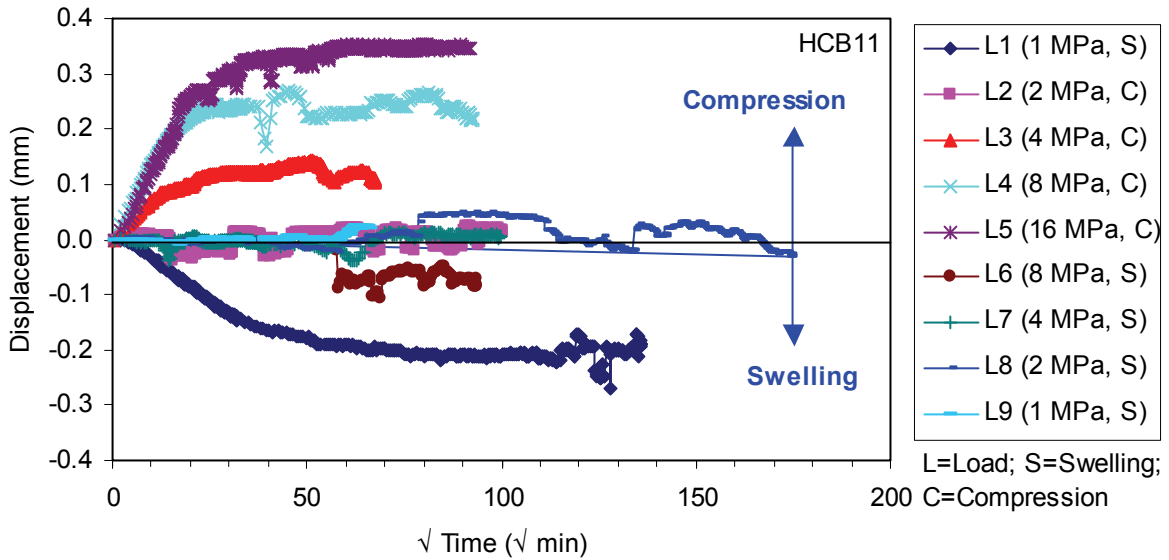
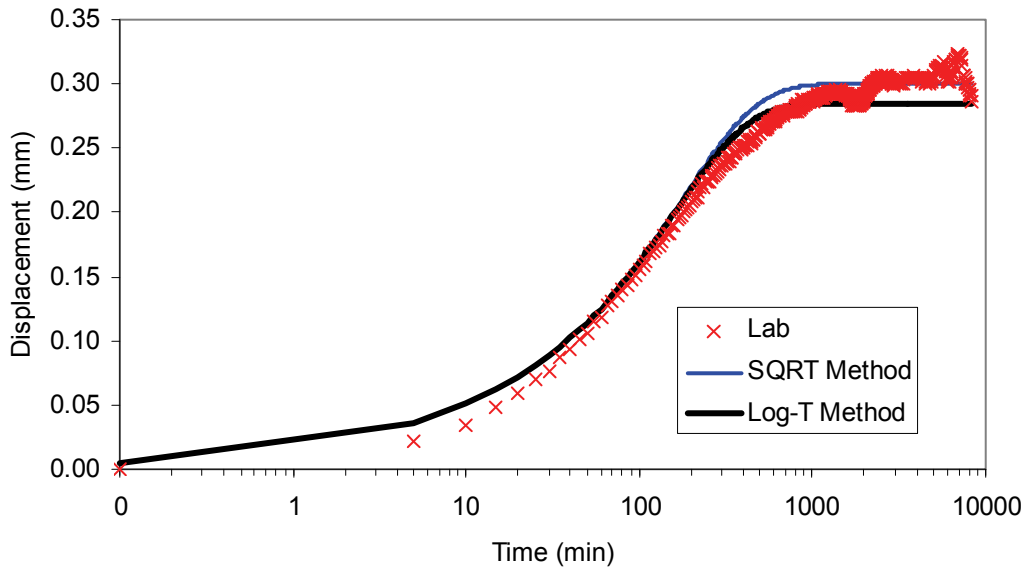


Figure A27: Displacement versus Square Root of Time for Specimen HCB11



**Figure A28: Displacement Calculated Using the Parameters Generated from Sqrt and Log-T Methods Compared with the Laboratory Test Data for Specimen HCB 8, Load 5 (16 MPa, Compression)**

**Table A6: Coefficient of Consolidation ( $c_v$ ) for Specimen HCB7**

Stage	Vertical stress (MPa)	Thickness (mm)	Void Ratio	Dry density (Mg/m <sup>3</sup> )	EMDD (Mg/m <sup>3</sup> )	Coefficient of Consolidation (mm <sup>2</sup> /min)					
						Compression			Swelling		
						Sqrt Time	Log Time	Average	Sqrt Time	Log Time	Average
Pre-Test	0	10.45	0.75	1.57	1.38						
1	1	10.53	0.76	1.56	1.37				0.006	0.004	0.005
2	2	10.43	0.74	1.57	1.39	0.040	0.036	0.038			
3	4	10.21	0.71	1.61	1.42	0.040	0.063	0.051			
4	8	9.89	0.66	1.66	1.48	0.041	0.057	0.049			
5	16	9.64	0.61	1.70	1.52	0.031	0.032	0.032			
6	8	9.80	0.64	1.67	1.49				0.036	0.038	0.037
7	4	9.96	0.67	1.65	1.46				0.020	0.023	0.021
8	2	10.12	0.69	1.62	1.44				0.003	0.002	0.003
9	1	10.28	0.72	1.60	1.41				0.015	0.016	0.016
10	2	10.22	0.71	1.61	1.42	0.066	0.065	0.066			
Average						0.044	0.051	0.047	0.016	0.017	0.016

**Table A7: Coefficient of Consolidation ( $c_v$ ) for Specimen HCB8**

Stage	Vertical stress (MPa)	Thickness (mm)	Void Ratio	Dry density (Mg/m <sup>3</sup> )	EMDD (Mg/m <sup>3</sup> )	Coefficient of Consolidation (mm <sup>2</sup> /min)						
						Compression			Swelling			
						Sqrt Time	Log Time	Average	Sqrt Time	Log Time	Average	
Pre-Test	0	10.27	0.68	1.63	1.44							
1	1	10.30	0.69	1.62	1.44							
2	2	10.23	0.68	1.64	1.45	0.043	0.116	0.079				
3	4	9.95	0.63	1.68	1.50	0.109	0.084	0.097				
4	8	9.57	0.57	1.75	1.57	0.109	0.084	0.097				
5	16	9.26	0.52	1.81	1.63	0.052	0.058	0.055				
6	8	9.36	0.54	1.79	1.61				0.089	0.114	0.102	
7	4	9.50	0.56	1.76	1.59				0.050	0.061	0.055	
8	2	9.67	0.59	1.73	1.55				0.030	0.025	0.027	
9	1	9.68	0.59	1.73	1.55							
10	2	9.69	0.59	1.73	1.55							
Average						0.078	0.085	0.082	0.056	0.067	0.061	

**Table A8: Coefficient of Consolidation ( $c_v$ ) for Specimen HCB9**

Stage	Vertical stress (MPa)	Thickness (mm)	Void Ratio	Dry density ( $Mg/m^3$ )	EMDD ( $Mg/m^3$ )	Coefficient of Consolidation ( $mm^2/min$ )					
						Compression			Compression		
						Sqrt Time	Log Time	Average	Sqrt Time	Log Time	Average
Pre-Test	0.1	9.60	0.61	1.71	1.53	N/A	N/A	N/A	N/A	N/A	N/A
1A	3.6	9.82	0.64	1.67	1.49	N/A	N/A	N/A	N/A	N/A	N/A
1B	5.0	9.84	0.65	1.67	1.49	N/A	N/A	N/A	N/A	N/A	N/A
2	8.0	9.73	0.63	1.69	1.51	0.058	0.081	0.069			
3	16.0	9.44	0.58	1.74	1.56	0.036	0.044	0.040			
5	16.0	9.26	0.55	1.77	1.60	0.048	0.061	0.055			
6	8.0	9.43	0.58	1.74	1.56				0.037	0.035	0.036
7	4.0	9.88	0.65	1.66	1.48				0.013	0.015	0.014
8	2.0	10.38	0.74	1.58	1.39				0.013	0.013	0.013
9	1.0	10.79	0.80	1.52	1.33				0.012	0.008	0.010
Average						0.047	0.062	0.055	0.016	0.016	0.016

**Table A9: Coefficient of Consolidation ( $c_v$ ) for Specimen HCB10**

Stage	Vertical stress (MPa)	Thickness (mm)	Void Ratio	Dry density ( $\text{Mg/m}^3$ )	EMDD ( $\text{Mg/m}^3$ )	Coefficient of Consolidation ( $\text{mm}^2/\text{min}$ )					
						Compression			Swelling		
						Sqrt Time	Log Time	Average	Sqrt Time	Log Time	Average
Initial	0.8	10.09	0.66	1.66	1.47						
	0.9	10.10	0.66	1.66	1.47						
1	2.6	10.17	0.67	1.64	1.46						
2	4.0	10.09	0.66	1.66	1.47	0.127	0.078	0.102			
3	8.0	9.78	0.61	1.71	1.53	0.101	0.083	0.092			
4	16.0	9.43	0.55	1.77	1.60	0.067	0.055	0.061			
5	8.0	9.53	0.56	1.75	1.58	0.142	0.125	0.134			
6	4.1	9.66	0.59	1.73	1.55				0.043	0.043	0.043
7	1.9	9.85	0.62	1.70	1.52				0.025	0.023	0.024
8	0.1	11.01	0.81	1.52	1.33						
9	2.0	10.26	0.68	1.63	1.44						
10	0.1	10.63	0.75	1.57	1.39						
11	2.1	10.25	0.68	1.63	1.45	0.117	0.109	0.113			
12	0.9	10.37	0.70	1.61	1.43				0.093	0.065	0.079
Average						0.111	0.090	0.100	0.054	0.044	0.049

**Table A10: Coefficient of Consolidation ( $c_v$ ) for Specimen HCB11**

Stage	Vertical stress (MPa)	Thickness (mm)	Void Ratio	Dry density ( $Mg/m^3$ )	EMDD ( $Mg/m^3$ )	Coefficient of Consolidation ( $mm^2/min$ )					
						Compression			Swelling		
						Sqrt Time	Log Time	Average	Sqrt Time	Log Time	Average
Initial	1	9.81	0.65	1.67	1.49						
1	1	9.98	0.67	1.64	1.46				0.007	0.008	0.007
2	2	9.95	0.67	1.65	1.46						
3	4	9.79	0.64	1.67	1.49	0.065	0.061	0.063			
4	8	9.49	0.59	1.72	1.54	0.057	0.059	0.058			
5	16	9.15	0.53	1.79	1.61	0.024	0.022	0.023			
Average						0.048	0.047	0.048	0.007	0.008	0.007

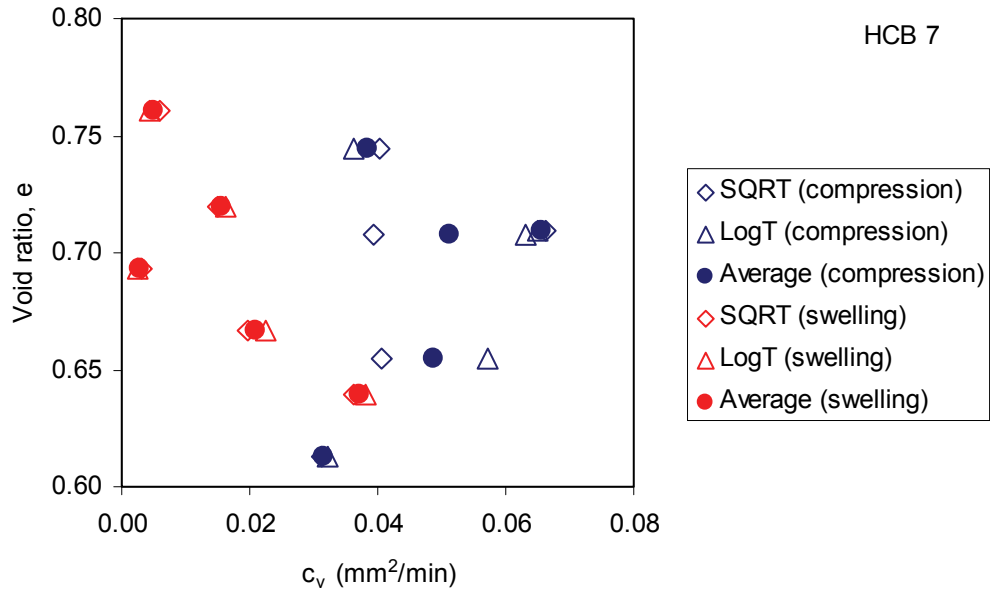


Figure A29: Void Ratio versus Coefficient of Consolidation ( $c_v$ ) of Specimen HCB7

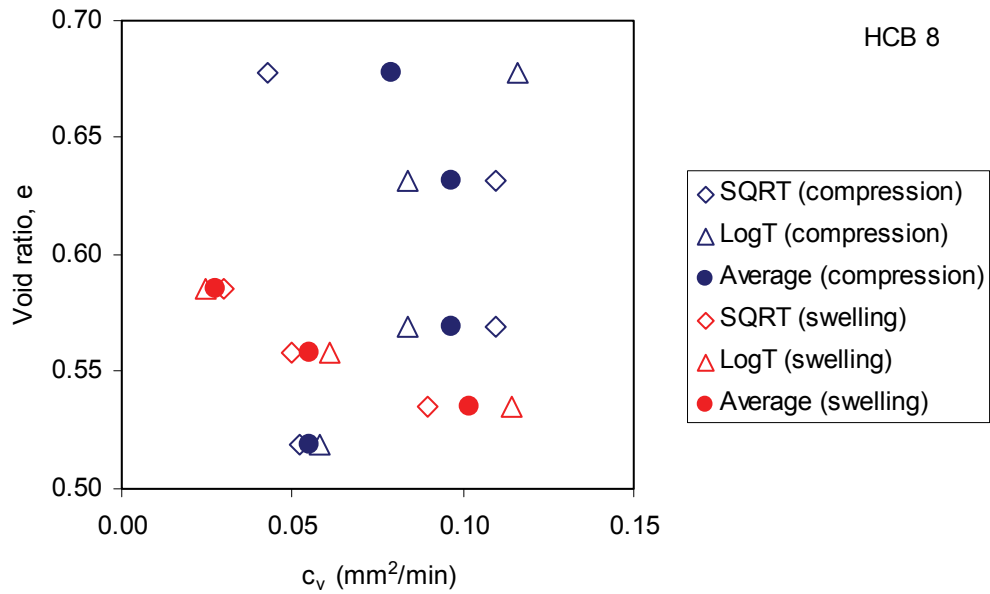


Figure A30: Void Ratio versus Coefficient of Consolidation ( $c_v$ ) of Specimen HCB8

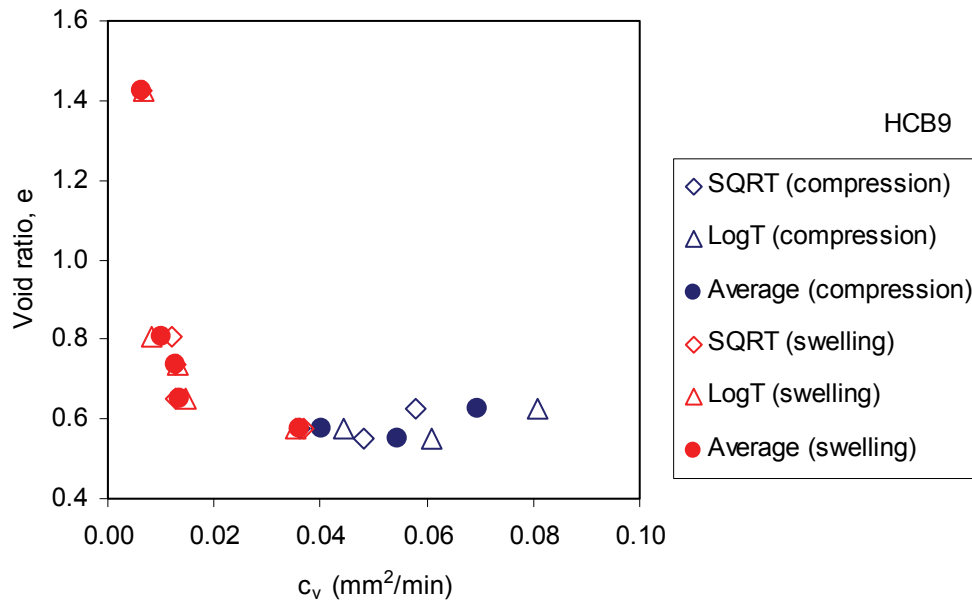


Figure A31: Void Ratio versus Coefficient of Consolidation (c<sub>v</sub>) of Specimen HCB9

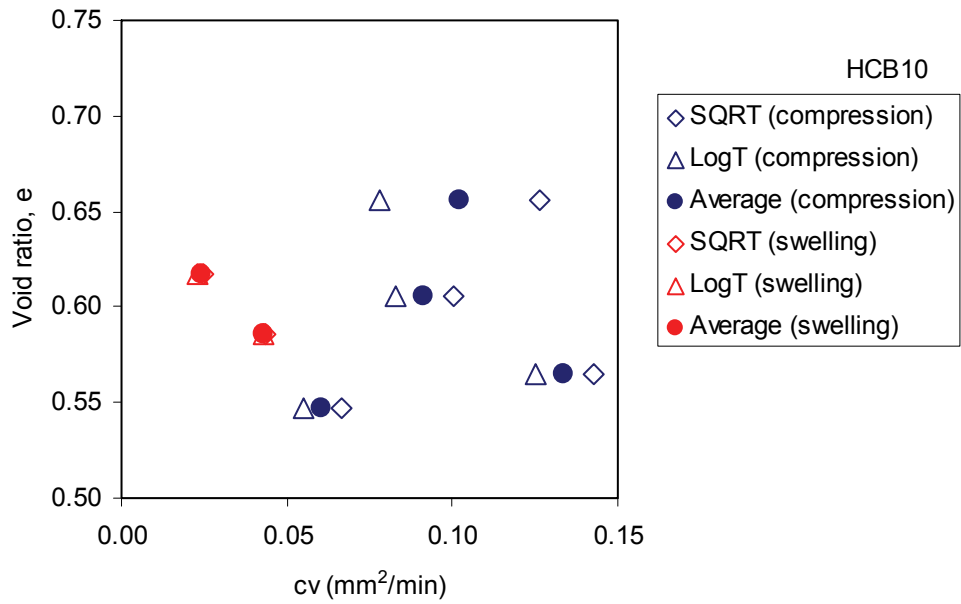
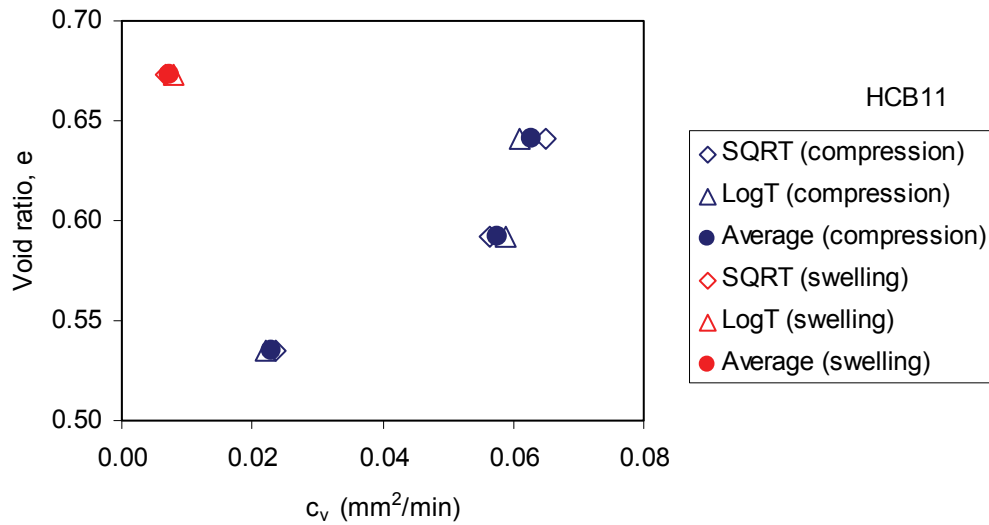


Figure A32: Void Ratio versus Coefficient of Consolidation (c<sub>v</sub>) of Specimen HCB10



**Figure A33: Void Ratio versus Coefficient of Consolidation ( $c_v$ ) of Specimen HCB11**

#### A4.4 HYDRAULIC CONDUCTIVITY (K)

The hydraulic conductivity (K) can be estimated from the coefficient of consolidation ( $c_v$ ) by assuming that the soil is linear elastic for each load increment.

$$K = c_v \cdot m_v \cdot \gamma_w \quad (A4)$$

where K - hydraulic conductivity (m/s);  
 $m_v$  - coefficient of volume compressibility (Pa<sup>-1</sup>);  
 $\gamma_w$  - unit weight of water (N/m<sup>3</sup>)

The hydraulic conductivity (K) estimated from Equation A4 as a function of EMDD is shown in Figure A34. The hydraulic conductivity (K) calculated from the results of 1D consolidation tests is within the range of  $1 \cdot 10^{-15}$  to  $1 \cdot 10^{-11}$  m/s for EMDD within the range of 1.1 to 1.6 Mg/m<sup>3</sup>; and it decreases with an increase of EMDD. This is comparable with the hydraulic conductivity (K) of the bentonite measured using hydraulic conductivity cells by Dixon et al. (1999) as shown in Figure A35.

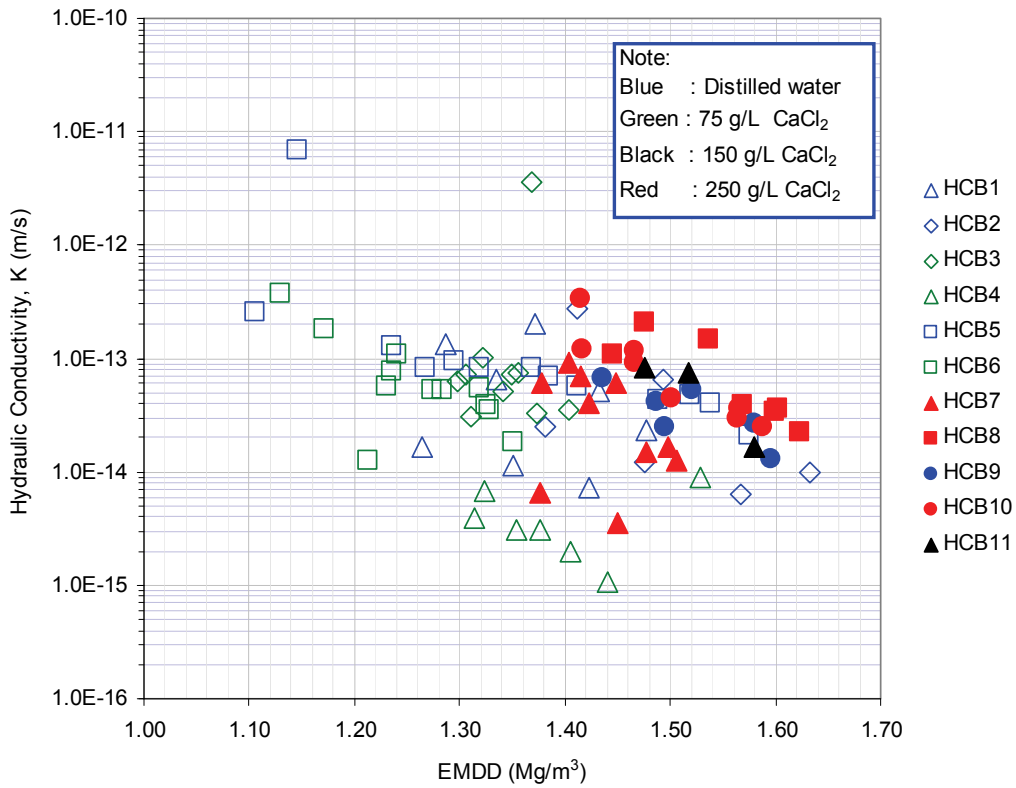


Figure A34: Hydraulic Conductivity Estimated from 1D-Consolidation Test for Highly Compacted Bentonite (HCB)

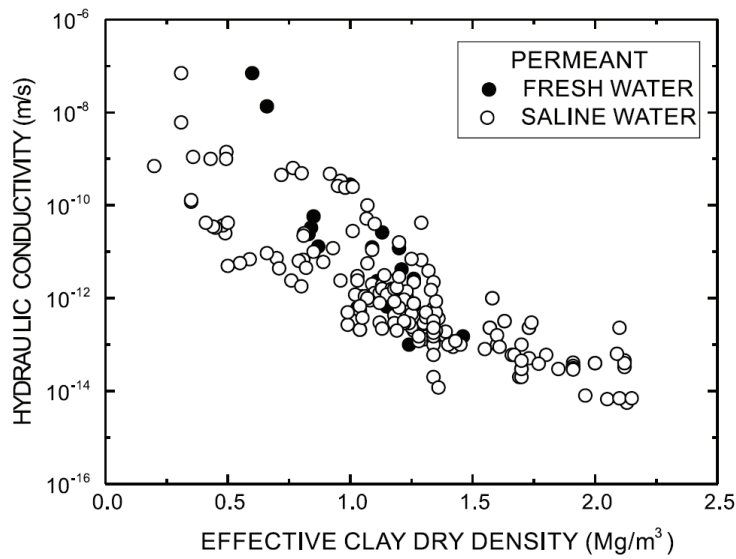


Figure A35: Hydraulic Conductivity ( $K$ ) of Bentonite Measured using Hydraulic Conductivity Cell (Dixon et al. 1999)

### A4.5 1D-MODULUS

The 1D consolidation tests only measure the displacement and stress in vertical direction. The horizontal stress during an oedometer test is unknown. Consequently only a 1D-constrained modulus ( $M$ ) can be estimated from the results of these tests. The 1D-constrained modulus ( $M$ ) of the soil can be calculated from the relationship of vertical strain ( $\epsilon_v$ ) and vertical stress increment ( $\sigma_v$ ). The 1D-constrained modulus ( $M$ ) for increasing loads is less than for decreasing loads. It should be recognized that the behaviour of soil is not linear elastic, especially for large strain changes. The soil can only be considered as a linear elastic material for a small strain increment. The mechanical behaviour of soils is also stress path dependent. The estimate values of 1D-constrained modulus ( $M$ ) for Specimens HCB1 to HCB11 versus EMDD are illustrated in Figure A36, the data are shown in Tables A11 to A21.

Numerical modelling usually starts using the simplest constitutive model, such as linear elastic model. In two-dimensional modelling, the linear elastic model requires two parameters to describe the mechanical behaviour: Young's modulus ( $E$ ) and Poisson's ratio ( $\nu$ ). The Young's modulus ( $E$ ) can be estimated from the 1D-constrained modulus ( $M$ ) by assuming the value of Poisson's ratio ( $\nu$ ). Representative Poisson's ratio ( $\nu$ ) for soft clay is 0.15-0.25. For medium clay Poisson's ratio ( $\nu$ ) is in the range of 0.2 to 0.5 (Das 1998). The Poisson's ratio ( $\nu$ ) of soil can be determined from the results of the triaxial test.

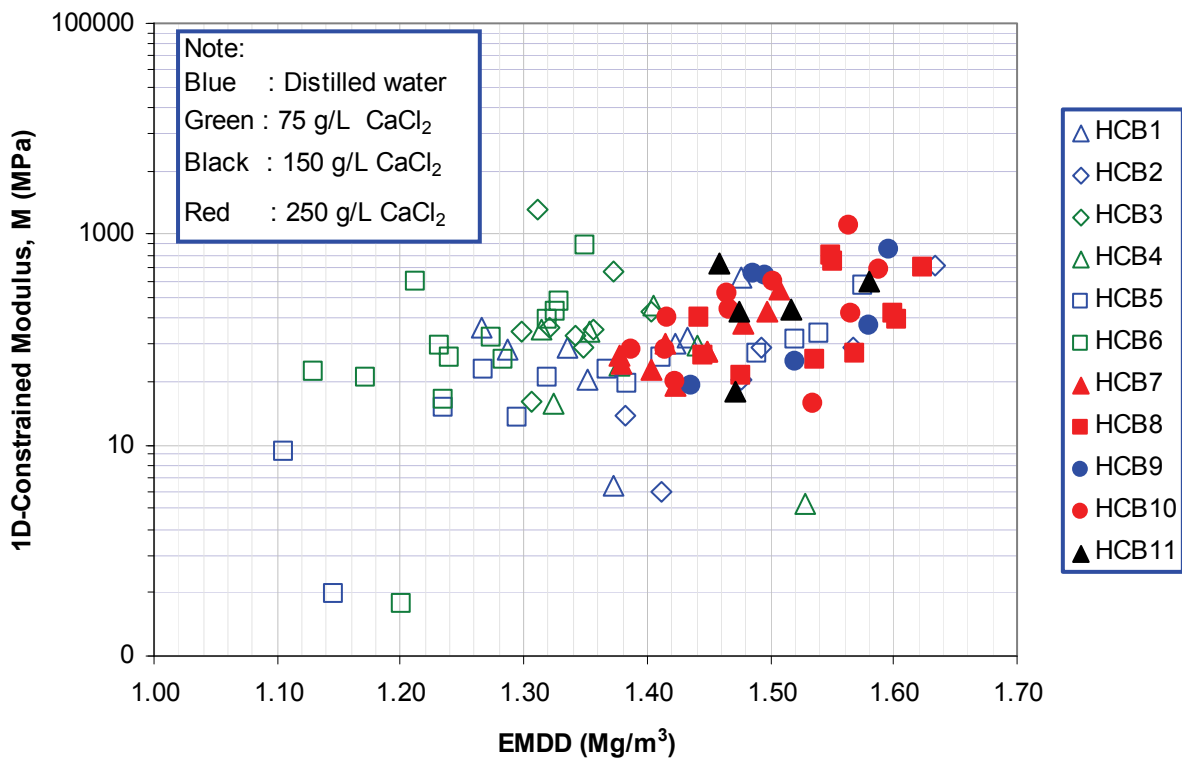


Figure A36: 1D-Constrained Modulus versus EMDD

**Table A11: 1D-Constrained Modulus for Specimens HCB1**

Stage	Vertical stress (MPa)	Vertical strain (%)	Vertical stress-mid value (MPa)	Void ratio-mid value, e	EMDD-mid value (Mg/m <sup>3</sup> )	1D-Constrained Modulus (MPa)			
						All	Initial	Loading	Unloading
start	0.38	0.0							
1	0.99	15.0	0.7	0.77	1.37	4	4		
2	2.1	14.2	1.5	0.88	1.27	130		130	
3	3.98	11.8	3.0	0.86	1.29	79		79	
4	7.97	7.1	6.0	0.80	1.34	85		85	
5	15.93	-0.6	12.0	0.70	1.43	103		103	
6	8.01	1.5	12.0	0.65	1.48	383			383
7	4.02	5.9	6.0	0.70	1.42	90			90
8	2	10.8	3.0	0.78	1.35	42			42
		Max	12.0	0.88	1.48	383	4	130	383
		Min	0.7	0.65	1.27	4	4	79	42
		Average	5.5	0.77	1.37	115	4	99	171

**Table A12: 1D-Constrained Modulus for Specimens HCB2**

Stage	Vertical stress (MPa)	Vertical strain (%)	Vertical stress-mid value (MPa)	Void ratio-mid value, e	EMDD-mid value (Mg/m <sup>3</sup> )	1D-Constrained Modulus (MPa)			
						All	Initial	Loading	Unloading
start	0.98	0.0							
1	1.31	9.2	1.1	0.72	1.41	4	4		
2	15.98	-8.4	8.6	0.65	1.49	83		83	
3	8.59	-6.9	12.3	0.52	1.63	506			506
4	4.27	-1.8	6.4	0.57	1.57	85			85
5	2.34	2.9	3.3	0.65	1.48	41			41
6	1.02	9.8	1.7	0.75	1.38	19			19
		Max	12.3	0.75	1.63	506	4	83	506
		Min	1.1	0.52	1.38	4	4	83	19
		Average	5.6	0.64	1.49	123	4	83	163

**Table A13: 1D-Constrained Modulus for Specimens HCB3**

Stage	Vertical stress (MPa)	Vertical strain (%)	Vertical stress-mid value (MPa)	Void ratio-mid value, e	EMDD-mid value (Mg/m <sup>3</sup> )	1D-Constrained Modulus (MPa)			
						All	Initial	Loading	Unloading
start	1.02	0.0							
1	1.03	11.1	1.0	0.76	1.37	0.1	0.1		
2	2.07	11.1	1.6	0.83	1.31	1710		1710	
3	3.94	9.7	3.0	0.82	1.32	128		128	
4	8.05	6.4	6.0	0.78	1.36	125		125	
5	3.99	7.3	6.0	0.76	1.37	445			445
6	1.96	9.7	3.0	0.78	1.35	86			86
7	1	13.4	1.5	0.83	1.31	26			26
8	3.98	10.8	2.5	0.84	1.30	117		117	
9	7.97	7.1	6.0	0.79	1.34	108		108	
10	15.88	2.7	11.9	0.73	1.40	181		181	
		Max	11.9	0.8	1.40	1710	0.1	1710	445.0
		Min	1.0	0.7	1.30	0.1	0.1	108	25.9
		Average	4.2	0.8	1.34	292	0.1	395	185.5

**Table A14: 1D-Constrained Modulus for Specimens HCB4**

Stage	Vertical stress (MPa)	Vertical strain (%)	Vertical stress-mid value (MPa)	Void ratio-mid value, e	EMDD-mid value (Mg/m <sup>3</sup> )	1D-Constrained Modulus (MPa)			
						All	Initial	Loading	Unloading
start	8.06	0.0							
1	8.22	5.8	8.1	0.61	1.53	3	3		
2	4.17	10.5	6.2	0.69	1.44	87			87
3	2.04	14.2	3.1	0.75	1.38	57			57
4	1.08	18.1	1.6	0.81	1.32	25			25
5	4.14	15.6	2.6	0.82	1.31	122		122	
6	7.95	12.4	6.0	0.78	1.35	119		119	
7	16	8.5	12.0	0.72	1.40	209		209	
		Max	12.0	0.8	1.53	209.3	3	209	87
		Min	1.6	0.6	1.31	2.7	3	119	25
		Average	5.7	0.7	1.37	88.9	3	150	56

**Table A15: 1D-Constrained Modulus for Specimens HCB5**

Stage	Vertical stress (MPa)	Vertical strain (%)	Vertical stress-mid value (MPa)	Void ratio-mid value, e	EMDD-mid value (Mg/m <sup>3</sup> )	1D-Constrained Modulus (MPa)			
						All	Initial	Loading	Unloading
start	1.03	0.0							
1	0.96	17.9	1.0	1.07	1.15	0.4	0.4		
2	1.98	6.2	1.5	1.13	1.11	9		9	
3	4.06	-3.1	3.0	0.93	1.24	23		23	
4	8.11	-11.0	6.1	0.77	1.37	51		51	
5	15.85	-18.8	12.0	0.62	1.52	99		99	
6	8.12	-16.3	12.0	0.57	1.58	319			319
7	4.04	-10.7	6.1	0.64	1.49	72			72
8	2.02	-5.4	3.0	0.75	1.38	38			38
9	1.02	0.1	1.5	0.85	1.30	18			18
10	1.98	-1.8	1.5	0.88	1.27	52	52		
11	4.01	-6.5	3.0	0.82	1.32	43	43		
12	8.07	-12.4	6.0	0.72	1.41	69	69		
13	15.78	-19.2	11.9	0.60	1.54	114	114		
		Max	12.0	1.1	1.54	318.9	114.3	99.3	318.9
		Min	1.0	0.6	1.27	0.4	0.4	8.7	18.4
		Average	5.3	0.8	1.37	69.8	55.7	45.4	111.9

**Table A16: 1D-Constrained Modulus for Specimens HCB6**

Stage	Vertical stress (MPa)	Vertical strain (%)	Vertical stress-mid value (MPa)	Void ratio-mid value, e	EMDD-mid value (Mg/m <sup>3</sup> )	1D-Constrained Modulus (MPa)			
						All	Initial	Loading	Unloading
start	1.01	0.0							
1	0.97	12.9	1.0	0.98	1.20	0.3	0.3		
2	1.99	10.8	1.5	1.08	1.13	50		50	
3	4.1	6.0	3.0	1.02	1.17	44		44	
4	7.94	0.3	6.0	0.92	1.24	68		68	
5	15.82	-4.7	11.9	0.82	1.32	158		158	
6	7.94	-3.7	11.9	0.78	1.35	771			771
7	3.99	-1.5	6.0	0.81	1.33	184			184
8	1.95	1.7	3.0	0.86	1.28	63			63
9	1.02	5.2	1.5	0.92	1.24	27			27
10	1.98	4.9	1.5	0.95	1.21	357		357	
11	4.04	2.6	3.0	0.93	1.23	89		89	
12	7.94	-1.0	6.0	0.87	1.27	107		107	
13	15.94	-4.6	11.9	0.81	1.33	225		225	
		Max	11.9	1.1	1.33	771.0	0.3	356.9	771.0
		Min	1.0	0.8	1.21	0.3	0.3	43.6	26.6
		Average	5.2	0.9	1.26	164.7	0.3	137.1	261.1

**Table A17: 1D-Constrained Modulus for Specimens HCB7**

Stage	Vertical stress (MPa)	Vertical strain (%)	Vertical stress-mid value (MPa)	Void ratio-mid value, e	EMDD-mid value (Mg/m <sup>3</sup> )	1D-Constrained Modulus (MPa)			
						All	Initial	Loading	Unloading
Pre-Test	0	74.83							
1	1	76.11	0.56	0.75	1.38	72	72		
2	2	74.45	1.51	0.75	1.38	59		59	
3	4	70.81	2.94	0.73	1.40	52		52	
4	8	65.51	5.91	0.68	1.45	77		77	
5	16	61.28	11.92	0.63	1.50	188		188	
6	8	63.97	11.91	0.63	1.51	297			297
7	4	66.68	6.00	0.65	1.48	142			142
8	2	69.32	3.04	0.68	1.45	79			79
9	1	71.98	1.51	0.71	1.42	37			37
10	2	70.90	1.50	0.71	1.42	90		90	
			Max	1.51	297	72	188		297
			Min	1.42	37	72	52		37
			Average	1.46	109	72	93		139

**Table A18: 1D-Constrained Modulus for Specimens HCB8**

Stage	Vertical stress (MPa)	Vertical strain (%)	Vertical stress-mid value (MPa)	Void ratio-mid value, e	EMDD-mid value (Mg/m <sup>3</sup> )	1D-Constrained Modulus (MPa)			
						All	Initial	Loading	Unloading
Pre-Test	0	68.47							
1	1	69.02	0.55	0.69	1.44	162	162		
2	2	67.74	1.45	0.68	1.45	71		71	
3	4	63.16	2.93	0.65	1.48	45		45	
4	8	56.96	5.96	0.60	1.54	64		64	
5	16	51.92	11.94	0.54	1.60	158		158	
6	8	53.55	11.94	0.53	1.62	489			489
7	4	55.79	5.99	0.55	1.60	176			176
8	2	58.56	3.01	0.57	1.57	73			73
9	1	58.74	1.50	0.59	1.55	546			546
10	2	58.90	1.50	0.59	1.55	617		617	
				Max	1.62	617	162	617	546
				Min	1.54	45	162	45	73
				Average	1.58	240	162	191	321

**Table A19: 1D-Constrained Modulus for Specimens HCB9**

Stage	Vertical stress (MPa)	Vertical strain (%)	Vertical stress-mid value (MPa)	Void ratio-mid value, e	EMDD-mid value (Mg/m <sup>3</sup> )	1D-Constrained Modulus (MPa)			
						All	Initial	Loading	Unloading
Pre-Test	0.1								
1A	3.6	-34.79							
1B	5.0	-34.71	4.31	0.64	1.49	1823	1823		
2	8.0	-35.42	6.51	0.64	1.50	423		423	
3	16.0	-37.38	11.99	0.60	1.53	408		408	
5	16.0	-38.53	15.97	0.55	1.60				
6	8.0	-37.43	12.01	0.56	1.58	725			725
7	4.0	-34.41	6.02	0.61	1.52	133			133
8	2.0	-31.12	3.01	0.69	1.44	61			61
9	1.0	-28.37	1.51	0.77	1.36	36			36
				Max	1.60	1823	1823	423	725
				Min	1.36	36	1823	408	36
				Average	1.50	516	1823	416	239

**Table A20: 1D-Constrained Modulus for Specimens HCB10**

Stage	Vertical stress (MPa)	Vertical strain (%)	Vertical stress-mid value (MPa)	Void ratio-mid value, e	EMDD-mid value (Mg/m <sup>3</sup> )	1D-Constrained Modulus (MPa)			
						All	Initial	Loading	Unloading
Initial	0.8								
	0.9	-34.67							
1	2.6	-34.20	1.73	0.66	1.47	368	368		
2	4.0	-34.74	3.30	0.66	1.47	273		273	
3	8.0	-36.75	6.01	0.63	1.50	197		197	
4	16.0	-39.02	11.97	0.58	1.56	350		350	
5	8.0	-38.36	11.98	0.56	1.59	1193			1193
6	4.1	-37.52	6.06	0.58	1.56	464			464
7	1.9	-36.26	3.03	0.60	1.53	173			173
8	0.1	-28.78	1.02	0.71	1.42	25			25
9	2.0	-33.62	1.06	0.75	1.39	40		40	
10	0.1	-31.24	1.06	0.71	1.42	80			80
11	2.1	-33.69	1.09	0.71	1.42	80		80	
12	0.9	-32.96	1.49	0.69	1.44	160		160	
				Max	1.56	1193	368	350	1193
				Min	1.39	25	368	40	25
				Average	1.44	284	368	183	387

**Table A21: 1D-Constrained Modulus for Specimens HCB11**

Stage	Vertical stress (MPa)	Vertical strain (%)	Vertical stress-mid value (MPa)	Void ratio-mid value, e	EMDD-mid value (Mg/m <sup>3</sup> )	1D-Constrained Modulus (MPa)			
						All	Initial	Loading	Unloading
Initial	1	-34.85							
1	1	-33.74	0.83	0.66	1.47	32	32		
2	2	-33.93	1.49	0.67	1.46	530		530	
3	4	-35.00	2.97	0.65	1.48	185		185	
4	8	-36.95	5.87	0.62	1.52	195		195	
5	16	-39.22	11.86	0.56	1.58	360		360	
				Max	1.58	530	32	530	
				Min	1.46	32	32	185	
				Average	1.50	260	32	317	

## A5. DISCUSSION

### A5.1 BOUNDARY CONDITIONS DURING INITIAL SATURATION

Two types of boundary conditions are used in this test series: initial saturation under constant pressure (HCB7, HCB8, and HCB11) and constant volume (HCB9 and HCB10). In the case of swelling under constant pressure, the displacement of the soil increases with time and eventually equilibrates as shown in Figure A37 for specimen HCB7. Under constant volume boundary conditions, the vertical stress increases up to certain pressure level to maintain constant volume as shown in Figures A12 and A15 for Specimens HCB9 and HCB10. The swelling pressure for specimen with distilled water was higher (i.e., approximately 5 MPa) compared with the specimen with 250 g/L CaCl<sub>2</sub> (i.e., approximately 2.5 MPa).

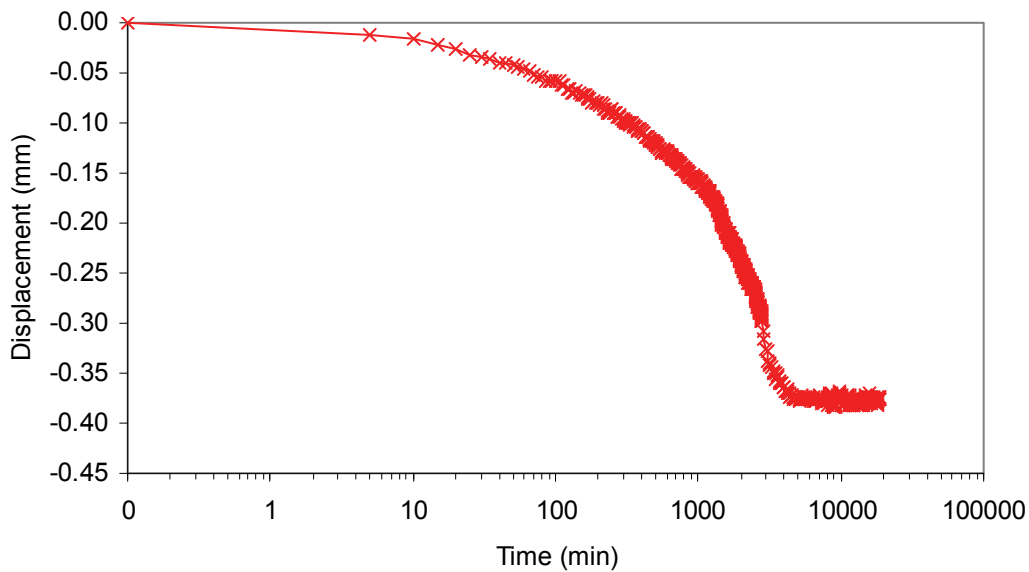


**Figure A37: Displacement During Initial Saturation Under Constant Vertical Stress of 1 MPa for Specimen HCB7**

### A5.2 MECHANICAL CONSTITUTIVE MODEL

The results of 1D-consolidation tests of HCB are evaluated in the framework of two different mechanical constitutive models.

1. Model 1: Log-Linear Relationship;
2. Model 2: Modification of Model 1.

### A5.2.1 Model 1: Log-Linear Relationship

The linear elastic constitutive model can only describe the mechanical behaviour of soil within small stress-strain increments. Alternatively, more rigorous constitutive models, such as the critical state model (e.g., Modified Cam-Clay (Roscoe et al. 1958, Roscoe and Burland 1968; Schofield and Wroth 1968)) may be used to define the mechanical behaviour of soil within larger range of stress-strain increments.

Log-linear relationships are used to interpret the results of the oedometer tests. This relationship is a component of a critical state model. In order to develop a complete critical-state model, the results of the oedometer tests need to be combined with the triaxial test results. However, a number of parameters can be determined from the oedometer tests alone, including: compression index ( $C_c$ ); swelling index ( $C_s$ ); and pre-consolidation pressure ( $\sigma_c$ ). The parameters  $C_c$ ,  $C_s$ , and  $\sigma_c$  are illustrated in Figure A38. These parameters can be determined from the relationship of void ratio ( $e$ ) versus vertical stress ( $\sigma_v$ ) (in log scale). The compression index ( $C_c$ ) is the slope in the compression line; the swelling index ( $C_s$ ) is the slope in the swelling line; and the consolidation pressure is the intersection of the swelling line and the compression line. It is recognized that the pre-consolidation pressure ( $\sigma_c$ ) is not clearly observed from the results of the 1D-consolidation test. The initial pre-consolidation pressure ( $\sigma_c$ ) is estimated from the changes of slopes defining  $C_c$  and  $C_s$  during the initial load increase.

The values of  $C_c$ ,  $C_s$ , and  $\sigma_c$  for each specimen are summarized in Tables A22. The calculated response using these parameters (i.e., Calculated (model 1)) compared with the results of laboratory tests are illustrated in Figures A39 to A43. These figures show that the critical state model can be used to define the mechanical behaviour of the Highly Compacted Bentonite (HCB) when the vertical stress is greater than 1 MPa. The compression index ( $C_c$ ) and swelling index ( $C_s$ ) for all HCB specimens versus void ratio ( $e$ ) are shown in Figures A43 and A44 respectively.

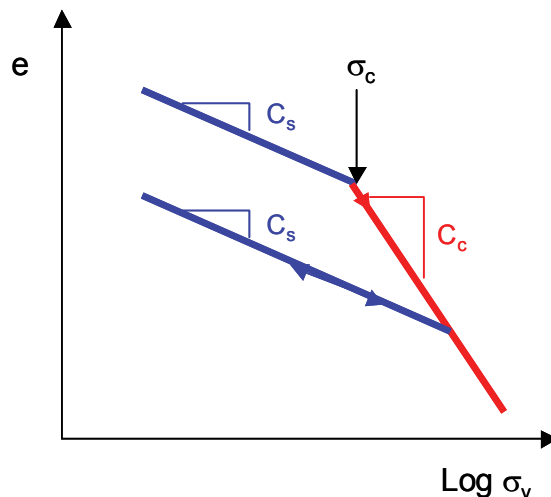
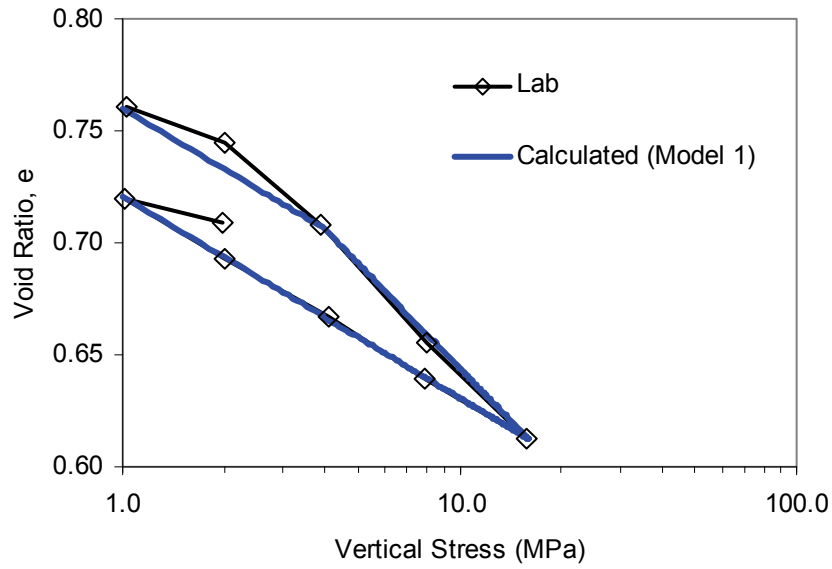


Figure A38: Model 1: Critical State Soil Mechanics Model for 1D-Consolidation

**Table A22: Compression Index (C<sub>c</sub>), Swelling Index (C<sub>s</sub>), and Initial Consolidation Pressure of HCB Specimens**

Speci-men No.		Void ratio, e	Dry density (Mg/m <sup>3</sup> )	EMDD (Mg/m <sup>3</sup> )	C <sub>c</sub>	C <sub>s</sub>	C <sub>sf</sub> *	Initial Consolidation pressure, σ <sub>c</sub> (MPa)	Void ratio corresponds to consolidation pressure, e <sub>c</sub>
HCB1	Min	0.63	1.45	1.26	0.42	0.11	0.25	4.00	0.84
	Mid-point	0.76	1.56	1.38	0.42	0.11	0.25	4.00	0.84
	Max	0.89	1.68	1.50	0.42	0.11	0.25	4.00	0.84
HCB2	Min	0.51	1.52	1.33	0.27	0.09	0.30	N/A	N/A
	Mid-point	0.66	1.67	1.49	0.27	0.09	0.30	N/A	N/A
	Max	0.81	1.82	1.65	0.27	0.09	0.30	N/A	N/A
HCB3	Min	0.69	1.47	1.28	0.15	0.09	0.21	4.50	0.83
	Mid-point	0.78	1.55	1.36	0.15	0.09	0.21	4.50	0.83
	Max	0.86	1.62	1.44	0.15	0.09	0.21	4.50	0.83
HCB4	Min	0.56	1.49	1.30	0.19	0.07	0.22	N/A	N/A
	Mid-point	0.70	1.62	1.44	0.19	0.07	0.22	N/A	N/A
	Max	0.84	1.76	1.58	0.19	0.07	0.22	N/A	N/A
HCB5	Min	0.54	1.22	1.04	0.57	0.30	0.00	NA	NA
	Mid-point	0.89	1.50	1.32	0.57	0.30	0.00	NA	NA
	Max	1.24	1.78	1.60	0.57	0.30	0.00	NA	NA
HCB6	Min	0.77	1.31	1.12	0.32	0.15	NA	2.34	1.05
	Mid-point	0.94	1.43	1.24	0.32	0.15	NA	2.34	1.05
	Max	1.10	1.55	1.36	0.32	0.15	NA	2.34	1.05
HCB7	Min	0.61	1.56	1.37	0.16	0.09	NA	4.01	0.74
	Mid-point	0.69	1.63	1.45	0.16	0.09	NA	4.01	0.74
	Max	0.76	1.70	1.52	0.16	0.09	NA	4.01	0.74
HCB8	Min	0.52	1.62	1.44	0.18	0.06	NA	2.35	0.67
	Mid-point	0.60	1.72	1.54	0.18	0.06	NA	2.35	0.67
	Max	0.69	1.81	1.63	0.18	0.06	NA	2.35	0.67
HCB9	Min	0.55	1.52	1.33	0.16	0.09	0.26	8.00	0.64
	Mid-point	0.68	1.65	1.46	0.16	0.09	0.26	8.00	0.64
	Max	0.80	1.77	1.60	0.16	0.09	0.26	8.00	0.64
HCB10	Min	0.55	1.52	1.33	0.19	0.06	0.15	4.13	0.65
	Mid-point	0.68	1.65	1.46	0.19	0.06	0.15	4.13	0.65
	Max	0.81	1.77	1.60	0.19	0.06	0.15	4.13	0.65
HCB11	Min	0.53	1.64	1.46	0.18	NA	NA	3.00	0.67
	Mid-point	0.60	1.71	1.54	0.18	NA	NA	3.00	0.67
	Max	0.67	1.79	1.61	0.18	NA	NA	3.00	0.67

\*C<sub>sf</sub> = slope during unloading under low pressure, see Figure A46.



**Figure A39: Calculated Response using Critical State Constitutive Model Compared with the Laboratory Results for Specimen HCB7**

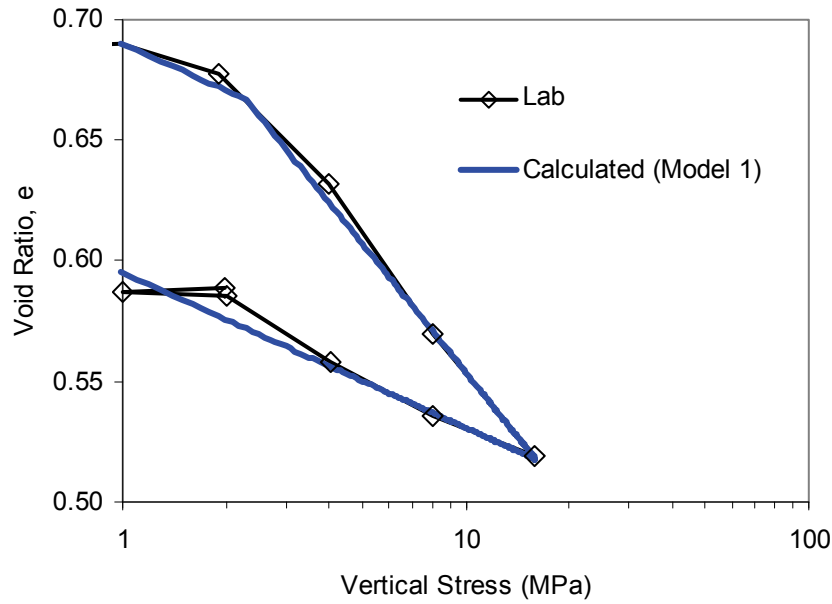


**Figure A40: Calculated Response using Critical State Constitutive Model Compared with the Laboratory Results for Specimen HCB8**

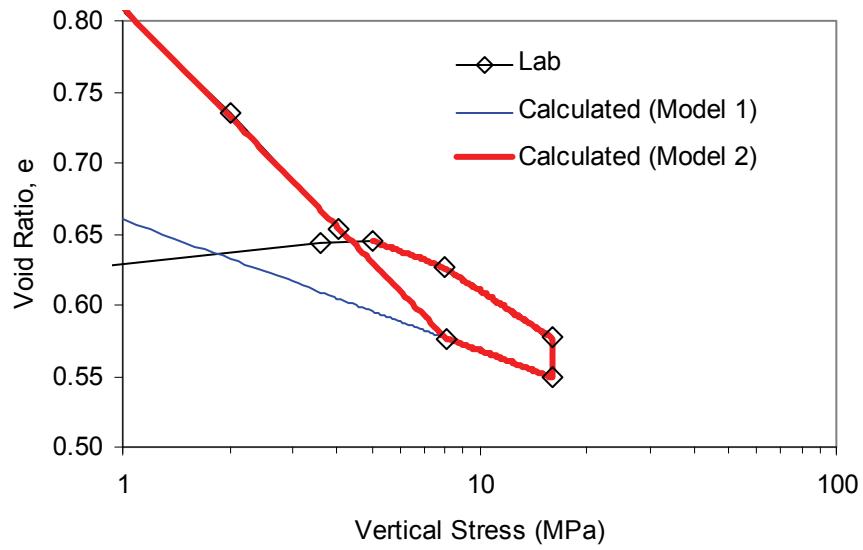


**Figure A41: Calculated Response using Critical State Constitutive Model (Model 1) and Modified Model (Model 2) Compared with the Laboratory Results for Specimen HCB9**

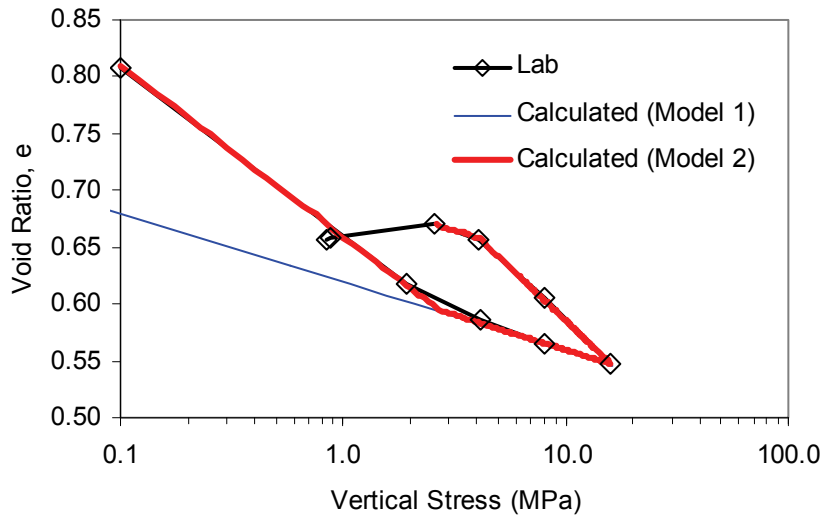


**Figure A42: Calculated Response using Critical State Constitutive Model (Model 1) and Modified Model (Model 2) Compared with the Laboratory Results for Specimen HCB10**

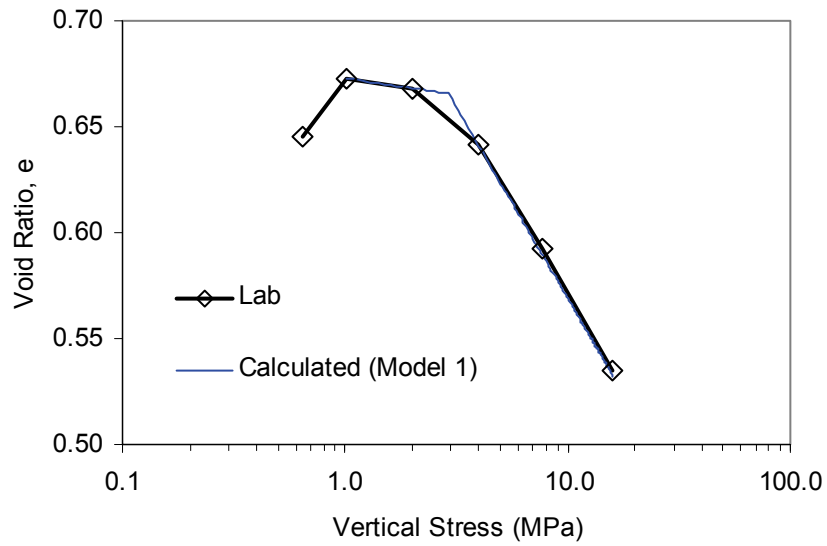


**Figure A43: Calculated Response using Critical State Constitutive Model (Model 1) Compared with the Laboratory Results for Specimen HCB11**

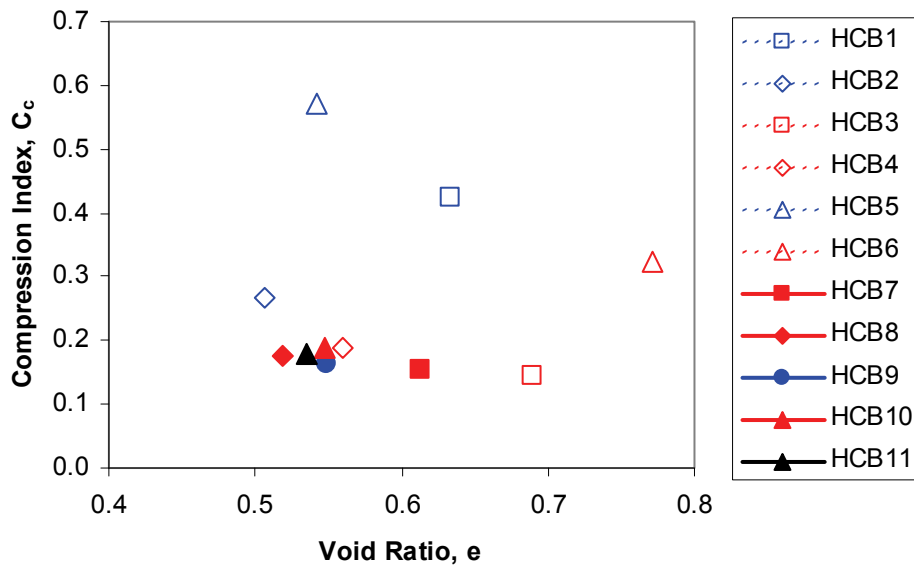


**Figure A44: Compression Index ( $C_c$ ) for HCB Specimens**

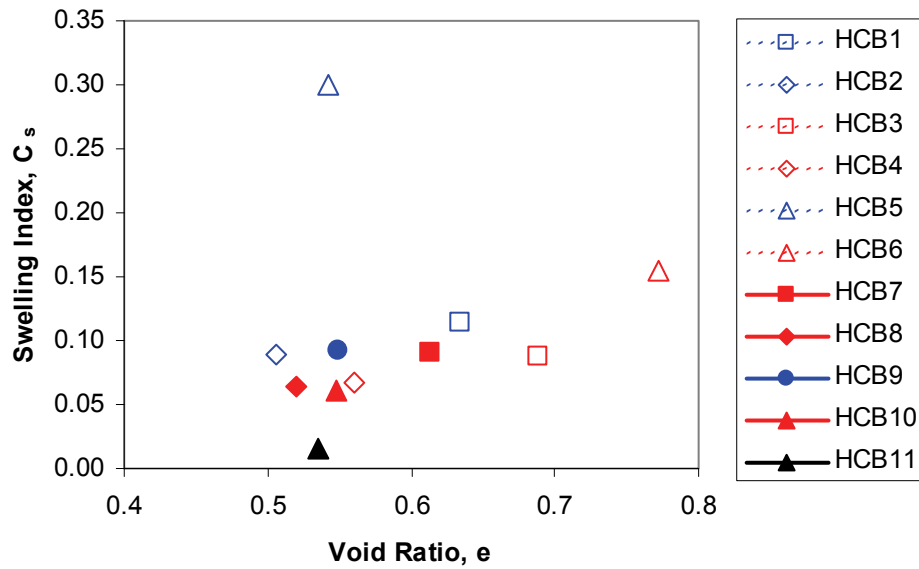


Figure A45: Swelling Index ( $C_s$ ) for HCB Specimens

#### A5.2.2 Model 2: Modification Of Model 1

The 1D-consolidation test results of HCB9 and HCB10 (Figures A41 and A42) show that in log-linear scale the slope of the swelling curve under high vertical stress is less than that under low vertical stress. Similar behaviour was also observed on DBF materials with various sand contents (i.e., 70% to 85%) (N. A. Chandler, personal communication, 2007). The log-linear relationship (i.e., Model 1) described in section A5.2.1 underestimates the swelling under low vertical stress. This suggests the modification of model 1 in order to simulate the behaviour of the HCB under low pressure.

A possible modification of model 1 is shown in Figure A46. The vertical stress ( $\sigma_v^{cv}$ ) that results in constant volume of the specimen is dependent on the void ratio ( $e$ ). Assuming that  $\sigma_v^{cv}$  decreases with an increase of void ratio, the Constant Volume Line (CVL) can be created (Figure A46). When the vertical stress is less than this line, the swelling index ( $C_s$ ) increases becoming the new swelling index ( $C_{sf}$ ) (Figure A46).

The response calculated using this constitutive model compared to the laboratory data is shown in Figures A41 and A42 as Model 2 for Specimens HCB9 and HCB10 respectively. Further investigation to develop the Constant Volume Line (CVL) is still required. The work scope in 2008 discussed in Section 6.1 includes the investigation the HCB under low pressure.

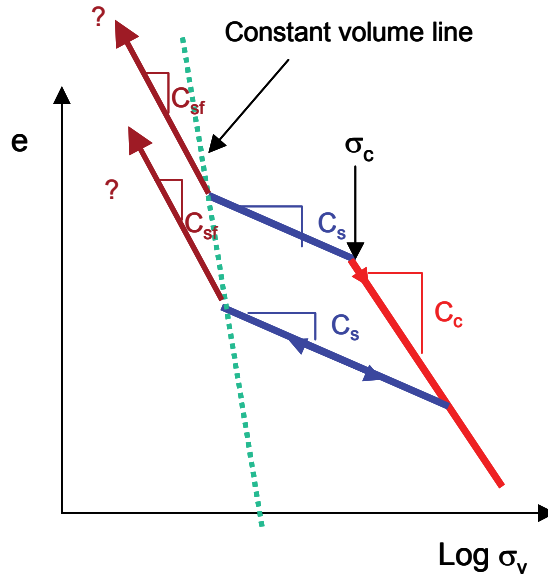


**Figure A46: Model 2: Modification of Log-Linear Relationship (Model 1) for HCB Specimen**

### **A5.3 APPLICATIONS OF PARAMETERS IN NUMERICAL MODELLING**

The parameters from 1D consolidation results should be combined with the results of the triaxial tests (Blatz et al. 2008) to provide a complete critical state mechanical constitutive model. The parameters  $C_c$  and  $C_s$  are generated from the slope of void ratio ( $e$ ) versus vertical stress ( $\sigma_v$ ) results from the oedometer tests. This forms the critical state description in specific volume ( $V$ ) –  $\ln p'$  space. The triaxial test data provide the  $q$ - $p'$  space description, which completes the critical state model. The combined oedometer and triaxial test derived critical state model can then be used directly in numerical modelling using Finite Element (FE) or Finite Different (FD) computer code.

### **A5.4 EFFECTS OF PORE LIQUID CHEMISTRY, LIQUID USED IN SPECIMEN PREPARATION, AND BOUNDARY CONDITIONS APPLIED DURING INITIAL SATURATION**

#### **A5.4.1 Effect Of Pore Liquid Chemistry**

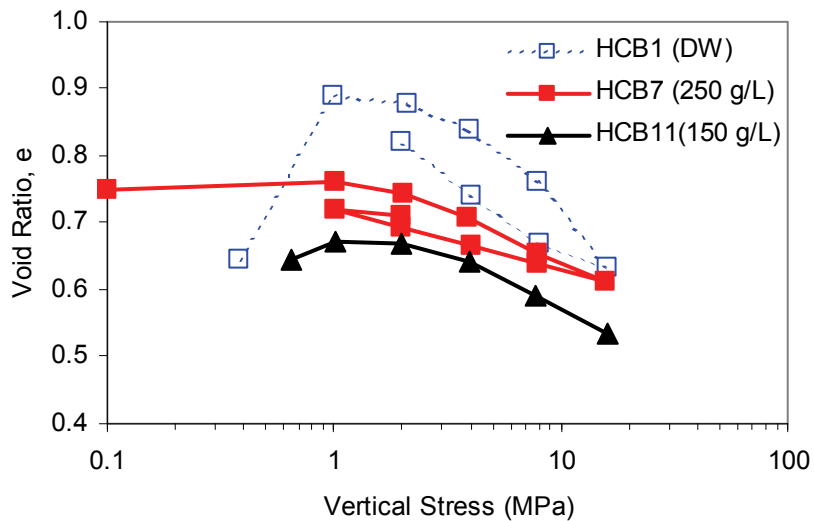
##### **A5.4.1.1 Specimens Prepared with Distilled Water**

Figure A47 shows comparison of the results of specimens prepared with distilled water (DW) having different pore liquid concentration in the oedometer reservoir (i.e., HCB1 (DW); HCB7 (250 g/L  $\text{CaCl}_2$ ); and HCB11 (150 g/L  $\text{CaCl}_2$ )). The reductions of void ratio ( $e$ ) due to an increase in vertical stress from 1 MPa to 16 MPa are 0.27 for specimen HCB1 (DW), 0.14 for specimen HCB11 (150 g/L), and 0.15 for specimen HCB7 (250 g/L). The reduction of void ratio ( $e$ ) for specimen with distilled water (i.e., HCB1) is greater than specimens with saline pore liquid (i.e., HCB11 and HCB7). The reductions of void ratio ( $e$ ) for specimens HCB11(150 g/L) and HCB7 (250 g/L) are relatively similar (i.e., 0.14 versus 0.15). The different initial void

ratio ( $e$ ) of specimen HCB7 and HCB11 prior to the load increase (i.e., 1 MPa) causes the reduction of void ratio ( $e$ ) for specimens HCB7 (250 g/L) greater than HCB11 (150 g/L). Greater initial void ratio ( $e$ ) means lower dry density ( $\rho_{dry}$ ) and increases the compressibility of the specimen.

The slopes of compression index ( $C_c$ ) and swelling index ( $C_s$ ) illustrated in Figure A38 are calculated for each specimen. The compression index ( $C_c$ ) and swelling index ( $C_s$ ) versus pore liquid concentration are shown in Figures A48 and A49. The compression index ( $C_c$ ) and swelling index ( $C_s$ ) decrease with an increase in  $\text{CaCl}_2$  concentration indicating that material becomes stiffer. For a concentration increase from 0 to 250 g/L, the compression index ( $C_c$ ) decreases from 0.4 to 0.1 and the swelling index ( $C_s$ ) decreases from 0.15 to 0.09.

The values of compression index ( $C_c$ ) and the reduction of void ratio ( $e$ ) for specimens HCB7 and HCB11 are relatively similar. It may indicate that the increase of the pore liquid salinity only decreases the compression index up to certain concentration (i.e, less than 150 g/L in this case). When the pore liquid concentration is greater than this value, the change of pore liquid concentration does not change the value of compression index ( $C_c$ ). This relationship is illustrated in Figure A48 and A49 as “possible relationship”. The relationships in Figures A48 and A49 can be used to incorporate the effect of pore liquid concentration on the mechanical behaviour in numerical modelling of HCB. This figure shows that the addition of saline pore liquid reduces the amount of swelling and reduces the slope of  $e$ -log  $\sigma_v$  curves.



**Figure A47: Void Ratio ( $e$ ) versus Vertical Stress ( $\sigma_v$ ) for Specimens Prepared with Distilled Water with Different Reservoir Liquid**

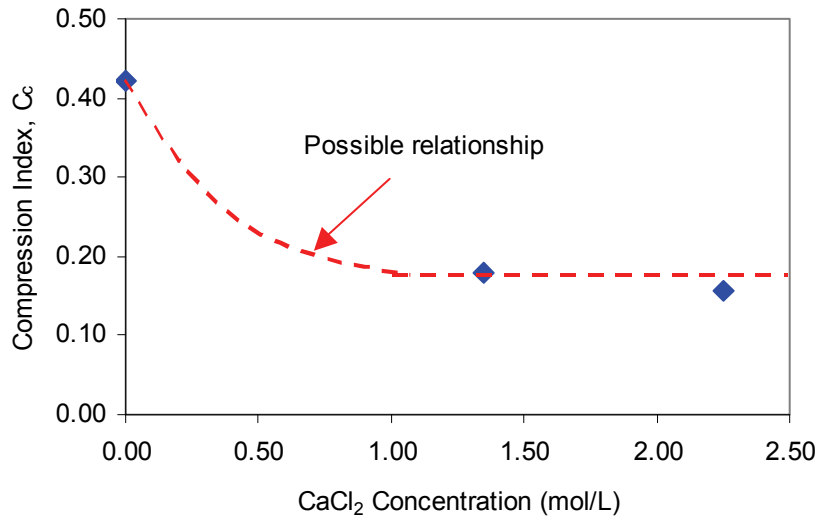


**Figure A48: Compression Index ( $C_c$ ) versus Concentration of  $\text{CaCl}_2$  in Pore Liquid for Specimens Prepared using Distilled Water with Different Reservoir Liquid**

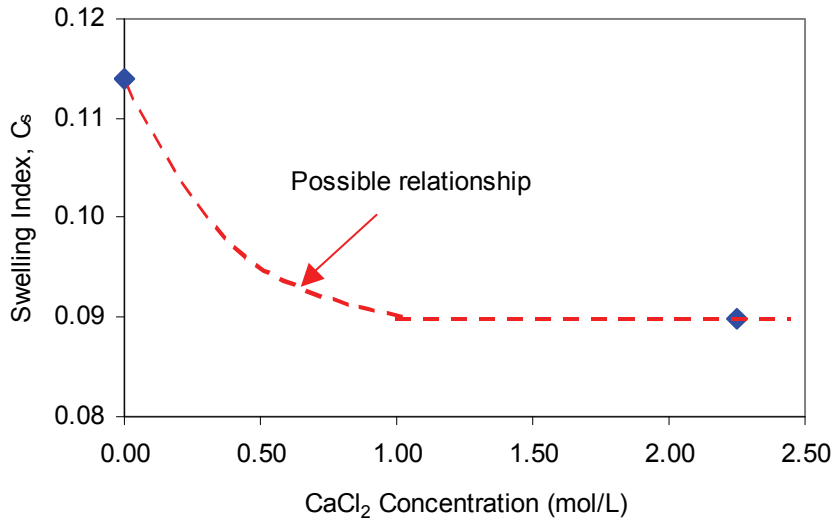


**Figure A49: Swelling Index ( $C_s$ ) versus Concentration of  $\text{CaCl}_2$  in Pore Liquid for Specimens Prepared using Distilled Water with Different Reservoir Liquid**

#### A5.4.1.2 Specimens Prepared with Salt Solution

Specimen HCB3 and HCB8 are prepared with 75 g/L and 250 g/L  $\text{CaCl}_2$  respectively and similar liquids are added in the reservoir. Specimen HCB1 uses distilled water in specimen preparation and reservoir liquid. Comparison of the results of specimens HCB1, HCB3, and

HCB8 is used to examine the effect of pore liquid concentration. Specimens HCB1 and HCB3 have a higher void ratio compared to Specimen HCB8 due to different conditions applied during initial saturation. The compression index ( $C_c$ ) and swelling index ( $C_s$ ) versus pore liquid concentration are shown in Figures A51 and A52. The compression index ( $C_c$ ) and swelling index ( $C_s$ ) decrease with an increase of  $\text{CaCl}_2$  concentration. The relationship in Figures A51 and A52 may be used to incorporate the effect of pore liquid concentration on the mechanical behaviour in numerical modelling of HCB.

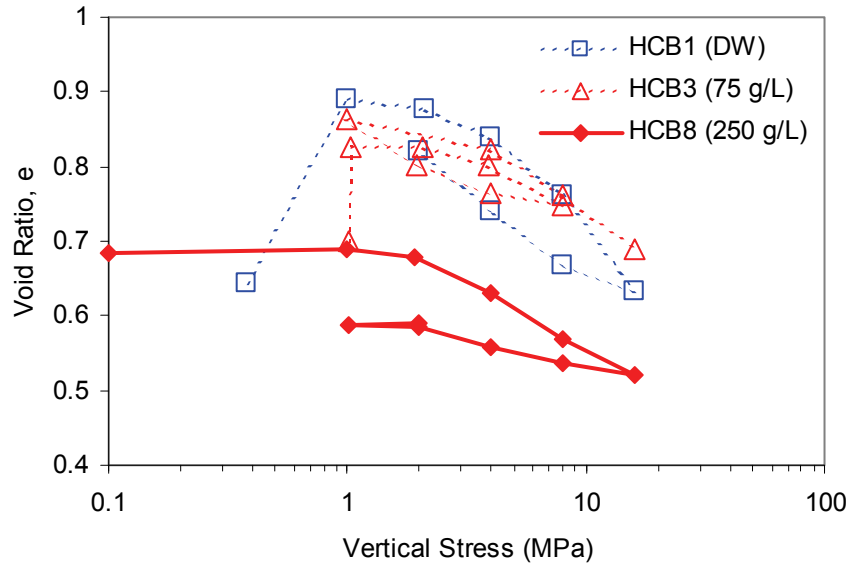


**Figure A50: Void Ratio ( $e$ ) versus Vertical Stress ( $\sigma_v$ ) for Specimens Prepared with Different Mixing and Reservoir Liquid**

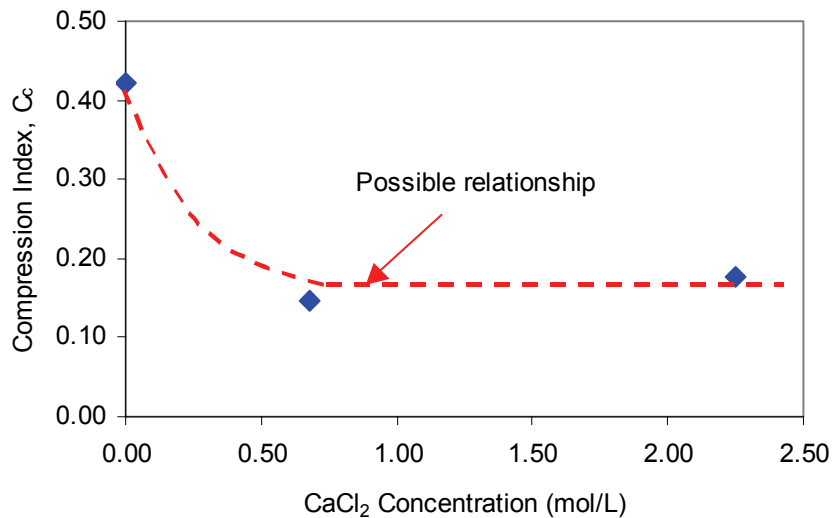


**Figure A51: Compression Index ( $C_c$ ) versus Concentration of  $\text{CaCl}_2$  in Pore Liquid for Specimens Prepared with Different Mixing and Reservoir Liquid**

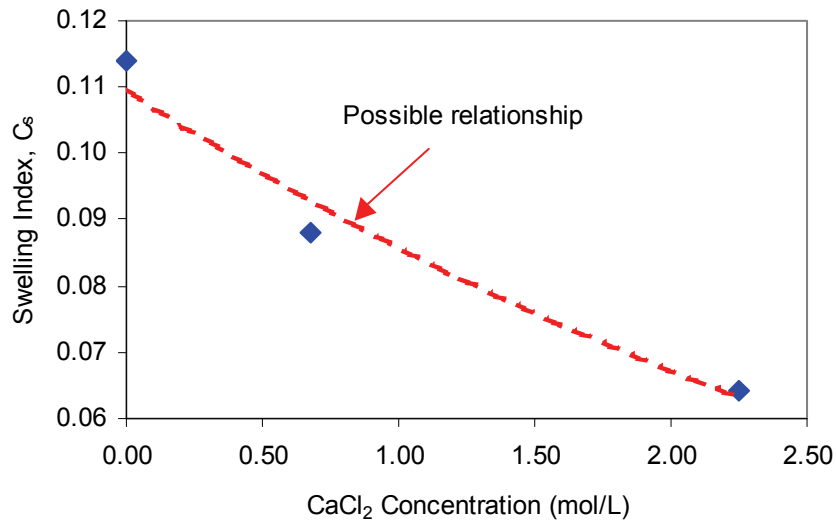


**Figure A52: Swelling Index ( $C_s$ ) versus Concentration of  $\text{CaCl}_2$  in Pore Liquid for Specimens Prepared with Similar Mixing and Reservoir Liquid**

#### **A5.4.2 Effect Of Pore Liquid Used In Specimen Preparation**

The effect of the liquid used in the specimen preparation can be examined by the comparison of specimens HCB1, HCB7, and HCB11 for specimens mixed with distilled water (Figure A47) and specimens HCB1, HCB3 and HCB8 for specimens mixed with salt solution with different concentrations (Figure A50). Distilled water is used in preparation of specimen HCB1 and provided in the reservoir during the test. Specimens HCB7 and HCB11 are prepared with distilled water, but  $\text{CaCl}_2$  solutions with different concentrations are provided in the reservoir during the test. Specimens HCB3 and HCB8 are prepared with  $\text{CaCl}_2$  solution with different concentrations and similar solutions are provided in the reservoir during the test.

The compression index ( $C_c$ ) and swelling index ( $C_s$ ) versus pore liquid concentration of these specimens are shown in Figures A53 and A54, which indicate that different liquids used in specimen preparation may only affect the swelling index ( $C_s$ ) (Figure A54), but may not affect the compression index ( $C_c$ ) (Figure A53).

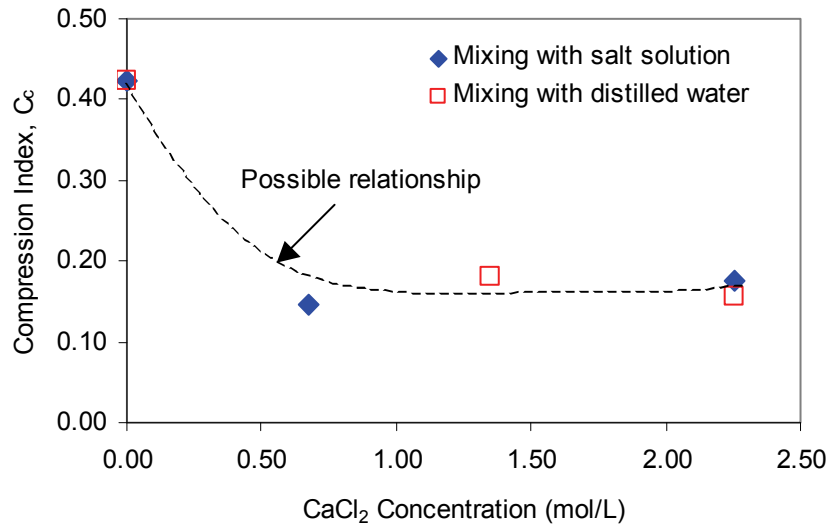


Figure A53: Compression Index ( $C_c$ ) versus Concentration of  $\text{CaCl}_2$  in Pore Liquid

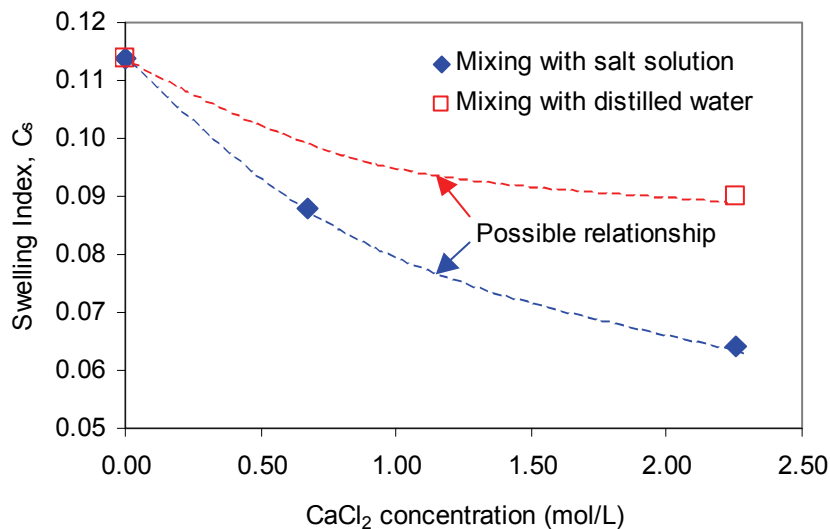
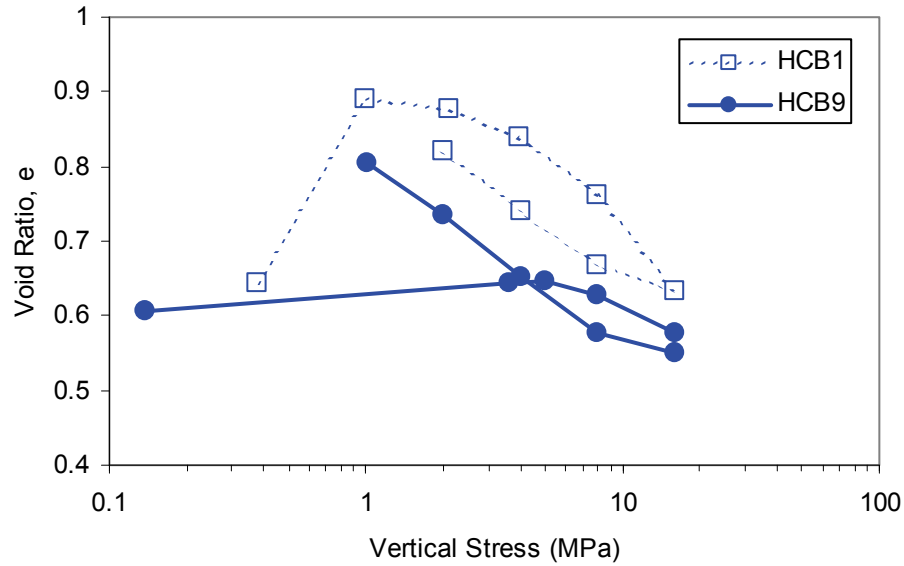


Figure A54: Swelling Index ( $C_s$ ) versus Concentration of  $\text{CaCl}_2$  in Pore Liquid

#### A5.4.3 Effect Of Boundary Conditions During Initial Saturation

The effect of boundary conditions applied during initial saturation can be examined by comparison of specimens HCB1 and HCB9 for specimens prepared with distilled water (DW) (Figure A55) and comparison of specimens HCB8 and HCB10 for specimens prepared with 250 g/L  $\text{CaCl}_2$  (Figure A56). However, the compression index ( $C_c$ ) and swelling index ( $C_s$ ) versus pore liquid concentration of these specimens are shown in Figures A57 and A58. For specimens with 250 g/L  $\text{CaCl}_2$ , the initial boundary condition applied at initial saturation does

not affect the mechanical behaviour of HCB. However, the specimens prepared with distilled water with constant volume conditions has lower  $C_c$  and  $C_s$  values compared to the specimens with constant pressure conditions (Figures A57 and A58). This difference in  $C_c$  and  $C_s$  is likely due to the higher initial void ratio of specimens HCB1 than HCB9. The higher initial void ratios increase the value of  $C_c$  and  $C_s$  indicating that these parameters are stress path-dependent. Further investigation is required to better define the effect of boundary conditions.



**Figure A55: Void Ratio ( $e$ ) versus Vertical Stress ( $\sigma_v$ ) for Specimens having Distilled Water as Mixing and Reservoir Liquid with Different Boundary Condition during Initial Saturation (HCB1-Constant Pressure; HCB9 - Constant Volume)**

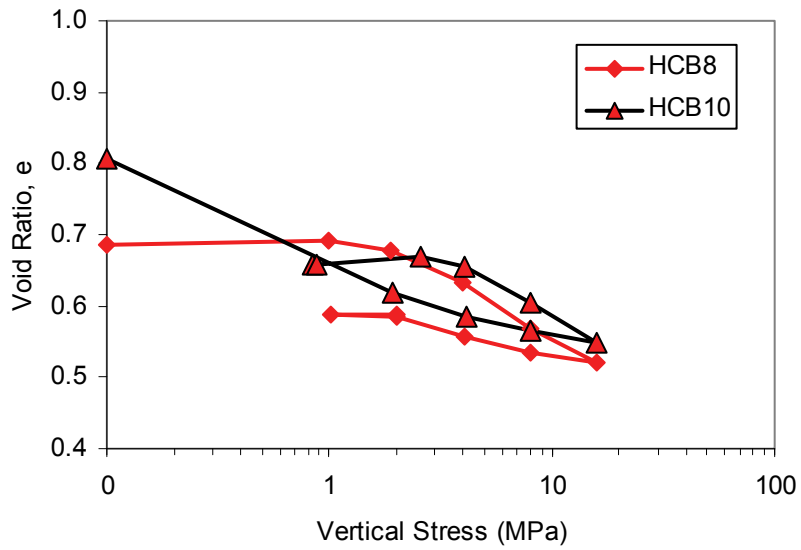


**Figure A56: Void Ratio ( $e$ ) versus Vertical Stress ( $\sigma_v$ ) for Specimens having 250 g/L  $\text{CaCl}_2$  as Mixing and Reservoir Liquid with Different Boundary Condition during Initial Saturation (HCB8-Constant Pressure; HCB10-Constant Volume)**

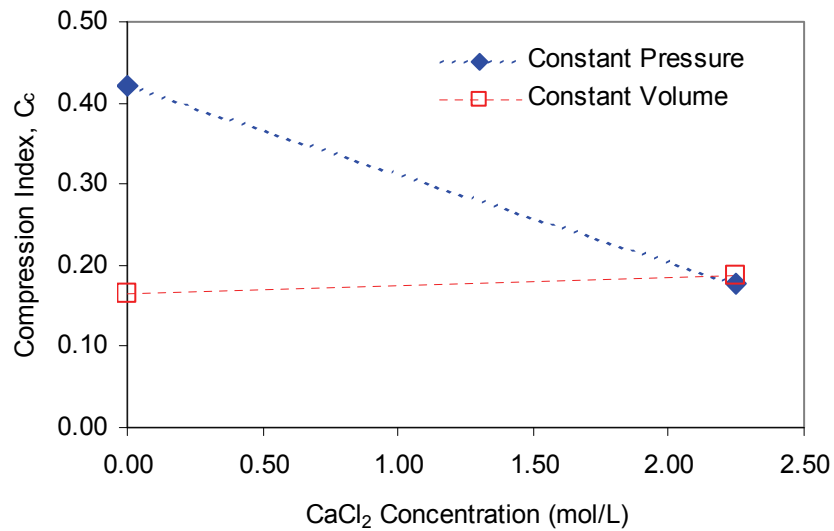


**Figure A57: Compression Index ( $C_c$ ) versus Pore Liquid Concentration for Specimens with Different Boundary Condition during Initial Saturation**

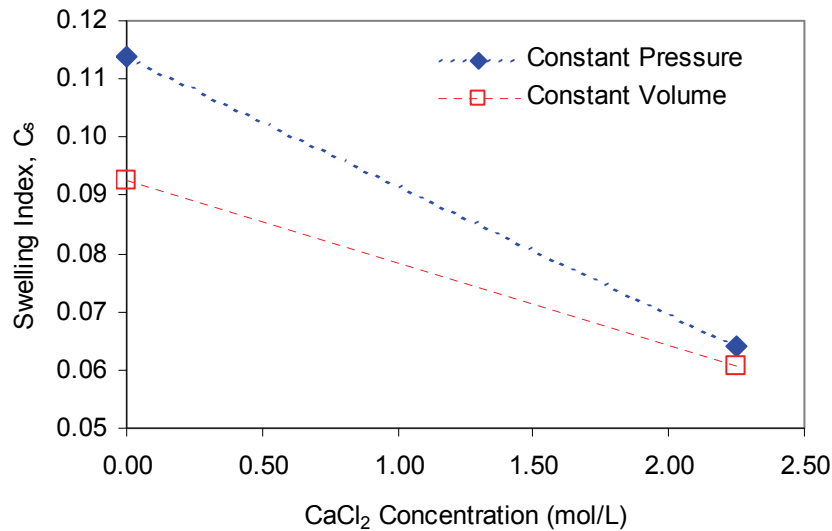


**Figure A58: Swelling Index ( $C_s$ ) versus Pore Liquid Concentration for Specimens with Different Boundary Condition during Initial Saturation**

## A6. CONCLUDING REMARKS

1. 1D-Constrained modulus ( $M$ ) of HCB has been calculated from the stress-strain increments, which varies from 10 to 1000 MPa for EMDD within the range of 1.2 to 1.6  $\text{Mg/m}^3$ . The results indicate that a linear-elastic model can only be used to describe mechanical behaviour of the HCB within small stress-strain increments. A more rigorous constitutive model (i.e., Modified Cam-Clay (Roscoe and Burland 1968)) should be used to define mechanical behaviour of HCB involving high range of stress-strain increments.
2. Mechanical constitutive model parameters including compression index ( $C_c$ ), swelling index ( $C_s$ ) and preconsolidation pressure ( $\sigma_c$ ) were determined from the 1D consolidation tests on HCB. The range of the  $C_c$  and  $C_s$  parameters are 0.15 to 0.42 and  $C_s = 0.06$  to 0.15, respectively. Combined with the results of triaxial tests, these parameters can be used to develop a modified cam-clay model (Roscoe and Burland 1968) to describe the behaviour of HCB.
3. The effects of the pore liquid concentration, liquid type used in the specimen preparation, and boundary conditions applied during initial saturation were examined and the following has been note.
  - The Compression Index ( $C_c$ ) and the Swelling Index ( $C_s$ ) of HCB decrease with an increase of the concentration of  $\text{CaCl}_2$  as pore liquid. The relationship of these indices with the  $\text{CaCl}_2$  concentration in pore liquid has been presented in this report. This relationship can be used to incorporate the effect of change in pore liquid chemistry to the mechanical behaviour of HCB.

- The liquid used in specimen preparation affects the value of swelling index ( $C_s$ ), but it does not appear to affect the compression index ( $C_c$ ).
  - The boundary condition applied during the initial saturation establishes the initial void ratio or dry density of the specimen. It does not affect the behaviour of HCB specimens prepared with 250 g/L  $\text{CaCl}_2$ , but it affects the behaviour of specimens prepared with distilled water. Further investigation is still required to examine this effect.
4. The coefficients of consolidation ( $c_v$ ) have been determined from the results of 1D consolidation tests. The hydraulic conductivity ( $K$ ) calculated from  $c_v$  is within the range of  $1 \times 10^{-15}$  to  $1 \times 10^{-11}$  m/s for EMDD within the range of 1.6 to 1.1  $\text{Mg/m}^3$  respectively and it decreases with increasing EMDD. The results are comparable with the hydraulic conductivity ( $K$ ) of the bentonite measured using hydraulic conductivity cells by Dixon et al. (1999).
  5. The 1D consolidation result indicates that the swelling index ( $C_s$ ) significantly increases for specimens under low vertical stress. A suggested modification of the existing constitutive model has been presented to incorporate this behaviour.

#### **ACKNOWLEDGEMENTS**

The authors gratefully acknowledge the technical support from P. Baumgartner, the careful and dedicated laboratory work by C.L. Kohle and D. Drew, and assistance of F. Johnston and T. Reimer during the laboratory tests.

## REFERENCES

- ASTM (ASTM International). 2004. Standard test methods for one-dimensional consolidation properties of soils using incremental loading. Standard D2435-04, ASTM International, West Conshohocken, Pennsylvania, USA.
- ASTM (ASTM International). 2005. Standard Test Methods for Laboratory determination of water (moisture) content of soil and rock by mass. Standard D 2216-05, ASTM International, West Conshohocken, Pennsylvania, USA.
- Baumgartner, P. and G.R. Snider. 2002. Seal Evaluation and Assessment Study (SEAS): Light backfill placement trials. Atomic Energy of Canada Limited Technical Record, TR-793.
- Baumgartner, P., D. G. Priyanto, J. R. Baldwin, J. A. Blatz, B. H. Kjartanson, and H. Batenipour. 2008. Preliminary Results of One-Dimensional Consolidation Testing on Bentonite Clay-Based Sealing Components Subjected to Two Pore-Fluid Chemistry Conditions. Nuclear Waste Management Organization (NWMO) Technical Report No. TR-2008-04. Toronto, Canada.
- Blatz, J.A., Siemens, G.A. and A. G. Man. 2008. Triaxial characterization of light and dense backfill to determine properties for use in numerical modeling. Nuclear Waste Management Organization (NWMO) Technical Report No. TR-2008-05. Toronto, Canada.
- Budhu, M. 2000. Soil Mechanics and Foundations. John Wiley and Sons.
- Cassagrande, A., and Fadum, R. E. 1940. "Notes on Soil Testing for Engineering Purposes." Soil Mechanics Series, Graduate School of Engineering, Harvard University, Cambridge, MA, Vol. 8(268), p. 37.
- Craig, R.F. 1992. Soil Mechanics, 5<sup>th</sup> Edition. E & FN Spoon, London.
- Das, B.M. 1998. Principles of Geotechnical Engineering, 4<sup>th</sup> Edition. PWS Publishing Company, Boston, MA.
- JNC (Japan Nuclear Cycle Development Institute). 2000. H12: Project to establish the scientific and technical basis for HLW disposal in Japan. Supporting report 2: Repository design and engineering technology. Japan Nuclear Cycle Development Institute Report, JNC TN 1400 2000-003.
- Lide, D.R., ed. 2007. CRC Handbook of Chemistry and Physics, Internet Version 2007, (87th Edition), <http://www.hbcernetbase.com>
- Priyanto, D.G. 2007. Development and Application of New Constitutive Models to Simulate the Hydraulic and Mechanical Behaviours of Unsaturated Swelling Clay. Ph.D Thesis. Department of Civil Engineering, University of Manitoba, Canada.

Roscoe, K. H., Schofield, A. N., & Wroth, C. P. 1958. On the yielding of soils. *Géotechnique*, 8, 22-53.

Roscoe, K. H., & Burland, J. B. 1968. On the generalized stress-strain behaviour of 'wet' clay. In J. Heyman & F. Leckie (Eds.), *Engineering Plasticity* (pp. 535-609). Cambridge:

Schofield, A. N., & Wroth, C. P. 1968. *Critical state soil mechanics*. London: McGraw Hill.

Taylor, D. W. 1942. Research on Consolidation of Clays. Serial No. 82, Massachusetts Institute of Technology, Cambridge.

Terzaghi, K. 1943. *Theoretical Soil Mechanics*. Wiley, New York.

**APPENDIX B:  
DENSE BACKFILL (DBF)**

D. G. Priyanto<sup>1</sup>, J. A. Blatz<sup>2</sup>, and R. Offman<sup>2</sup>  
<sup>1</sup>Atomic Energy of Canada Limited  
<sup>2</sup>University of Manitoba

**CONTENTS**

	<b><u>Page</u></b>
<b>B1. DBF .....</b>	<b>97</b>
<b>B2. TESTING MATRIX IN 2007 .....</b>	<b>97</b>
<b>B3. PRELIMINARY RESULTS.....</b>	<b>98</b>
<b>B4. COMPLETION OF TESTS.....</b>	<b>101</b>
<b>REFERENCES .....</b>	<b>101</b>

**LIST OF TABLES**

	<b><u>Page</u></b>
Table B1: Testing Matrix for 1D Consolidation Tests for DBF at the University of Manitoba in 2007 .....	97
Table B2: Loading Sequence for the DBF Samples .....	98

**LIST OF FIGURES**

	<b><u>Page</u></b>
Figure B1: Sample Thickness and Vertical Stress versus Time for Test No 1 (Mixing Liquid: 250 g/L CaCl <sub>2</sub> ; Reservoir Liquid: 250 g/L CaCl <sub>2</sub> ) Results Current to December 2007 .....	99
Figure B2: Void Ratio (e) versus Vertical Stress ( $\sigma_v$ ) for Test No 1 (Mixing Liquid = 250 g/L CaCl <sub>2</sub> ; Reservoir Liquid = 250 g/L CaCl <sub>2</sub> ) Results Current to December 2007 .....	99
Figure B3: Sample Thickness and Vertical Stress versus Time for Test No 2 (Mixing Liquid = DDW; Reservoir Liquid = 250 g/L CaCl <sub>2</sub> ) Result Current to December 2007 .....	100
Figure B4: Void Ratio (e) versus Vertical Stress ( $\sigma_v$ ) for Test No 2 (Mixing Liquid = DDW; Reservoir Liquid = 250 g/L CaCl <sub>2</sub> ) Result Current to December 2007 .....	100

## B1. DBF

Dense backfill (DBF) is a clay-based sealing-system component proposed for use in a nuclear fuel waste repository (Maak and Simmons 2005). The DBF proposed for repository use is composed of 5% bentonite, 25% glacial clay and 70% crushed granite aggregate by mass (Russell and Simmons 2003). It is to be compacted to a dry density of 2120 kg/m<sup>3</sup> at a water content of 8.5%, producing an initial degree of saturation of ~80%. For the consolidation tests, a DBF, composed of 75% crushed granite, 18.75% crushed illite clay (i.e., Sealbond) and 6.25% Avonlea bentonite, from a previous experiment in the URL (the BCE (Graham et al. 1997)), was supplied to the University of Manitoba's Geotechnical Laboratory by Atomic Energy of Canada Limited. This previously prepared material was used for two main reasons. Firstly, this material is well characterised and is consistent with DBF previously used in geotechnical testing and secondly, there is no commercial source of glacial lake clay. Any backfill material produced in an effort to match the reference DBF composition of Russell and Simmons (2003) would not necessarily be representative of backfill proposed for use in a repository. The bulk mechanical behaviour of the DBF used in the testing and the reference material is also anticipated to be similar. Therefore for consistency of testing and comparability of previous study results, the DBF used is the 75% granite – 25% clay blend material.

## B2. TESTING MATRIX IN 2007

The testing plans for 1D consolidation tests in 2007 are shown in Table 1, which include two boundary conditions and two types of liquid used in sample mixing (i.e., distilled water (DW), and 250 g/L calcium chloride (CaCl<sub>2</sub>) solution). Table 2 shows the loading sequence used in all four tests. Due to the low hydraulic conductivity and the large size of the DBF specimens, the tests took longer time than it was anticipated. Only two tests are shown in this report, the complete results of the tests will be presented in the technical report in the following year.

**Table B1: Testing Matrix for 1D Consolidation Tests for DBF at the University of Manitoba in 2007**

Test No.	Sample No.	Mixing Liquid	Reservoir Liquid	Swelling % on Initial Saturation	Loading Path *
1.	DBF1	250 g/L CaCl <sub>2</sub>	250 g/L CaCl <sub>2</sub>	20	Load to 4000 kPa after initial swelling
2.	DBF2	DDW	250 g/L CaCl <sub>2</sub>	20	Load to 4000 kPa after initial swelling
3.	DBF3	250 g/L CaCl <sub>2</sub>	250 g/L CaCl <sub>2</sub>	Rigidly confined	Load to 4000 kPa after initial swelling
4.	DBF4	DDW	250 g/L CaCl <sub>2</sub>	Rigidly confined	Load to 4000 kPa after initial swelling

\* See Table 2

**Table B2: Loading Sequence for the DBF Samples**

<b>Stage</b>	<b>Load Schedule Type 2</b>
Step 1	Load to 1 MPa
Step 2	Load to 2 MPa
Step 3	Load to 4 MPa
Step 4	Unload to 2 MPa
Step 5	Unload to 1 MPa
Step 6	Unload to 0.5 MPa
Step 7	Load to 1 MPa
Step 8	Load to 2 MPa
Step 9	Load to 4 MPa

### **B3. PRELIMINARY RESULTS**

Physical tests of Specimen DBF1 and DBF2 are current to December 2007. The next two tests (i.e., Tests No. 3 and 4) have been installed in the oedometer cells. These tests are expected to be complete in March 2008. The preliminary results up to December 2007 are shown in Figures B1 to B4. Figures B1 and B3 show the sample thickness and vertical stress versus time for Specimen DBF1 and DBF2. Figures B2 and B4 show the void ratio ( $e$ ) versus vertical stress ( $\sigma_v$ ) for Specimens DBF1 and DBF2. Specimens DBF1 and DBF2 were originally planned to experience 20% swelling on initial saturation, but 20% swelling did not occur during initial saturation. It may be due to the initial load applied to the specimen was too high, the low montmorillonite content of the material, and low initial dry density of the specimens. Considering the length of initial saturation that required 35 days, the tests continued. The load applied on specimens DBF1 and DBF2 were increased from 0, 1, 2, and 4 MPa. The load was decreased to 2 and 1 MPa. The specimens DBF1 and DBF2 were in the initial stage of 1 MPa load increment in December 2007.

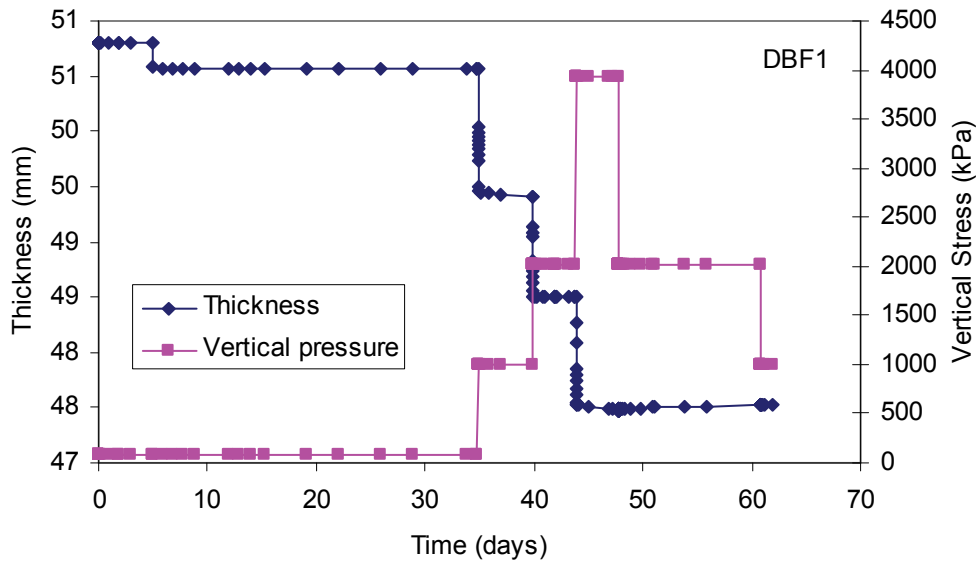


**Figure B1: Sample Thickness and Vertical Stress versus Time for Test No 1 (Mixing Liquid: 250 g/L CaCl<sub>2</sub>; Reservoir Liquid: 250 g/L CaCl<sub>2</sub>) Results Current to December 2007**

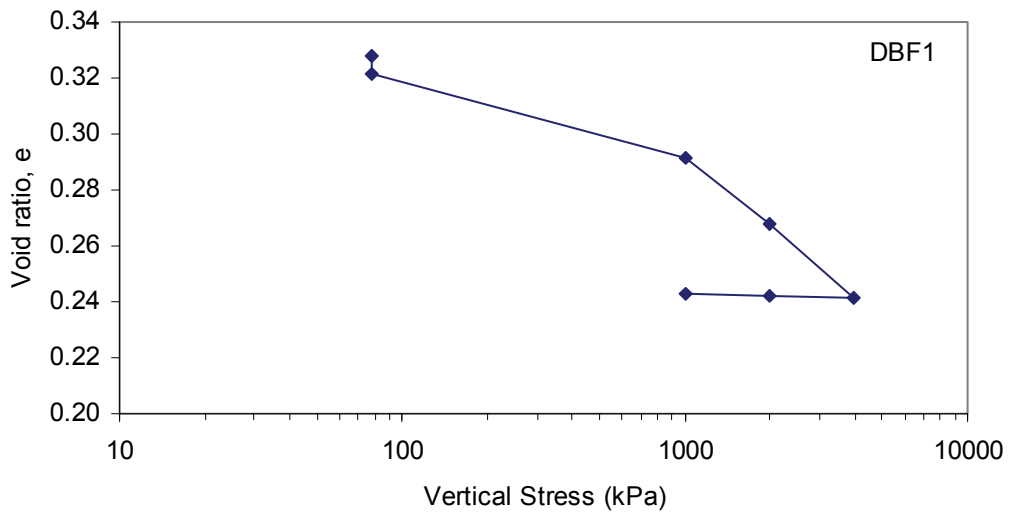


**Figure B2: Void Ratio ( $e$ ) versus Vertical Stress ( $\sigma_v$ ) for Test No 1 (Mixing Liquid = 250 g/L CaCl<sub>2</sub>; Reservoir Liquid = 250 g/L CaCl<sub>2</sub>) Results Current to December 2007**

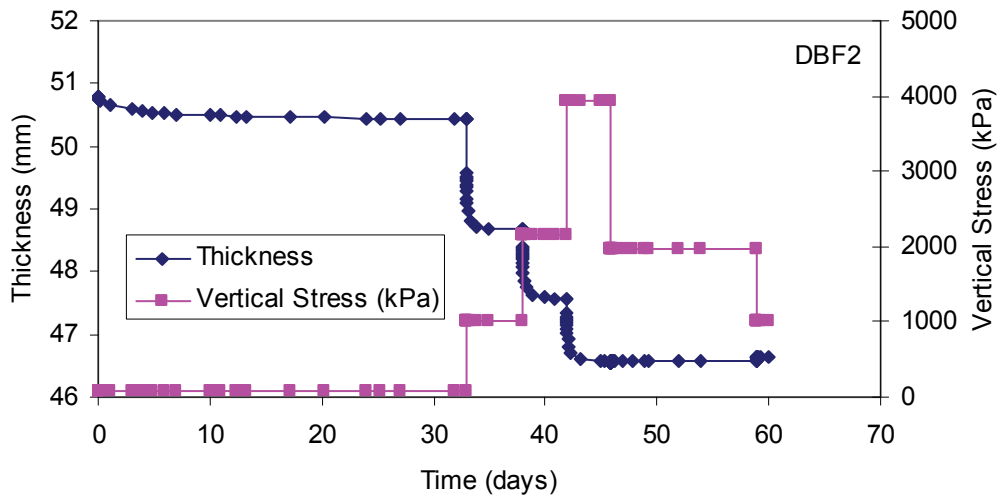


**Figure B3: Sample Thickness and Vertical Stress versus Time for Test No 2 (Mixing Liquid = DDW; Reservoir Liquid = 250 g/L CaCl<sub>2</sub>) Result Current to December 2007**

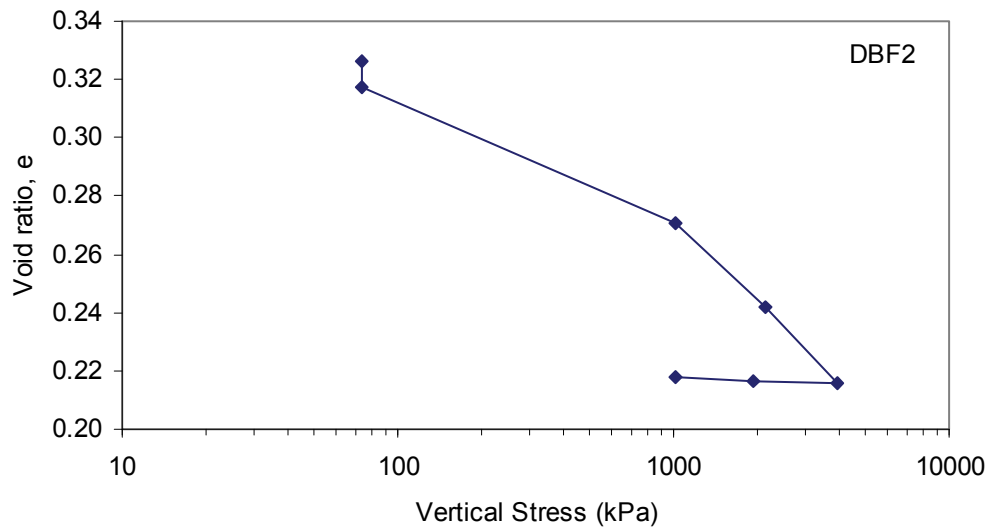


**Figure B4: Void Ratio (e) versus Vertical Stress ( $\sigma_v$ ) for Test No 2 (Mixing Liquid = DDW; Reservoir Liquid = 250 g/L CaCl<sub>2</sub>) Result Current to December 2007**

#### **B4. COMPLETION OF TESTS**

The final report will provide:

- parameters  $C_c$  and  $C_s$  interpreted from the 1D consolidation tests; and
- the discussions on the effects of pore liquid salinity used as mixing liquid in sample preparation and boundary condition applied during initial saturation.

#### **REFERENCES**

- Maak, P. and G.R. Simmons. 2005. Deep geologic repository concepts for isolation of used fuel in Canada. In Proc. Canadian Nuclear Society conference Waste Management, Decommissioning and Environmental Restoration for Canada's Nuclear Activities: Current Practices and Future Needs. 2005 May 8-11, Ottawa.
- Russell, S.B. and G.R. Simmons. 2003. Engineered barrier system for a deep geologic repository. Presented at the 2003 International High-Level Radioactive Waste Management Conference. 2003 March 30-April 2, Las Vegas, NV.



**APPENDIX C:  
LIGHT BACKFILL (LBF)**

S. Boyle and G. A. Siemens  
Royal Military College of Canada

**CONTENTS**

	<b><u>Page</u></b>
<b>C1. INTRODUCTION .....</b>	<b>105</b>
<b>C1.1 LBF.....</b>	<b>105</b>
<b>C2. LBF OEDOMETER TESTING.....</b>	<b>105</b>
<b>C2.1 LBF TEST DESCRIPTION.....</b>	<b>105</b>
<b>C2.2 LBF TEST PROCEDURE .....</b>	<b>106</b>
C2.2.1 Calcium Chloride Solution.....	106
C2.2.2 LBF .....	106
<b>C3. LBF TEST RESULTS .....</b>	<b>107</b>
<b>C3.1 INDIVIDUAL TEST RESULTS.....</b>	<b>107</b>
<b>C3.2 COMPARISON OF MIXING AND RESERVOIR CONDITIONS .....</b>	<b>116</b>
<b>C3.3 COMPARISON OF INITIAL CONDITIONS.....</b>	<b>117</b>
<b>C4. SUMMARY .....</b>	<b>119</b>
<b>C5. CONCLUSIONS AND RECOMMENDATIONS .....</b>	<b>119</b>
<b>ACKNOWLEDGEMENTS .....</b>	<b>119</b>
<b>REFERENCES .....</b>	<b>119</b>

**LIST OF TABLES**

	<b><u>Page</u></b>
Table C1: Actual Testing Matrix for LBF 1-D Consolidation Testing.....	106
Table C2: Initial Properties of LBF Samples.....	107
Table C3: Compression and Swelling Indices .....	115

**LIST OF FIGURES**

	<b><u>Page</u></b>
Figure C1: LBF_1: a) Change in void ratio vs. pressure b) Sample displacement vs. square root of time .....	109
Figure C2: LBF_2: a) Change in void ratio vs. pressure; b) Sample displacement vs. square root of time .....	110
Figure C3: LBF_3: a) Change in void ratio vs. pressure b) Sample displacement vs. square root of time .....	111
Figure C4: LBF_4: a) Change in void ratio vs. pressure b) Sample displacement vs. square root of time .....	112
Figure C5: LBF_5B: a) Change in void ratio vs. pressure b) Sample displacement vs. square root of time .....	113
Figure C6: LBF_6: a) Change in void ratio vs. pressure b) Sample displacement vs. square root of time .....	114
Figure C7: Calculation of Compression & Swell Indices.....	115
Figure C8: Void Ratio Comparison for Tests in Distilled Water .....	116
Figure C9: Void Ratio Comparison for Tests in Calcium Chloride Solution .....	117
Figure C10: Void Ratio Comparison for Tests under Unconfined Swelling.....	118
Figure C11: Void Ratio Comparison for Tests under Constant Volume.....	118

## **C1. INTRODUCTION**

This appendix summarizes the laboratory procedures and results of the one-dimensional (1D) consolidation testing on Light Backfill (LBF). LBF is one of the proposed engineered barrier components (Russell and Simmons 2003) for the Deep Geologic Repository (DGR). The testing program consisted of six samples with varying initial conditions including changes to the pore fluid chemistry. This testing is part of the ongoing work being undertaken to determine parameters for Hydraulic-Mechanical modelling of LBF by the Atomic Energy of Canada Limited (AECL). The LBF was tested at the Royal Military College of Canada (RMC).

### **C1.1 LBF**

LBF is composed of 50% (by dry weight) of silica sand and 50% of sodium bentonite from Avonlea Saskatchewan (Russell and Simmons 2003). This composition is similar to the previous tests (Baumgartner et al. 2008), so the results of these tests can be compared with the previous program. As received from AECL, the LBF material used in this testing program was taken from the same sample stockpile of Bentonite Sand Buffer (BSB) that was used in the Isothermal Test (Dixon et al. 2002) but has lower dry density than the BSB.

## **C2. LBF OEDOMETER TESTING**

### **C2.1 LBF TEST DESCRIPTION**

The LBF material used in the following tests was dry and crushed when it arrived at RMC. Fluid was added to the material, using a spray bottle for even distribution, to obtain target gravimetric water content of 19.1%. The sample was then mixed thoroughly. Once the target gravimetric water content was achieved, the sample was placed into the oedometer ring and compacted. Test specimens were compacted to a target dry density of  $1.3 \text{ Mg/m}^3$ . Two Wykeham Farrance Model 24001, rear-loading consolidation frames were used to conduct the 1D oedometer tests. Standard 50-mm-diameter and 19-mm-height, consolidation rings were used. Six samples were tested according to the testing matrix, shown in Table C1.

**Table C1: Actual Testing Matrix for LBF 1-D Consolidation Testing**

Test No.	Mixing Fluid	Reservoir Fluid	Swelling % on Initial Water Uptake	Loading Path
LBF_1	227 g/L CaCl <sub>2</sub>	227 g/L CaCl <sub>2</sub>	8.3 %	Load to 1702 kPa after initial swelling
LBF_2	Distilled Water	227 g/L CaCl <sub>2</sub>	4.2 %	Load to 1709 kPa after initial swelling
LBF_3	227 g/L CaCl <sub>2</sub>	227 g/L CaCl <sub>2</sub>	Rigidly Confined	Load to 1703 kPa after initial swelling
LBF_4	Distilled Water	227 g/L CaCl <sub>2</sub>	Rigidly Confined	Load to 1709 kPa after initial swelling
LBF_5B	91 g/L CaCl <sub>2</sub>	91 g/L CaCl <sub>2</sub>	7.7 %	Load to 1701 kPa after initial swelling
LBF_6	Distilled Water	91 g/L CaCl <sub>2</sub>	Rigidly Confined	Unload, swell to 2.2%, load to 1711 kPa

## C2.2 LBF TEST PROCEDURE

### C2.2.1 Calcium Chloride Solution

Three different liquids (distilled water, 91 g/L CaCl<sub>2</sub> and 227 g/L CaCl<sub>2</sub> solutions) were used during the course of this testing. The 91 g/L solution was prepared using anhydrous calcium chloride and the 227 g/L solution was prepared using the dihydrate form of calcium chloride. For the 91 g/L solution, 91 g of CaCl<sub>2</sub> was mixed with 1L of water to obtain a TDS of 91 g/L and a concentration of 0.82M. For the 227 g/L solution, 331.16 g of CaCl<sub>2</sub> was added to 1L of water to obtain a TDS of 227 g/L and a concentration of 1.54mol/L. Although these solution concentrations of 91g/L and 227 g/L were less than the original target of 100 g/L and 250 g/L, the difference of solution concentration within this range does not significantly affect the result of each test. To minimize evaporation and maintain a constant concentration, the solutions were stored in covered containers.

### C2.2.2 LBF

Standard ASTM D2435-04 procedures were generally followed for the consolidation testing unless otherwise specified. Samples were prepared from the dry, crushed LBF material supplied to RMC. Prior to testing, the LBF was placed in the oven for a minimum of 24 hours. The oven-dried samples were then wetted with the specified fluid, as outlined in the testing matrix, to obtain a target water content of 19.1%. Using a target density of 1.3 Mg/m<sup>3</sup>, the wetted LBF was added to the oedometer ring and compacted, by hand, to a target height of 10 mm. Each sample was then loaded according to the testing schedule summarized in Table C1. The initial properties for each test are outlined in Table C2. Due to the high montmorillonite content of LBF and the associated low hydraulic conductivity, primary consolidation was rarely achieved in the standard 24-hour increment. Therefore each load and

unload increment was considered complete when the vertical deformation rate was less than 0.02 mm/day.

Two broadly different loading schedules and were used for testing as outlined in Table C1. Inundation with the cell fluid was accompanied by either swell under a constant load to a specified height or rigidly confined. Following initial conditions, standard oedometer loading and unloading increments were applied.

During initial testing, corrosion of the lifting and tie down screws was observed when the oedometer cell was filled with the calcium chloride solution. Following observation of corrosion, the test (LBF\_5) was aborted until the corrosion issue was resolved. The corrosion was alleviated by using stainless steel wing nuts coated in "Marine Goop" (i.e., a product of Eclectic Products, Inc. 101 Dixie Mae Drive Pineville, LA 71360-3993) for the remainder of the testing program, as discussed with AECL. Following solution of the issue, test LBF\_5B was then initiated.

**Table C2: Initial Properties of LBF Samples**

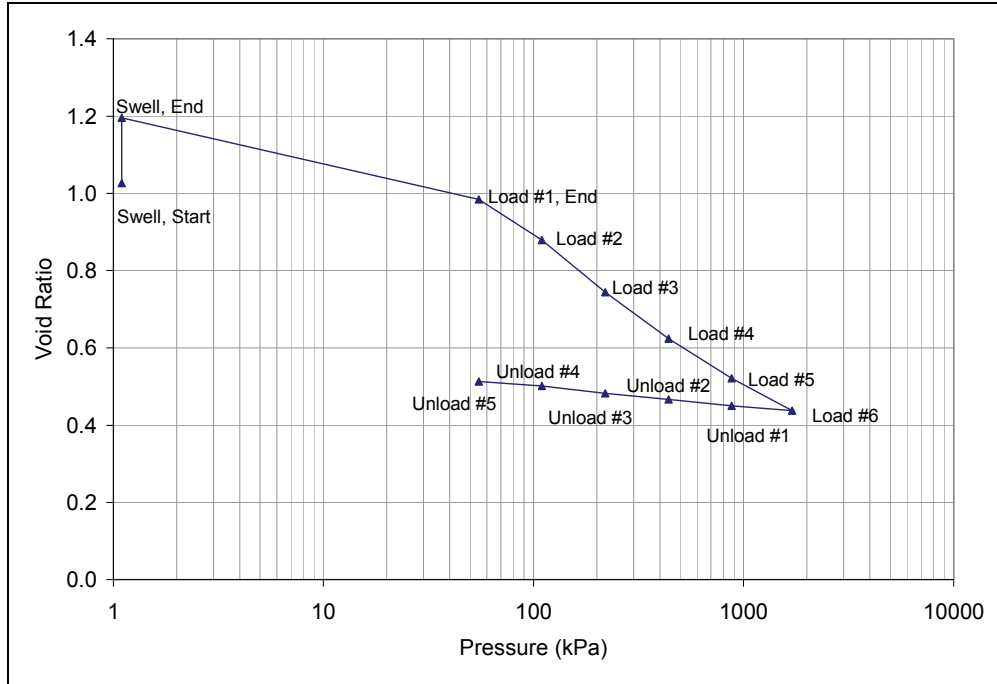
<b>Test</b>	<b>Water Content (%)</b>	<b>Height (mm)</b>	<b>Dry Density (Mg/m<sup>3</sup>)</b>
LBF_1	19.1	9.69	1.33
LBF_2	18.7	10.75	1.27
LBF_3	19.8	9.81	1.37
LBF_4	18.4	10.46	1.30
LBF_5B	18.6	10.10	1.29
LBF_6	19.5	10.29	1.28
Averages	19.0	10.18	1.31

### **C3.LBF TEST RESULTS**

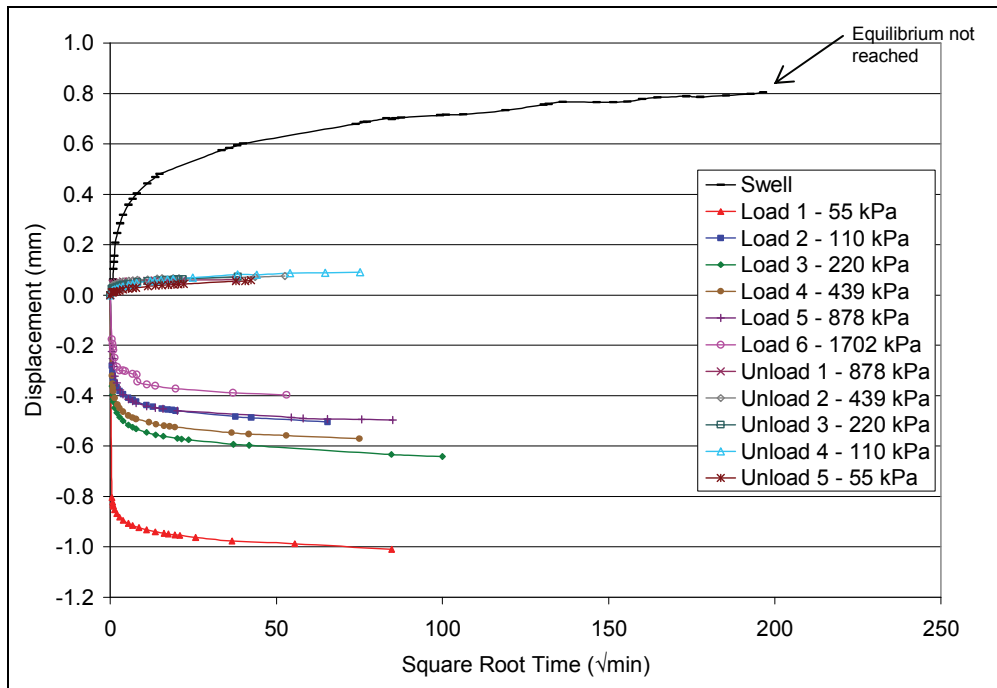
#### **C3.1 INDIVIDUAL TEST RESULTS**

Test results of the six individual samples are plotted in Figures C1 through C6 including void ratio versus applied pressure and displacement versus square root of time. Tests LBF\_1, LBF\_2, and LBF\_5 included initial free swell phases while tests LBF\_3, LBF\_4, and LBF\_6 began with rigid boundary conditions applied. In tests LBF\_1 and LBF\_2, minimal weight (20 g) was applied during the initial swell phase as water uptake occurred. After 27 days, specimen LBF\_1 swelled at a rate of 0.005 mm/day however it did not appear to have reached equilibrium as seen in Figure C1b. AECL was contacted and the decision to proceed with subsequent loading increments was made. LBF\_2 did reach equilibrium, however there is a jump in the data near the end of the swelling period as observed in Figure C2b. One possible explanation is due to dial gauge error that was also observed in subsequent compression loadings. Following the

jump in reading no further increase in height was observed and equilibrium was determined. Throughout the entire test (LBF\_2), problems with this dial gauge were noticed. The gauge tended to stick during middle portions of a test but always came to equilibrium towards the end of the test. This is also highlighted in Figure C2b. LBF\_5 was allowed to swell to 7.4 % as designated by testing matrix and LBF\_3, LBF\_4 and LBF\_6 were all rigidly confined during water uptake.



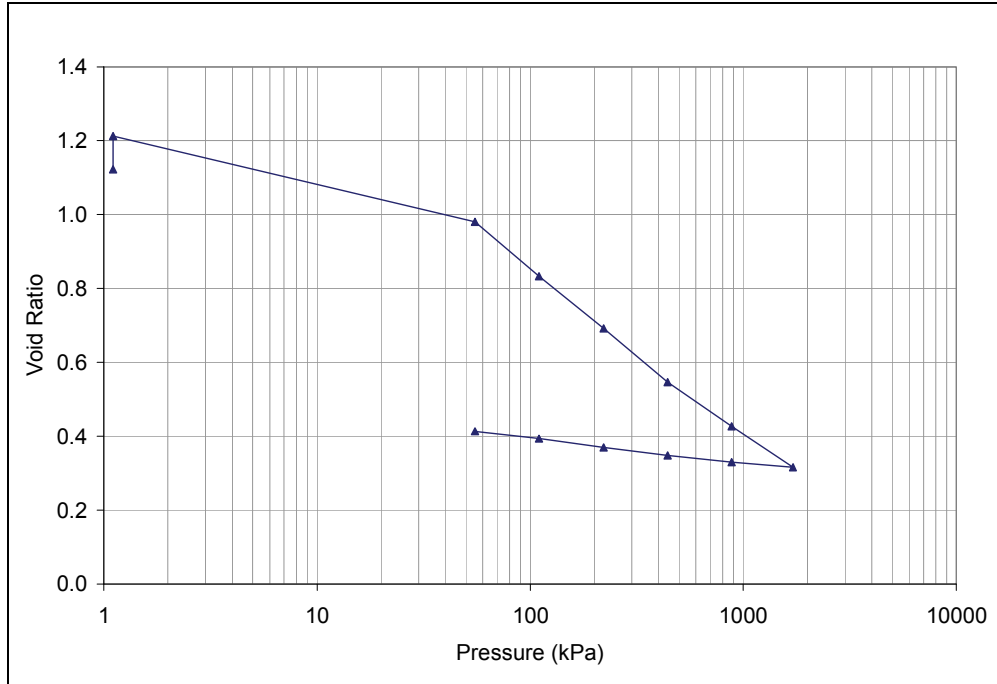
a)



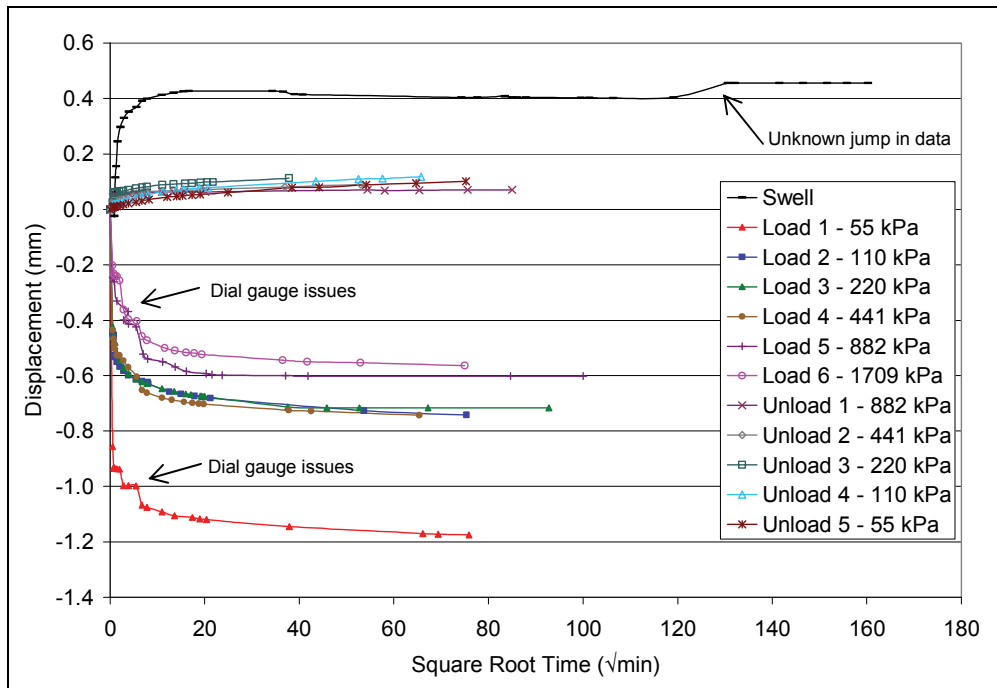
b)

**Figure C1: LBF\_1: a) Change in void ratio vs. pressure  
b) Sample displacement vs. square root of time**

(Mixing Liquid = Reservoir Liquid = 227 g/L CaCl<sub>2</sub>; Initial Swelling ~ 8.3%)



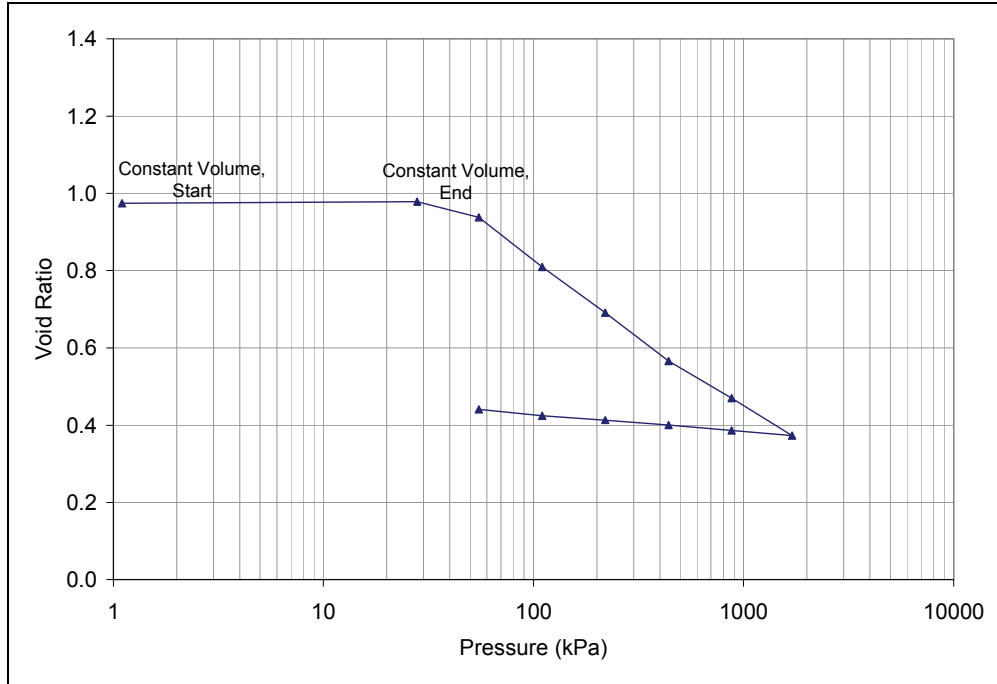
a)



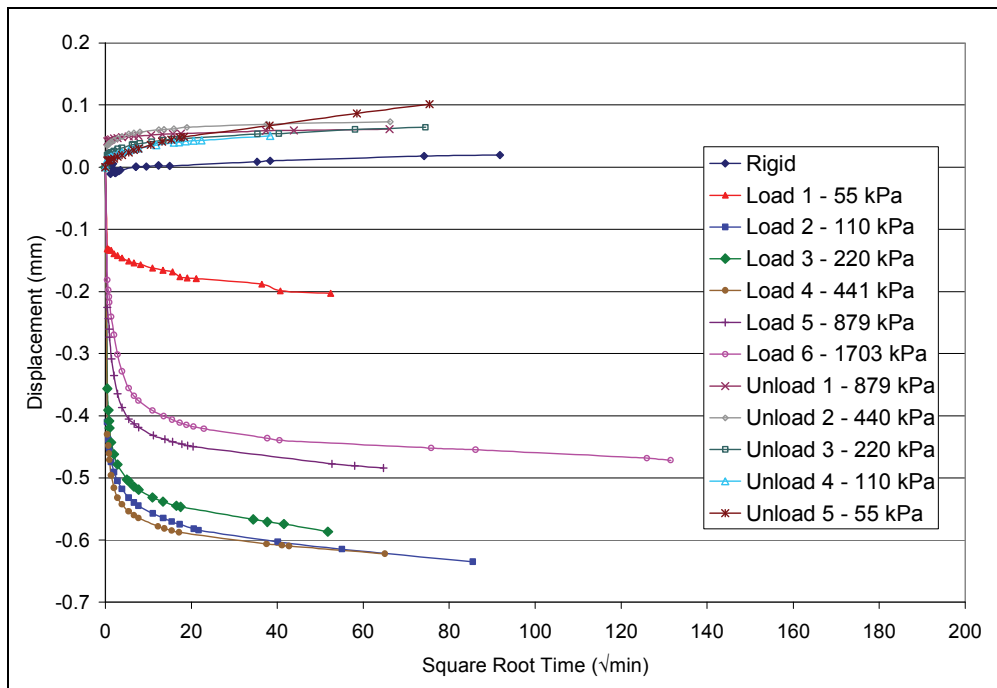
b)

**Figure C2: LBF\_2: a) Change in void ratio vs. pressure;  
b) Sample displacement vs. square root of time**

(Mixing Liquid = Distilled Water; Reservoir Liquid = 227 g/L CaCl<sub>2</sub> ; Initial Swelling = 4.2%)



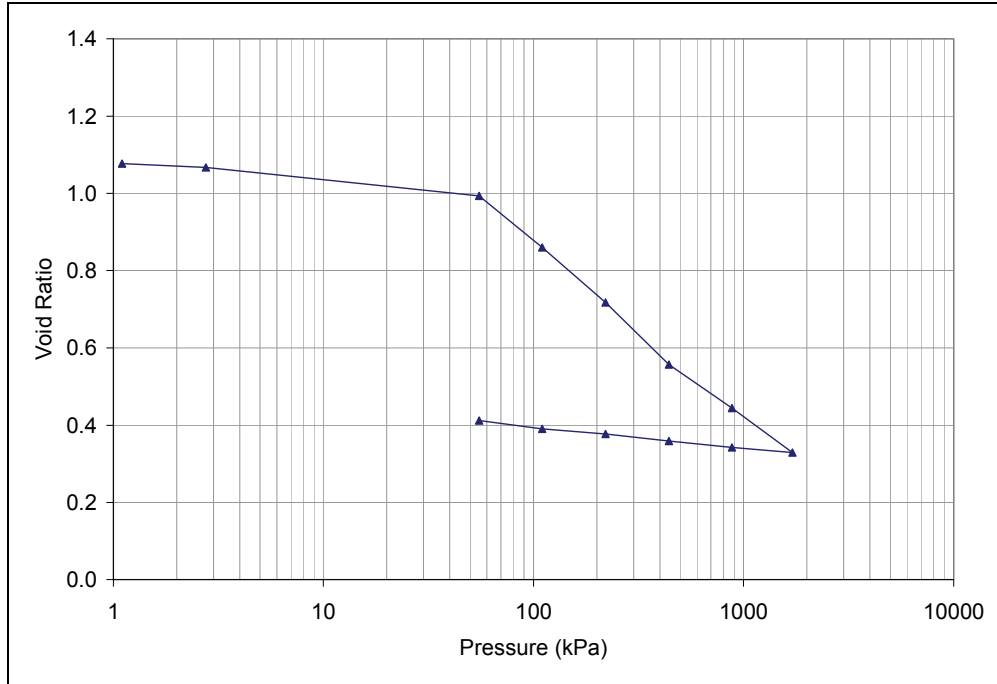
a)



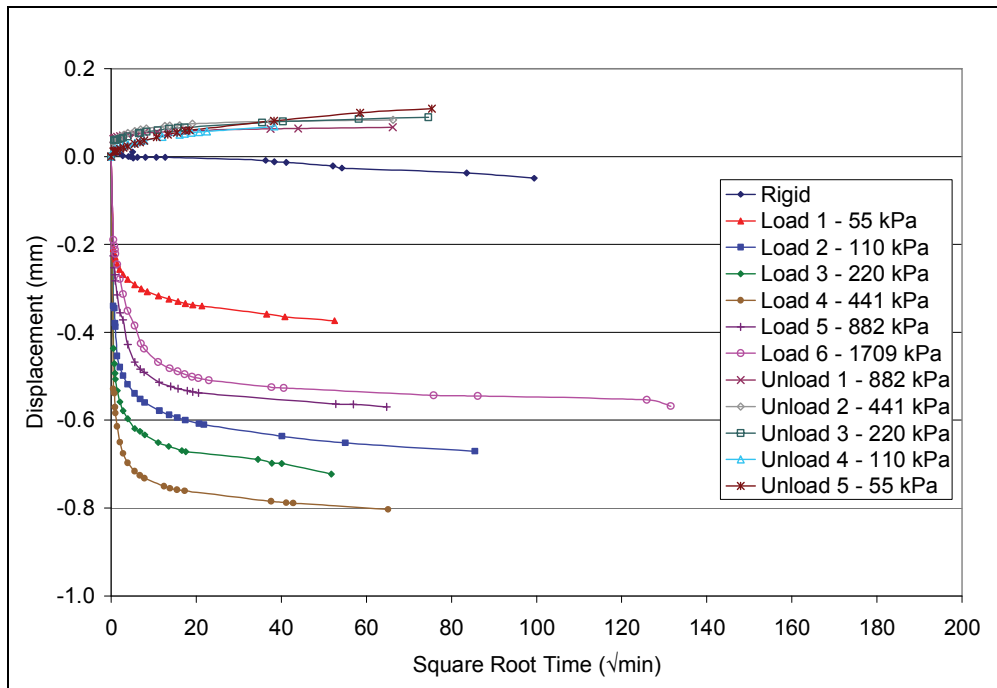
b)

**Figure C3: LBF\_3: a) Change in void ratio vs. pressure  
b) Sample displacement vs. square root of time**

(Mixing Liquid = Reservoir Liquid = 227 g/L CaCl<sub>2</sub> ; Rigidly Confined)



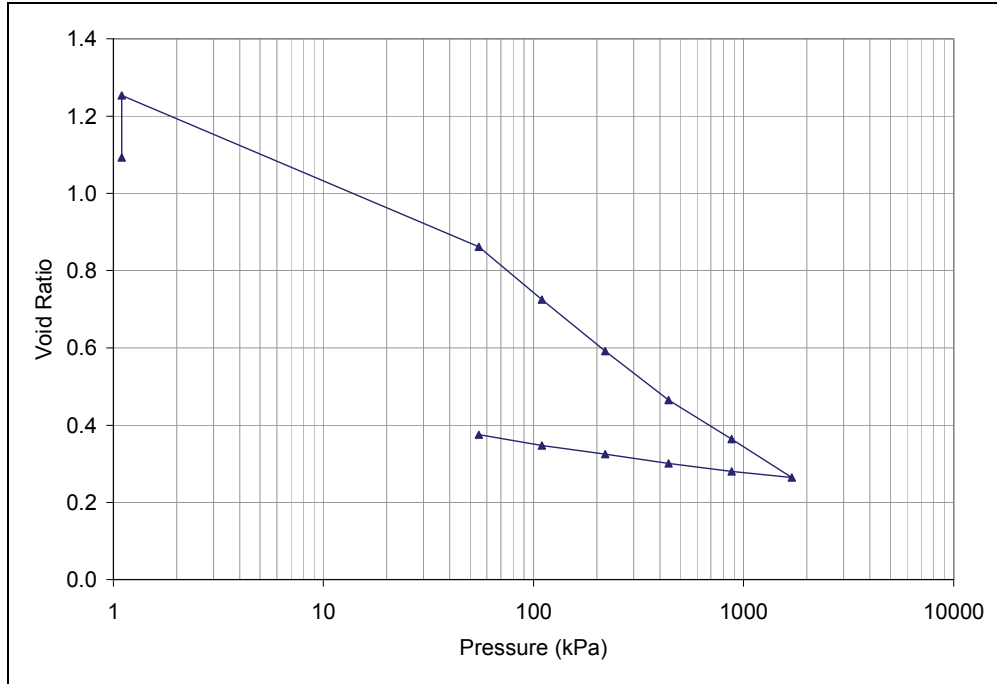
a)



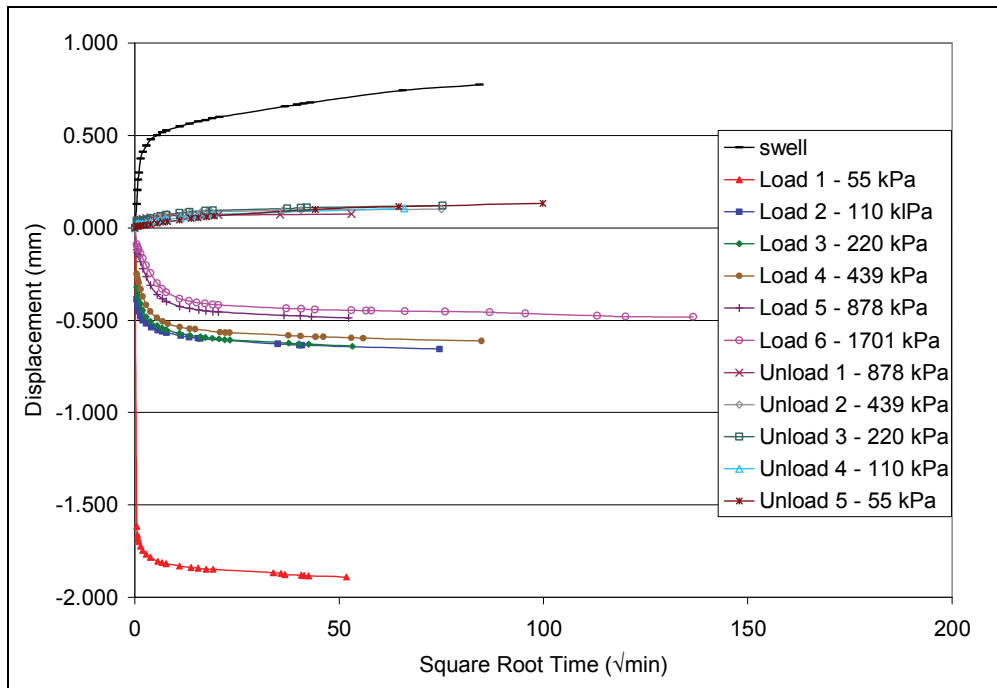
b)

**Figure C4: LBF\_4: a) Change in void ratio vs. pressure  
b) Sample displacement vs. square root of time**

(Mixing Liquid = Distilled Water; Reservoir Liquid = 227 g/L  $\text{CaCl}_2$ ; Rigidly Confined)



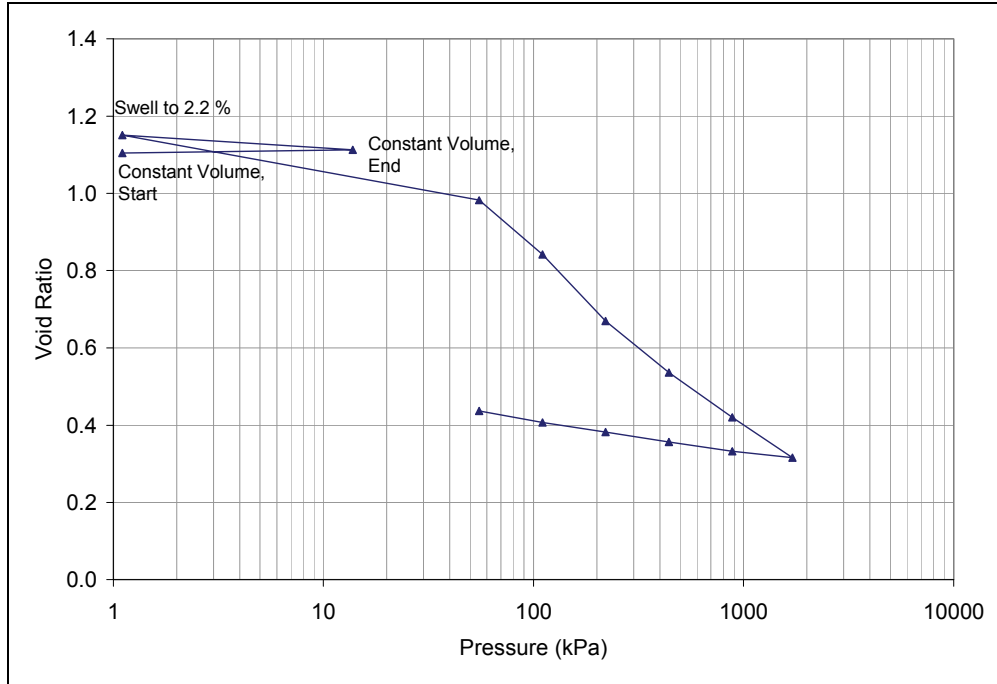
a)



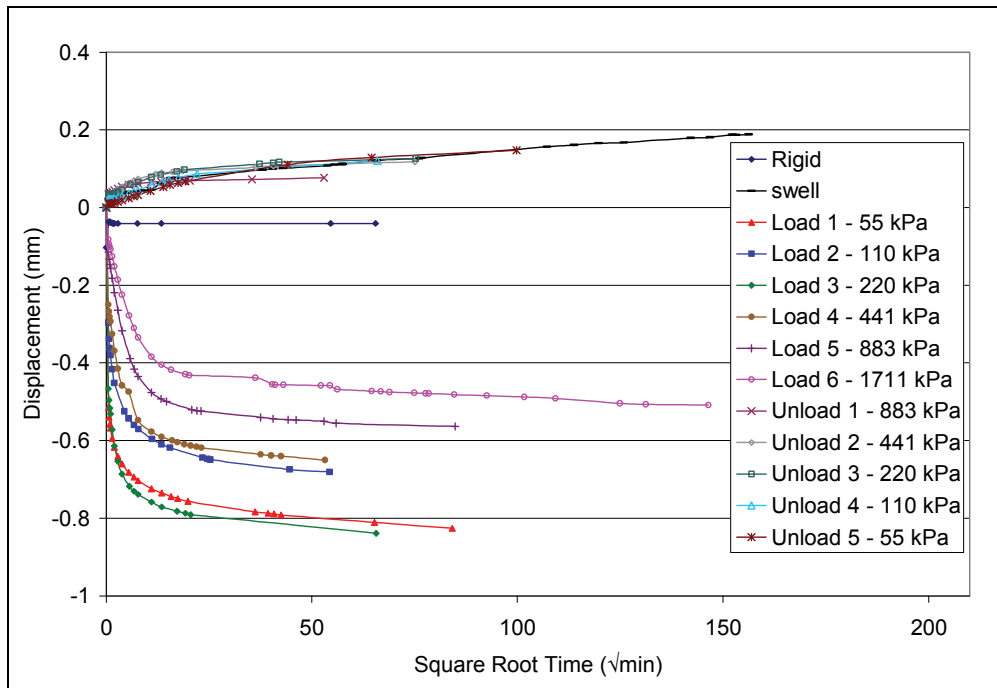
b)

**Figure C5: LBF\_5B: a) Change in void ratio vs. pressure  
b) Sample displacement vs. square root of time**

(Mixing Liquid = Reservoir Liquid = 91 g/L  $\text{CaCl}_2$ ; Initial Swelling  $\sim 7.7\%$ )



a)



b)

**Figure C6: LBF\_6: a) Change in void ratio vs. pressure  
b) Sample displacement vs. square root of time**

(Mixing Liquid = Distilled Water; Reservoir Liquid = 91 g/L  $\text{CaCl}_2$ ; Rigidly Confined)

From the test data, compression and swelling indices for each test were determined and summarized in Table C3. An example of the procedure used to calculate the indices is illustrated in Figure C7. The compression index ( $C_c$ ) was calculated from the end of the first load increment to the end of the sixth load increment and the swelling index ( $C_s$ ) was taken from the end of the sixth load increment to the end of the 5<sup>th</sup> unloading increment as shown in Figure C7.

**Table C3: Compression and Swelling Indices**

Test	Mixing Liquid	Reservoir Liquid	$C_c$	$C_s$
LBF_1	227 g/L CaCl <sub>2</sub>	227 g/L CaCl <sub>2</sub>	0.37	0.05
LBF_2	Distilled Water	227 g/L CaCl <sub>2</sub>	0.45	0.07
LBF_3	227 g/L CaCl <sub>2</sub>	227 g/L CaCl <sub>2</sub>	0.38	0.05
LBF_4	Distilled Water	227 g/L CaCl <sub>2</sub>	0.45	0.06
LBF_5B	91 g/L CaCl <sub>2</sub>	91 g/L CaCl <sub>2</sub>	0.40	0.07
LBF_6	Distilled Water	91 g/L CaCl <sub>2</sub>	0.45	0.08

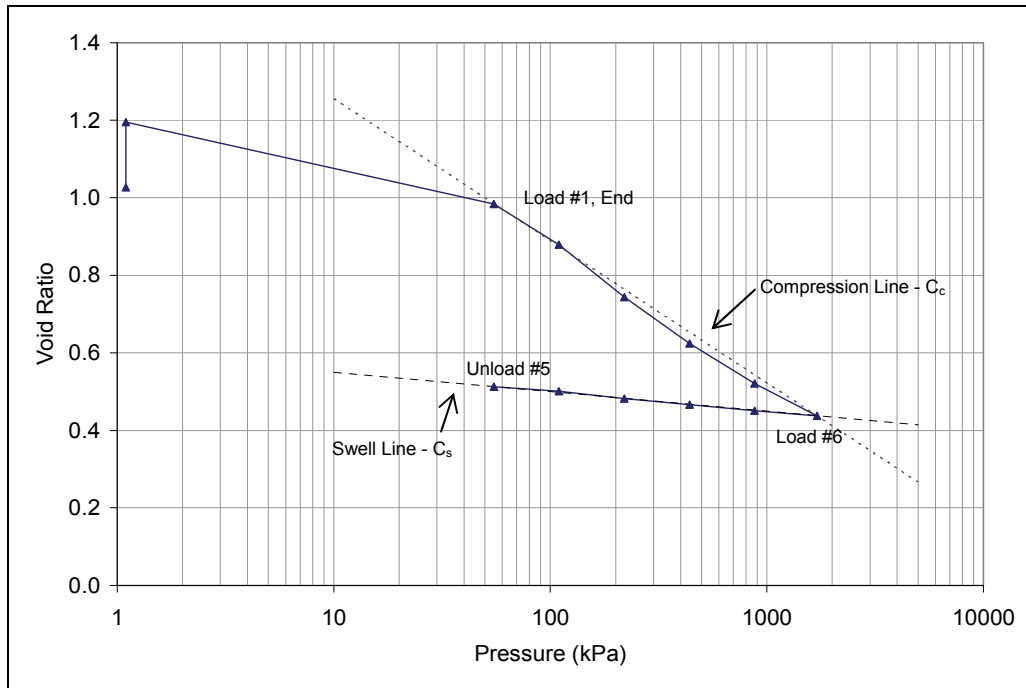


**Figure C7: Calculation of Compression & Swell Indices**

### C3.2 COMPARISON OF MIXING AND RESERVOIR CONDITIONS

For the specimens prepared with distilled water (LBF\_2, LBF\_4, and LBF\_6), the interpreted  $C_c$  and  $C_s$  values are consistent. Initial void ratios for the three distilled water tests were similar (Table C2). Although initial boundary conditions differed between free swell and rigidly confined, the resultant loading increments yielded void ratios that were almost identical (Figure C8). The  $C_c$  values for each test are the same at 0.45 and the  $C_s$  values are virtually the same at 0.07 and 0.08 as observed in Table C3. Behaviour observed during unloading (i.e., 1700 kPa to 50 kPa) is log-linear indicating the LBF is behaving similar to a non-swelling material. This may not be the case if the specimens were unloaded up to lower pressure (i.e., < 50 kPa). The investigation of the specimens under lower unloading pressure will be included in 2008 work scope as discussed in Section 6.

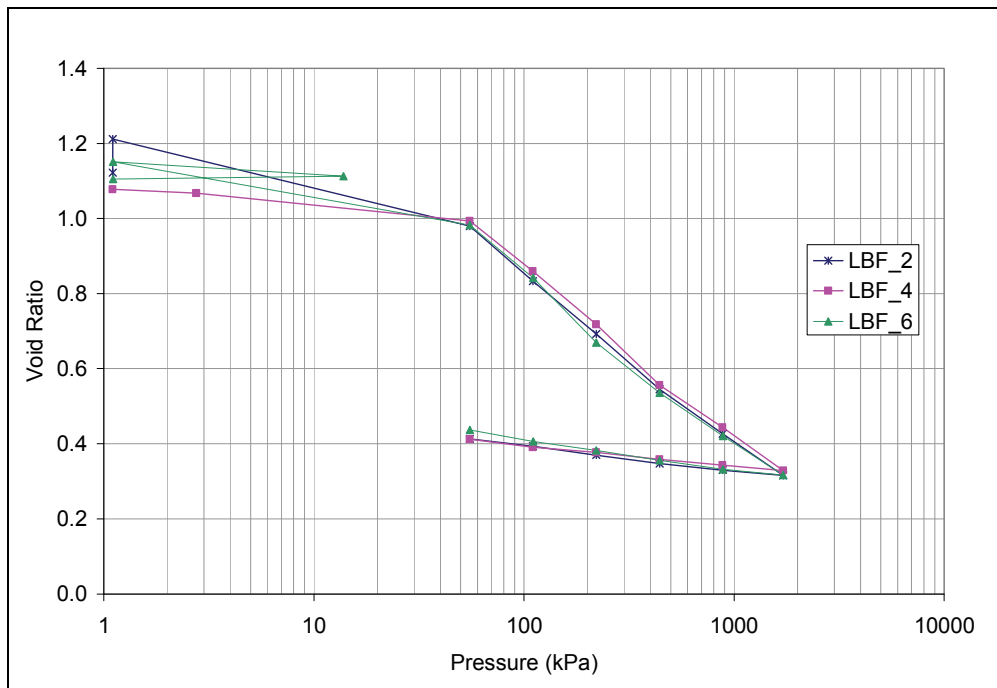


**Figure C8: Void Ratio Comparison for Tests in Distilled Water**

The two tests prepared with the 227 g/L  $\text{CaCl}_2$  solution (LBF\_1 and LBF\_3) result in essentially parallel curves with  $C_c$  values being 0.37 and 0.38 respectively (Figure C9). The prepared void ratios for these two tests are slightly different and this difference appears to be similar to the offset in the data. The sample prepared with 91 g/L  $\text{CaCl}_2$  resulted in a curve with a slightly less stiff  $C_c$  value of 0.4. Again, the difference in the initial dry density may account for the small offset seen in the curves.

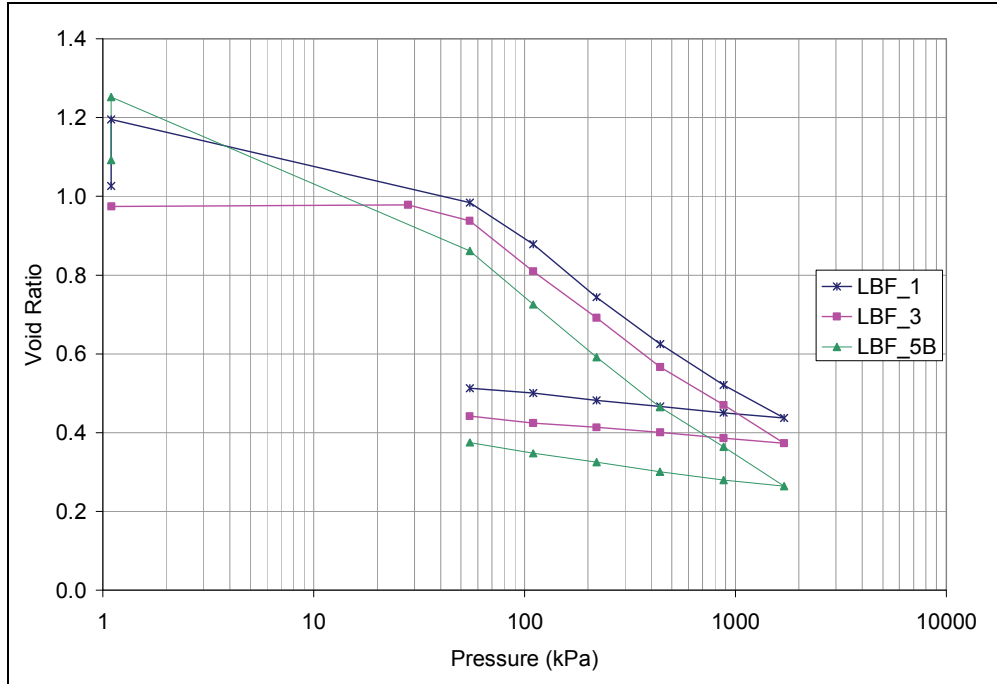


**Figure C9: Void Ratio Comparison for Tests in Calcium Chloride Solution**

Comparing the test specimens prepared in distilled water to those in saline solution finds that the saline prepared specimens have a stiffer compression behaviour, due to suppression of the swelling by the salts. This is consistent with earlier observed behaviour in compression.

### C3.3 COMPARISON OF INITIAL CONDITIONS

The initial conditions appear to play a less influential role into the compression behaviour of the material in comparison to the specimen mixing conditions. For the tests undergoing free swell during water uptake, Figure C10, it is seen that the tests prepared with the  $\text{CaCl}_2$  solution swell more than the sample mixed with distilled water. The test with 227 g/L  $\text{CaCl}_2$  for both the mixing and cell fluid swelled the most during the initial phase. The  $C_s$  values for the 91g/L  $\text{CaCl}_2$  test and distilled water (LBF\_2 and LBF\_5B) sample are equal at 0.07 where as the 227 g/L  $\text{CaCl}_2$  test is slightly stiffer at 0.05.

In the tests that were rigidly confined during water uptake (Figure C11) the mixing conditions are the dominant factor in the shape of the curve. The two samples mixed with distilled water (LBF\_4 and LBF\_6) are virtually identical were as the  $\text{CaCl}_2$  solution test plots with a shallower slope for both the compression and unloading. Interestingly, the sample with 227 g/L  $\text{CaCl}_2$  mixing and cell fluid (LBF\_3) required the highest load to maintain initial height compared with the two test specimens (LBF\_4 and LBF\_6) that used distilled water as the mixing fluid and saline solution as the cell fluid. This is consistent with the free swell testing where specimen LBF\_1 had the greatest initial swell.

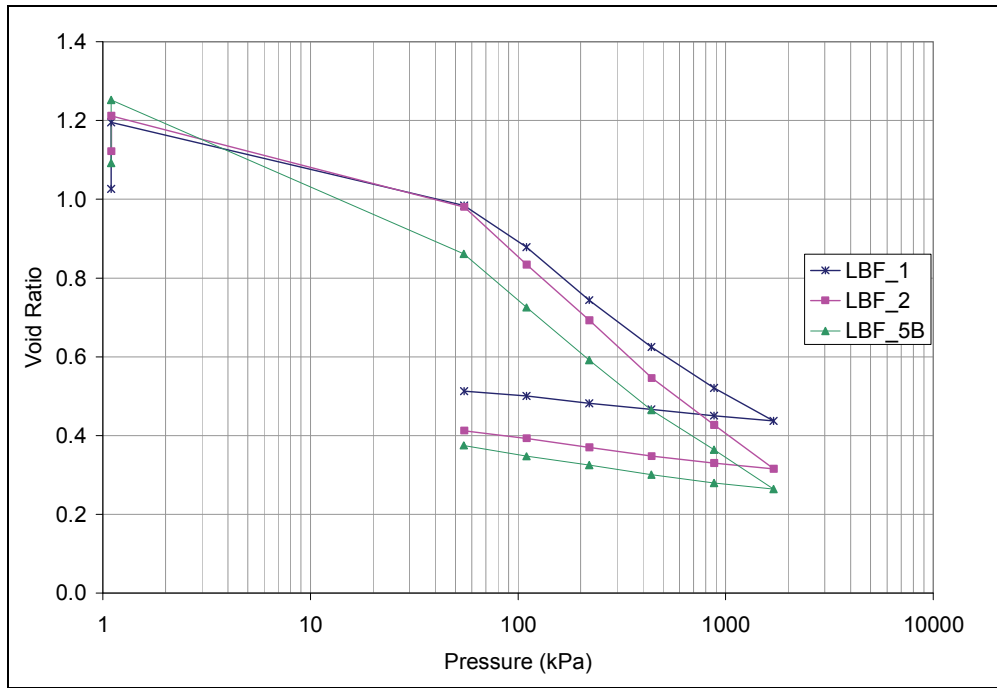


Figure C10: Void Ratio Comparison for Tests under Unconfined Swelling

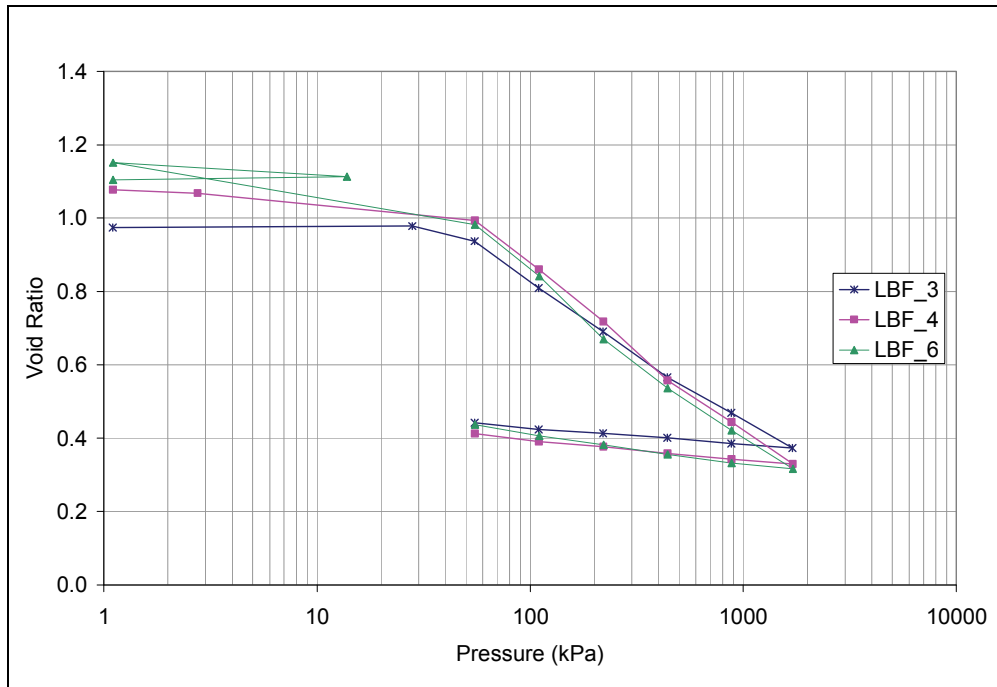


Figure C11: Void Ratio Comparison for Tests under Constant Volume

#### **C4. SUMMARY**

One-dimensional consolidation tests were performed on LBF material. In total, six tests were conducted using a variety of initial conditions and pore water chemistries. The resultant compression and swelling indices were determined from the test results. The test data is providing valuable input parameters for the Hydraulic-Mechanical modelling of LBF by Atomic Energy of Canada Limited (AECL).

#### **C5. CONCLUSIONS AND RECOMMENDATIONS**

It was observed that mixing conditions tend to be more influential in the behaviour of the material. The tests mixed with distilled water yielded identical  $C_c$  values and very similar  $C_s$  values. The two tests mixed with 227g/L  $\text{CaCl}_2$  as yielded virtually identical  $C_c$  values of 0.37 and 0.38 whereas the 91g/L  $\text{CaCl}_2$  tests has a slightly shallower slope but is similar at 0.40. In general, all the tests yielded consistent results with the curves plotting on top or parallel to one another. Consistent mixing and reservoir pore fluids strongly influence initial swell and compression behaviour observed. The pore fluid chemistry dominates compression behaviour above 55 kPa, which was the first loading applied following the initial swell or rigidly confined phase.

Unfortunately, prior to the first load increment at approximately 55 kPa, there are no data points and therefore this upper portion of the curve is undefined. In order to better understand compression behaviour in this stress level (<55 kPa) it would be beneficial to have additional load increments between water uptake and 55 kPa. For instance, load increments in the range of 2, 4, 8, 16, 25 kPa would allow for better definition of the curve under small loads both loading and unloading.

#### **ACKNOWLEDGEMENTS**

Technical assistance in the Geotechnical Laboratory at RMC was provided by Joe Dipietrantonio.

#### **REFERENCES**

- ASTM (ASTM International). 2004. Standard test methods for one-dimensional consolidation properties of soils using incremental loading. Standard D2435-04, ASTM International, West Conshohocken, Pennsylvania, USA.
- Dixon, D., Chandler, N., Graham, J., & Gray, M. N. (2002). Two large-scale sealing tests conducted at Atomic Energy of Canada's underground research laboratory: the buffer-container experiment and the isothermal test. *Can. Geotech. J.*, 39, 503-518.
- Russell, S.B. and G.R. Simmons. 2003. Engineered barrier system for a deep geologic repository. Presented at the 2003 International High-Level Radioactive Waste Management Conference. 2003 March 30 – April 2, Las Vegas, NV